Aus dem Max von Pettenkofer-Institut für Hygiene und
Medizinische Mikrobiologie der Ludwig-Maximilians-Universität München
Lehrstuhl: Bacteriologie

Kommissarische Leitung: Prof. Dr. Rainer Haas

Functional Characterization of the *Helicobacter pylori* Cag Type IV Secretion System Components CagH, CagI and CagL

Dissertation

zum Erwerb des Doktorgrades der Naturwissenschaften

an der Medizinischen Fakultät

der Ludwig-Maximilians-Universität München

vorgelegt von

Kieu Thuy Pham

aus Hanoi/ Vietnam

Germany 2015

Gedruckt mit Genehmigung der Medizinischen Fakultät

der Ludwig-Maximilians-Universität München

Betreuer: Priv. Doz. Dr. Wolfgang Fischer

Zweitgutachter: Prof. Dr. Gunnar Schotta

Dekan: Prof. Dr. med. dent. Reinhard Hickel

Tag der mündlichen Prüfung: 20/01/2016

TABLE OF CONTENT

LIST OF FIGURES

LIST OF TABLES

SUMMARY

Helicobacter pylori is a highly successful bacterial pathogen uniquely adapted to colonize the human stomach. It is an infectious agent responsible for causing type B gastritis, peptic ulcers, gastric adenocarcinoma and MALT lymphoma. Upon contact with the host cell, *H. pylori* forms a transmembrane multi-protein complex and a needle-like structure, termed the Cag Type IV Secretion System (Cag-T4SS), to mediate the injection of its effector protein CagA into gastric epithelial cells. The translocated CagA influences several host cell signaling pathways and results in reorgnization of the cytoskeleton and in inflammation.

The *cag* pathogenicity island (*cag*-PAI) harbors 27-30 genes coding for components of the Cag type IV secretion apparatus. CagH, CagI and CagL, which are encoded by contiguous genes on the *cag*-PAI, are known to play roles as essential components of the Cag-T4SS. It has been shown that several Cag proteins, including CagI and CagL, contribute to the interaction between the secretion apparatus and the integrin β1 receptor, which might facilitate the translocation of CagA across the host cell membrane. However, the functional roles and the interactions between these three proteins and other Cag proteins, which lead to Cag-T4SS assembly, are not well defined.

In this thesis, we show that CagH, CagI and CagL are independently required for both CagA translocation and IL-8 induction, the hallmark of proinflammatory activity induced by the Cag-T4SS. Although the genes coding for these three proteins are located in the same operon and have overlapping open reading frames, there was no transcriptional effect of *cagI* deletion on *cagL*, but we found stabilizing effects at the protein level. Secondly, we show by immunoprecipitation and pull-down assays that CagH, CagI and CagL interact with each other to form a complex in *H. pylori*, which might play an important role in Cag-T4SS functionality. Additionally, using different biochemical methods, we provide evidence for different/distinct subcellular pools, as well as bacterial surface localization, of CagI and CagL. Importantly, we were able to identify functional domains of CagH, CagI and CagL. We found that the CagH, CagI and CagL proteins contain a conserved C-terminal motif, and that this motif is important

for the function of at least CagH and CagL, as well as for the interaction of CagH, CagI and CagL. Finally, we provide evidence for an influence of another *cag* gene, *cagP*, on production of CagI and CagL proteins. We show that there is no transcriptional effect exerted by deletion of *cagP*, or of the associated small non-coding RNA HPnc2630, on transcription of the *cagI* gene, but that the CagP protein is required for the full function of the Cag-T4SS. In conclusion, these findings reveal for the first time an important role of these proteins and their interaction for the activity of the Cag-T4SS and give novel insights for understanding the way how pili are assembled.

ZUSAMMENFASSUNG

Helicobacter pylori ist ein sehr erfolgreicher Krankheitserreger, der auf einzigartige Weise an die Kolonisierung des menschlichen Magens angepasst ist. Infektionen mit diesem Bakterium verursachen die Typ B-Gastritis, Magen- und Duodenalulzera sowie Magenkarzinome und MALT-Lymphome. Nach Kontakt mit Wirtszellen bildet *H. pylori* einen membranständigen Multiproteinkomplex sowie nadelartige Fortsätze oder Pili aus, das sogenannte Cag-Typ IV-Sekretionssystem (Cag-T4SS), und injiziert damit sein Effektorprotein CagA in Magenepithelzellen. Transloziertes CagA beeinflusst verschiedene Signaltransduktionswege der Wirtszelle und bewirkt eine Reorganisation des Zytoskeletts sowie eine Entzündungsreaktion.

Die *cag*-Pathogenitätsinsel (*cag*-PAI) enthält 27-30 Gene, die für Komponenten des Typ IV-Sekretionsapparats kodieren. CagH, CagI und CagL, die von benachbarten Genen der *cag*-PAI kodiert werden, sind als essenzielle Komponenten des Cag-T4SS beschrieben. Es wurde gezeigt, dass mehrere Cag-Proteine, darunter CagI und CagL, zu einer Wechselwirkung des Sekretionsapparats mit β1-Integrin-Rezeptoren beitragen, die die Translokation von CagA über die Wirtszellmembran ermöglicht. Die Funktionen dieser drei Proteine und ihre Wechselwirkungen untereinander bzw. mit anderen Proteinen des Sekretionsapparats sind hingegen bislang nicht untersucht.

In dieser Arbeit wurde eine umfassende funktionelle Analyse der Proteine CagH, CagI und CagL mittels verschiedener genetischer Deletions- und Komplementationsstrategien durchgeführt, um ihre Rolle für das Cag-T4SS zu bestimmen. Es konnte gezeigt werden, dass CagH, CagI und CagL unabhängig voneinander für die Translokation des CagA-Proteins und für die Induktion von Interleukin-8 (IL-8) als Marker für die proinflammatorische Aktivität des T4SS benötigt werden. Obwohl die Gene für diese drei Proteine im gleichen Operon lokalisiert sind und teilweise überlappende Leserahmen aufweisen, konnte kein transkriptioneller Effekt von Gendeletionen auf stromabwärts liegende Gene nachgewiesen werden, es wurden jedoch stabilisierende Effekte auf Proteinebene gefunden. Weiterhin konnte durch Immunpräzipitation und *Pulldown*-Experimente gezeigt werden, dass CagH, CagI und CagL miteinander interagieren und in *H. pylori* einen Komplex bilden, dem

vermutlich eine wichtige Rolle bei der Funktionalität des T4SS zukommt. Mit verschiedenen biochemischen Methoden konnten wir zeigen, dass CagI und CagL in verschiedenen Kompartimenten in der Bakterienzelle vorliegen, unter anderem auf der Bakterienoberfläche. Ein wichtiger Schritt war der Nachweis funktioneller Domänen von CagH, CagI und CagL. Alle drei Proteine enthalten unter anderem ein konserviertes C-terminales Motiv, das zumindest für die Funktion von CagH und CagL, sowie für die Wechselwirkung zwischen allen drei Proteinen von Bedeutung ist. Schließlich konnten Hinweise auf den Einfluss eines weiteren *cag*-Gens, *cagP*, auf die Menge an CagL und vor allem CagI in der Bakterienzelle erbracht werden. Wir zeigen, dass eine Deletion des *cagP*-Gens oder der assoziierten nichtkodierenden RNA HPnc2630 keinen transkriptionellen Effekt auf die Expression von *cagI* hat, dass die Anwesenheit des CagP-Proteins jedoch für die volle Funktion des Cag-T4SS notwendig ist.

Zusammengefasst belegen die Ergebnisse dieser Arbeit die bedeutende Rolle dieser Proteine und ihrer Wechselwirkung für die Aktivität des Cag-T4SS, und sie könnten ein wichtiger Schritt zum Verständnis der Assemblierung der Typ-IV-Sekretions-Pili sein.

Eidesstattliche Versicherung

Ich, Kieu Thuy Pham, erkläre hiermit an Eides statt, dass ich die vorliegende Dissertation mit dem Thema

Functional Characterization of the *Helicobacter pylori* Cag Type IV Secretion System Components CagH, CagI and CagL

selbständig verfasst, mich außer der angegebenen keiner weiteren Hilfsmittel bedient und alle Erkenntnisse, die aus dem Schrifttum ganz oder annähernd übernommen sind, als solche kenntlich gemacht und nach ihrer Herkunft unter Bezeichnung der Fundstelle einzeln nachgewiesen habe.

Ich erkläre des Weiteren, dass die hier vorgelegte Dissertation nicht in gleicher oder in ähnlicher Form bei einer anderen Stelle zur Erlangung eines akademischen Grades eingereicht wurde.

München, 25/01/2016

Ort, Datum Unterschrift

Teile dieser Arbeit werden veröffentlicht:

Pham KT, Weiss E, Jiménez Soto LF, Breithaupt U, Haas R, Fischer W. (2012). CagI is an essential component of the *Helicobacter pylori* Cag type IV secretion system and forms a complex with CagL. PLoS One. 7(4): e35341.

Publikation im Promotionszeitraum, die nicht in der Arbeit enthalten sind:

Pham KT, Fischer W. (2013). *Helicobacter pylori* utilizes DNA shuffling to modulate the gastric inflammatory response. Future Microbiol. 8(7): 835-838.

Bonsor DA1, Pham KT, Beadenkopf R, Diederichs K, Haas R, Beckett D, Fischer W, Sundberg EJ. (2015). Integrin Engagement by the Helical RGD Motif of the *Helicobacter pylori* CagL Protein Is Regulated by pH-induced Displacement of a Neighboring Helix. J Biol Chem. 15;290(20):12929-12940.

1 INTRODUCTION

1.1 *Helicobacter pylori*

1.1.1 Bacteriology

Helicobacter pylori (*H. pylori*) was first discovered in the stomachs of patients with gastritis and stomach ulcers in 1982 [Marshall and Warren, 1984]. It was originally named *Campylobacter pyloridis* and later was renamed as the first species of a new genus as *H. pylori.* It is a microaerophilic, Gram-negative bacterium with a curved rod shape (3.5 µm in length and 0.5 µm in width) [Goodwin and Worsley, 1993]. *H. pylori* is a highly motile bacterium and carries multiple unipolar flagella, usually 2-6 per bacterium. Each flagellum is approximately 3 µm in length. The motility facilitates rapid migration of *H. pylori* through the gastric mucus environment [O'Toole *et al.*, 2000]. The bacteria are able to transform their normal morphology to a coccoid morphology with a diversity in viability and ultrastructure in response to different stress conditions. These coccoid forms were observed to have metabolic activities, but are non-culturable *in vitro* [Bode *et al.*, 1993; Mizoguchi *et al.*, 1998]. The precoccoid forms were observed by negative staining to carry flagella filaments on a single pole and coccoid forms are usually devoid of flagella [Worku *et al.*, 1999]. In contrast, some coccoid forms are eletron-dense with intact membrane and flagella [Zheng *et al.*, 1999].

H. pylori requires a nutrient-rich medium containing serum or cholesterol, and a microaerobic environment for growth. Generally, under optimal conditions and on a nonselective solid medium, small colonies are formed after 2 to 3 days [Morgan *et al.*, 1987]. The optimal growth conditions comprise O_2 levels of 2 to 5% and additionally CO_2 levels of 5 to 10%, as well as a high humidity. A standard microaerobic condition of 85% N_2, 10% CO_2, and 5% O_2 is commonly used for *H. pylori* culture. Growth occurs at 34 to 40°C, with an optimum of 37°C and at pH values ranging from 5.5 to 8.0 (reviewed in [Kusters *et al.*, 2006]).

1.1.2 Epidemiology

Infection with *H. pylori* is one of the most common chronic bacterial infection of humans. The prevalence of *H. pylori* shows large geographical variations. *H. pylori* infection is more frequent in developing countries than in developed countries

(reviewed in [Pounder and Ng, 1995]). A recent review revealed a widely varying prevalence of *H. pylori* infection within populations of all ages, ranging from 31.7 to 93.6% in adults, and from 11 to 66.2% in children [Eusebi *et al.*, 2014]. Typically, acquisition of the bacteria happens early during childhood (reviewed in [Yucel, 2014]) and infection persists through life and leads to chronic gastric infection [Portal-Celhay and Perez-Perez, 2006]. Although more than 50% of the world population harbor *H. pylori* in their stomachs, most cases remain asymptomatic throughout life, with no specific clinical signs. The risk of being infected with *H. pylori* is associated with different factors such as socioeconomic status and living conditions. Persons of higher socioeconomic status, higher family income, and higher educational levels seem to have a lower risk of acquiring *H. pylori* infection (reviewed in [Eusebi *et al.*, 2014]). The exact route of *H. pylori* transmission remains unclear. The most likely mode of transmission is from person to person via fecal/oral or oral/oral contacts (reviewed in [Yucel, 2014]). *H. pylori* infection can be effectively cured by a proton pump inhibitor (PPI)-based triple therapy, including antibiotics such as clarithromycin, amoxicillin or metronidazole, and proton pump inhibitors such as pantoprazole. However, the increasing prevalence of regional antimicrobial resistance raised a challenge in *H. pylori* eradication treatment [Egan *et al.*, 2007; Egan and O'Morain, 2007].

1.1.3 Infection process

Originally, *H. pylori* was observed in the stomach of patients with gastritis and peptic ulcers [Marshall and Warren, 1984]. Additionally, it was later found to be involved in the development of gastric adenocarcinoma and MALT lymphoma (mucosa-associated lymphoid tissue) [Blaser *et al.*, 1995; Parsonnet *et al.*, 1991; Parsonnet *et al.*, 1994]. In 1994, *H. pylori* was classified as a type 1 carcinogen for gastric cancer by the International Agency for Research on Cancer (WHO) [Parkin *et al.*, 2005].

H. pylori is able to colonize the host stomach with the contribution of colonization factors and virulence factors (reviewed in [Dunn *et al.*, 1997]). Motility using the flagella and urease activity, which is required for neutralizing the microenvironment within the gastric lumen with pH values of 2 are important factors for a successful adaptation and colonization of the human gastric mucosa [Eaton *et al.*, 1991; Eaton *et al.*, 1992]. Once it reaches the mucus layer which is overlying the epithelial cells, *H.*

pylori induces gastric inflammatory responses and increases the secretion of interleukin (IL)-8 and other chemokines in gastric epithelial cells, which play a critical role for the survival of *H. pylori* [Censini *et al.*, 1996; Crabtree and Farmery, 1995; Huang *et al.*, 1995; Sharma *et al.*, 1995]. The ability of producing urease, catalase, phospholipases and further virulence factors (section 1.2) causes disruption of the gastric mucosal layer and damage of epithelial cells [Dunn *et al.*, 1997; Mauch *et al.*, 1993; Ottlecz *et al.*, 1993; Penta *et al.*, 2005]. For a long-term persistence of infection in the stomach, the tight adherence of *H. pylori* to gastric epithelial cells plays an important role, which is maintained by interaction between adhesins embedded in the bacterial outer membrane, such as BabA, SabA, AlpA, AlpB, OipA, HopZ and HomB, and gastric epithelium receptors (reviewed in [Oleastro and Menard, 2013]). In addition, *H. pylori* is able to produce and efficiently deliver virulence factors, such as the vacuolating cytotoxin VacA and the cytotoxin-associated antigen CagA, which exert multiple effects on host cells [Salama *et al.*, 2013].

1.2 Virulence factors of *H. pylori* and interaction with host cells

1.2.1 Outer membrane proteins (OMPs)

To maintain a persistent colonization through lifetime, *H. pylori* uses its ability to adhere to mucosal structures, like many other pathogens do. *H. pylori* is not only localized at the apical surface of gastric epithelial cells, but also within the surface mucous gel layer [Shimizu *et al.*, 1996]. Once inside the mucus, *H. pylori* penetrates the mucus layer using its spiral shape and flagellar motility, to reach the surface of epithelial cells and to adhere through interactions between outer membrane protein adhesins and different host receptors (reviewed in [Evans and Evans, 2000]). *H. pylori* adhesion to gastric epithelial cells is a crucial step in establishment of a long-term infection of the gastric mucosa. A variety of outer membrane proteins that serve as bacterial adhesins have been characterized (reviewed in [Oleastro and Menard, 2013]).

The blood group antigen-binding adhesin BabA (HopS or OMP28) is a major *H. pylori* adhesin of about 80 kDa. BabA recognizes Lewis b blood-group antigen and other fucosylated blood-group antigens such as the H-type 1 and the A and B blood group antigens, which are found on mucin proteins and on the surface of the gastric epithelium [Aspholm-Hurtig *et al.*, 2004; Boren *et al.*, 1993; Ilver *et al.*, 1998]. The BabA adhesin

also mediates binding of *H. pylori* to salivary mucin glycoprotein found in saliva and the non-mucin glycoprotein gp340 [Walz *et al.*, 2005; Walz *et al.*, 2009]. The presence of *babA* is typically associated with *cagA* and *vacA* toxigenic s1 strains [Fujimoto *et al.*, 2007], suggesting a crucial role of BabA in *H. pylori* pathogenesis.

SabA (SabA or HopP or OMP17) is a sialic acid-binding adhesin with a size of 70 kDa. It is known to adhere to sialyl-Lewis a and sialyl-Lewis x glycoprotein serving as additional functional receptors to promote binding of *H. pylori* to inflamed gastric mucosa [Mahdavi *et al.*, 2002]. Although there was no correlation between the *sabA* status and the severity of disease, a widely divergent prevalence of SabA in clinical isolates suggests differences between SabA and clinical outcome [Yamaoka, 2010].

The adherence-associated lipoproteins AlpA (HopC or OMP20) and AlpB (HopB or OMP21) are 56 kDa and 57 kDa proteins, respectively. AlpA and AlpB proteins seem to be produced by all clinical isolates, suggesting their important role for *H. pylori* [Odenbreit *et al.*, 2009]. Both lipoproteins were found to contribute to gastric colonization (reviewed in [Oleastro and Menard, 2013]). However, host receptors for both adhesins have not been identified. Recently, laminin, an extracellular matrix protein which is found in nearly every tissue, was demonstrated as a target for these two adhesins [Senkovich *et al.*, 2011].

The outer inflammatory protein A (OipA, HopH or OMP13) with a size of 34 kDa was initially reported as a surface protein capable of inducing IL-8 expression in a T4SS-independent manner [Yamaoka *et al.*, 2000]. Expression analysis of the *oipA* gene showed a significant correlation of OipA with high *H pylori* density, with severe neutrophil infiltration, and with development of duodenal ulcers and gastric cancer, [Yamaoka, 2010]. In addition, OipA influences the adherence capacity of *H. pylori* to the gastric cancer cell lines AGS and Kato-III [Dossumbekova *et al.*, 2006].

Further putative adhesins, HopZ [Peck *et al.*, 1999] and HomB [Oleastro *et al.*, 2008] have been identified.

1.2.2 Vacuolating cytotoxin A

The vacuolating cytotxin A (VacA), an immunogenic 95-kDa protein, is the most intensely investigated toxin secreted by *H. pylori*. The *vacA* gene is present in all strains

of *H. pylori* but about 50% of clinical isolates produce inactive or less active VacA toxins due to the different genotypes of the *vacA* gene. Based on diversity near the 5' end of the *vacA* gene (s-region) and in the mid-region of the gene (m-region). Different genotypes of *vacA,* generated from combination of different alleles (s1m1, s1m2 and s2m2), have been observed and correlated with different *H. pylori*-associated diseases. Strains containing *vacA* s1m1 have higher levels of cytotoxic activities in a wider range of cell types than strains *vacA* s1/m2, whereas strains harboring *vacA* s2 have cytotoxic activities for some cells only (reviewed in [Cover and Blanke, 2005]). The VacA protein encoded by the s1/m1 genotype is known to be correlated with the development of peptic ulcer disease and gastric cancer (reviewed in [Kusters *et al.*, 2006]). The *vacA* gene encodes for a 140 kDa precursor toxin, which contains an N-terminal signal sequence, a passenger domain and a C-terminal auto-transporter domain. This pretoxin undergoes proteolytic cleavage to release the mature 88 kDa toxin during transport to the extracellular space via an autotransporter (Type Va) pathway [Cover and Blanke, 2005; Fischer *et al.*, 2001a; Schmitt and Haas, 1994; Telford *et al.*, 1994]. The secreted 88 kDa monomers assemble into large water-soluble polymeric complexes with a molecular mass of about 900 kDa that insert into the host cell membrane to form anion-selective channels which are important for VacA cytotoxicity [Cover and Blanke, 2005; McClain *et al.*, 2013; Papini *et al.*, 2001]. VacA induces vacuole formation in the cytoplasm of gastric cells [de Bernard *et al.*, 1997]. In addition, VacA exerts a wide range of activities on host cells such as disruption of endosomal and lysosomal trafficking, triggering of apoptosis, and modulation of inflammatory responses (reviewed in [Cover and Blanke, 2005]). For these activities, VacA is able to intoxicate multiple types of human cells including gastric epithelial cells, and VacA alters the function of T lymphocytes, B cells, macrophages, and mast cells as well [Algood and Cover, 2006]. With respect to lymphocytes, VacA might contribute to pathogenesis by suppressing T-cell proliferation [Boncristiano *et al.*, 2003; Gebert *et al.*, 2003; Sundrud *et al.*, 2004] at the level of the Ca^{2+}-calmodulin-dependent phosphatase calcineurin [Gebert *et al.*, 2003]. *In vivo,* VacA was found to be associated in initial host colonization of *H. pylori* [Salama *et al.*, 2001].

1.2.3 The Cytotoxin-associated antigen and the *cag* pathogenicity island

The gene product of the Cytotoxin-Associated Gene (*cagA*) (120 to 145 kDa) is one of the most well-studied *H. pylori* virulence proteins. The CagA protein was demonstrated as a cancer-associated factor, since the gene is frequently found in *H. pylori* strains isolated from cancer patients, but less frequent from asymptomatic cases or patients with mild gastritis [Cover *et al.*, 1995]. In other studies, CagA production was associated with the development of atrophic gastritis, peptic ulcer disease and gastric carcinoma [Blaser *et al.*, 1995; Parsonnet *et al.*, 1997]. *H. pylori* producing active VacA (s1/i1/m1) and CagA proteins are classified as Type I strains, while Type II strains lack expression of these 2 proteins [Xiang *et al.*, 1995]. The CagA effector protein is delivered directly into host cells underneath the attachment site via the Cag-T4SS [Odenbreit *et al.*, 2000]. The Cag-T4SS is responsible for transporting the CagA virulence protein into gastric epithelial cells [Hatakeyama and Higashi, 2005]. CagA is the only known effector protein, which is transported by the Cag system to date. Immunogold-staining revealed that CagA is located at the tip of T4SS pili [Jimenez-Soto *et al.*, 2009; Kwok *et al.*, 2007] or on the bacterial surface [Murata-Kamiya *et al.*, 2010]. Following the translocation event, the CagA molecules localize to the inner surface of the plasma membrane [Higashi *et al.*, 2005].

Recently, structural studies showed that CagA consists of a structured N-terminal region and an intrinsically disordered C-terminal region. The N-terminal region contains three distinct domains: an alpha-helical N-terminal domain (Domain I), a more complex phosphatidylserine binding domain (Domain II), and Domain III interacting intramolecularly with the disordered C-terminal region [Hayashi *et al.*, 2012]. The core domain (Domain II) is formed by an extended single-layer β-sheet which is stabilized by two independent helical subdomains. The specific single-layer β-sheet region (SLB) was determined as a binding domain of CagA to β1 integrin. This interaction is critically involved in the delivery of CagA into host cells [Kaplan-Turkoz *et al.*, 2012].

The *cag* pathogenicity island (*cag*-PAI) found in *H. pylori* Type 1 strains is a 37 kbp genome island. This DNA region was acquired during the evolution of *H. pylori* [Akopyants *et al.*, 1998; Censini *et al.*, 1996]. The *cag*-PAI is well-characterized and is harbored by approximately 60-70% of Western *H. pylori* strains, while nearly 100% of

the East Asian *H. pylori* strains are *cag*-PAI-positive (reviewed in [Noto and Peek, 2012]). The *H. pylori cag*-PAI-bearing strains (cag^+) are found to be adjacent and frequently adherent to epithelial cells while *H. pylori cag*-PAI-negative (cag^-) predominate in the mucus gel, suggesting that the topology of colonization is influenced by the *cag* genotype [Camorlinga-Ponce *et al.*, 2004]. The *cag*-PAI contains ~30 putative open reading frames encoding multiple structural components of the type IV secretion apparatus, as well as the immunodominant antigen CagA. The *cagA* gene is localized to the end of the island (reviewed in [Hatakeyama and Higashi, 2005]).

1.2.4 Integrins as host cell receptors

Integrins belong to a large family of a αβ heterodimeric cell surface receptors found in multiple cellular organisms, from sponges to mammals [Humphries, 2000; Kim *et al.*, 2011]. These receptors are known to mediate cell-cell, cell-extracellular matrix and cell-pathogen interactions.

Integrins consist of two distinct subunits (α and β) forming heterodimers. These α and β subunits assemble into a head segment built on top of two V-shaped legs [Campbell and Humphries, 2011]. In mammals, integrins form 24 different receptors assembled from 18 α subunits and 8 β subunits [Barczyk *et al.*, 2010; Hynes, 2002].

Each subunit of the integrin αβ heterodimers consists of a large extracellular domain, a single-spanning transmembrane domain, and a short cytoplasmic tail. The extracellular part of the α and β subunits contains several subdomains organized into a globular ligand-binding-terminal head domain standing on two C-terminal legs, that connect to the transmembrane and cytoplasmic domain of each subunit. The transmembrane domains are single spanning structures (25-29 amino acid residues) forming α-helical coiled-coils that either homo- or heterodimerize. The cytoplasmic domains (10-70 amino acids) are generally short and unstructured (reviewed in [Takada *et al.*, 2007]).

Structural and functional studies revealed that integrins can exist in different affinity states: low, intermediate and high [Luo *et al.*, 2007]. Additionally, analysis of crystal structures showed that integrin heterodimers occur in the low affinity state (inactive form) as a bent V-shape with the head close to the membrane-proximal regions of the legs [Xiong *et al.*, 2001; Xiong *et al.*, 2002], maintained by the α/β salt bridges at the inner membrane region and the helix packing of the transmembrane regions [Partridge

et al., 2005]. This low affinity structure undergoes rapid, reversible conformational changes to increase ligand affinity, termed "activation", to release an active form. (reviewed in [Banno and Ginsberg, 2008; Calderwood, 2004; Shimaoka *et al.*, 2002]).

It has been shown that the translocation of CagA requires a cellular host cell receptor, the β1 integrin [Jimenez-Soto *et al.*, 2009; Kwok *et al.*, 2007]. Several Cag components have been demonstrated to bind to integrin, including CagA, CagI, CagY [Jimenez-Soto *et al.*, 2009] and CagL [Kwok *et al.*, 2007]. The binding of these proteins to β_1 integrin (extended, open conformation) was assumed to induce conformational changes of integrin heterodimers, which may allow translocation of CagA into host cells. Apart from α5β1, the αvβ5 and αvβ3 integrins were shown to be putative interacting partners of CagL in an RGD motif-dependent manner [Conradi *et al.*, 2012; Wiedemann *et al.*, 2012]. The interaction with αvβ5 activates gastrin expression via an integrin linked kinase (ILK) signaling complex [Wiedemann *et al.*, 2012]

1.2.5 Effects of CagA and the Cag-T4SS on host cells

Upon injection, CagA undergoes phosphorylation on tyrosine residues found in a five amino acid repeat, Glu-Pro-Ile-Tyr-Ala (EPIYA) motif by multiple members of either Abl or Src family kinases. The repeats were subclassified into EPIYA-A, -B, -C and -D motfis, based on the surrounding amino acids. *H. pylori* isolates from Western countries carry the 'A-B-C'-type CagA, whereas *H. pylori* strains from East-Asia CagA contain an 'A-B-D'-type CagA (reviewed in [Hatakeyama and Higashi, 2005]). The most outstanding event in *H. pylori* infection of some epithelial cell lines such as AGS cells is the induction of a morphological change termed the humming-bird phenotype, a form of cell scattering [Backert *et al.*, 2001], which is caused by interaction of phosphorylated CagA with the SHP2 (a cytoplasmic SRC homology domain-containing protein tyrosine phosphatase) [Jones *et al.*, 2010]. SHP2 links growth factor signaling with the activation of ERK1/2, which are members of the mitogen-activated protein kinase family (MAPK). The activation of the ERK-MAPK pathway may lead to enhanced cell-cycle progression and increased cell proliferation [Hatakeyama, 2004; Higashi *et al.*, 2002].

CagA exerts several effects on host cells in a phosphorylation independent manner, such as changes in cellular tight junction integrity, cellular polarity, cell proliferation and

differentiation, cell scattering, or induction of a pro-inflammatory response (reviewed in [Jones *et al.*, 2010]).

The resulting chronic inflammation caused by infection with *H. pylori* is a major step in the initiation and development of gastric cancer. *H. pylori* utilizes a variety of pathways to promote inflammation in the stomach (reviewed in [Lamb and Chen, 2013]). Inflammatory molecules found to be upregulated in the stomachs of *H. pylori*-infected patients include IL-1, IL-6, IL-8, TNF-α, and RANTES [McGee and Mobley, 2000]. Considerable induction of IL-8 during gastric infection has a key role in the pathogenesis of *H. pylori* [Crabtree, 1996; Naumann and Crabtree, 2004]. IL-8, a leukocyte chemotactic cytokine (chemokine), is produced by different cell types upon stimulation by various inflammatory stimuli and exerts a variety of functions on leukocytes as well as on neutrophils *in vitro* (reviewed in [Lamb and Chen, 2013]). Several studies showed that the expression of IL-8 upon *H. pylori* infection is triggered by various signaling pathways in a CagA-dependent or -independent manner [Fischer *et al.*, 2001b; Gorrell *et al.*, 2012; Kim *et al.*, 2006; Naito *et al.*, 2006; Nozawa *et al.*, 2004; Selbach *et al.*, 2002; Sharma *et al.*, 1998; Zhang *et al.*, 2006].

The CagA-dependent pathway of IL-8 induction involves in activation of NF-κB (nuclear factor kappa B), AP-1 (essential transcriptional factors for IL-8 gene transcription), and NFAT (nuclear factor of activated T cells) [Backert and Naumann, 2010]. Infection of Mongolian gerbils with the *cagA* deletion mutant led to a considerable reduction of NF-κB activation and the level of inflammation compared to infection with wild-type strain [Shibata *et al.*, 2006]. However, the ability of CagA to activate NF-κB and IL-8 production seems to be *H. pylori* strain-specific [Brandt *et al.*, 2005].

In a CagA-independent manner, binding of the type IV secretion apparatus to host cells has been proposed to induce IL-8 production [Fischer *et al.*, 2001b]. The Cag-T4SS triggers IL-8 secretion via interaction of the CagL protein which is surface exposed with the host receptor β1 integrin, and subsequent activation of MAPKs and NF- κB [Gorrell *et al.*, 2012]. Several adhesion proteins such as OipA and BabA were also found to be important for IL-8 production [Sugimoto *et al.*, 2011; Yamaoka *et al.*, 2000]. In addition, peptidoglycan is another virulence factor, which might be delivered into host

cells via the Cag apparatus or outer membrane vesicles [Kaparakis *et al.*, 2010]. Peptidoglycan is specifically recognized by a host intracellular sensor NOD1 (nuleotide oligomerization domain) [Boughan *et al.*, 2006; Viala *et al.*, 2004]. The activation of NOD1 triggers the proinflammatory cytokines MIP-2 (human IL-8 homolog), β-defensin, and IL-8 production through induction of signaling molecules in host cells such as NF-κB, p38, and ERK [Allison *et al.*, 2009; Viala *et al.*, 2004]. Furthermore, the activated NOD1 regulates the production of type I interferon (IFN), which likely affects Th1 cell differentiation [Watanabe *et al.*, 2010].

1.3 The Cag type IV secretion system

1.3.1 Functions of the T4SSs

The Type IV Secretion Systems (T4SSs) are multi-subunit cell-envelope-spanning structures of Gram-negative and Gram-positive bacteria. They are widely used for transport of a broad range of macromolecules, from single proteins to DNA-protein complexes across the cell [Alvarez-Martinez and Christie, 2009; Fronzes *et al.*, 2009; Juhas *et al.*, 2008]. These translocation systems usually consist of a secretion channel and often a pilus or other surface filament that might be used as a conduit for substrate transport or to establish contacts with target cells [Juhas *et al.*, 2008]. There are 3 subfamilies of the T4SSs that have been classified according to their functions:

Conjugation systems:

Conjugation systems are the most widely distributed of the T4SSs and found in a wide range of bacterial species [Alvarez-Martinez and Christie, 2009]. They are used to transfer DNA from one bacterial cell to another in a cell contact-dependent manner. These systems play major roles in the conjugative transfer of autonomously replicating plasmids and Integrative and conjugative elements (ICEs) in Gram (+) and Gram (-) bacteria [Smillie *et al.*, 2010; Wozniak and Waldor, 2010]. These ICEs can be found to be integrated into the chromosome, often as parts of transposons. The conjugation event contributes to bacterial genome plasticity and facilitates adaptation of bacteria to changes in the environment. Conjugation is also involved in the spread of antibiotic resistance genes among pathogenic bacteria [Fronzes *et al.*, 2009; Wallden *et al.*, 2010].

DNA transport is generally initiated by a multiprotein complex called relaxosome. The enzyme relaxase, which acts as a site-specific endonuclease, nicks double-stranded DNA and covalently binds to the 5' end of the resulting single-stranded DNA at the origin of transfer. This DNA-protein complex is subsequently specifically recognized by a type IV coupling protein (T4CP) for subsequent transfer via the T4SS (reviewed in [Zechner *et al.*, 2012]).

Agrobacterium tumefaciens (*A. tumefaciens*) VirB/D4 is a well-charaterized DNA transfer system which is similar to conjugation systems. *A. tumefaciens* uses this system for delivering transfer-DNA (T-DNA), a part of the tumor-inducing (Ti) plasmid as well as several virulence proteins to plant cells to cause formation of tumors [Christie, 2004].

DNA release or uptake systems

The second subfamily of the T4SSs consists of 2 transport systems involved in DNA uptake or release from/to the extracellular space: The ComB transformation competence system in *H. pylori* which is responsible for DNA uptake from the extracellular milieu and the DNA release system encoded on the *Neisseria gonorrhoeae* gonococcal genetic island (GGI) [Hamilton and Dillard, 2006; Hofreuter *et al.*, 2001; Smeets and Kusters, 2002].

Effector translocation systems

Many Gram-negative bacteria, such as the phytopathogen *A.tumefaciens* and some human pathogens, including *H. pylori, Legionella pneumophila*, and *Brucella* and *Bartonella* species use T4SSs for delivery of effector protein molecules across the cell envelope and directly into the cytosol of plant or mammalian host cells [Cascales and Christie, 2003; Zechner *et al.*, 2012]. These systems play important roles in bacterial colonization and survival within host cells or during infection [Alvarez-Martinez and Christie, 2009].

1.3.2 *Agrobacterium tumefaciens* VirB/D4 Type IV secretion system as a prototypical T4SS

A. tumefaciens is a phytopathogen, which causes crown gall disease in infected plant tissues. The VirB/D4 transport machinery of *A. tumefaciens* is a prototypical T4SS and has been thoroughly examined in terms of substrate recognition, translocation, assembly

mode and architecture, and the dynamics of substrate movement through the T4SS. The *A. tumefaciens* VirB/D4 T4SS mediates the transfer of not only nucleo-protein (T-DNA) complexes, but also a set of virulence effector proteins into the nuclei of plant cells. The 12 proteins (VirB1-VirB11 and VirD4) required for DNA transport and tumor formation are encoded by the *virB* and *virD* operons, located on the Ti plasmid [Cascales and Christie, 2004; Christie, 1997]. The T4SS is likely to form a secretion channel, which traverses the entire cell envelope and translocates proteins or protein-DNA complexes across 3 membranes directly to the cytosol of eukaryotic host cells (Figure 1.1). The VirB1 to VirB11 proteins are components of the secretion apparatus [Alvarez-Martinez and Christie, 2009], whereas VirD4 serves as a coupling protein, which recognizes the substrates (T-DNA and several independently translocated proteins) [Atmakuri *et al.*, 2004; De Vos and Zambryski, 1989]. The inner membrane channel is comprised of 4 subunits: VirB3, VirB6, VirB8 and VirB10, of which VirB10 spans the periplasmic space. The outer membrane pore (secretion channel) consists of VirB7 and VirB9. The VirB2 and VirB5 components do not only take part in the secretion channel, but also polymerize to form an extracellular pilus. The VirB4, VirB11 and VirD4 proteins are three ATPases which provide energy for substrate transfer and assembly of the system [Alvarez-Martinez and Christie, 2009; Fronzes *et al.*, 2009; Wallden *et al.*, 2010]. After translocation, the T-DNA moves to the plant cell nucleus where it integrates into the plant genomic DNA [Atmakuri *et al.*, 2004; De Vos and Zambryski, 1989]. The known effector proteins include VirD2, VirE2, VirE3 and VirF. The ssDNA-binding protein VirE2 binds to the T-strand and thus protects it from degradation in host cells. Both VirD2 and VirE2 facilitate transport of the T-complex into the nuclei of the host. VirF and VirE3 are required for full tumor formation [Vergunst *et al.*, 2003].

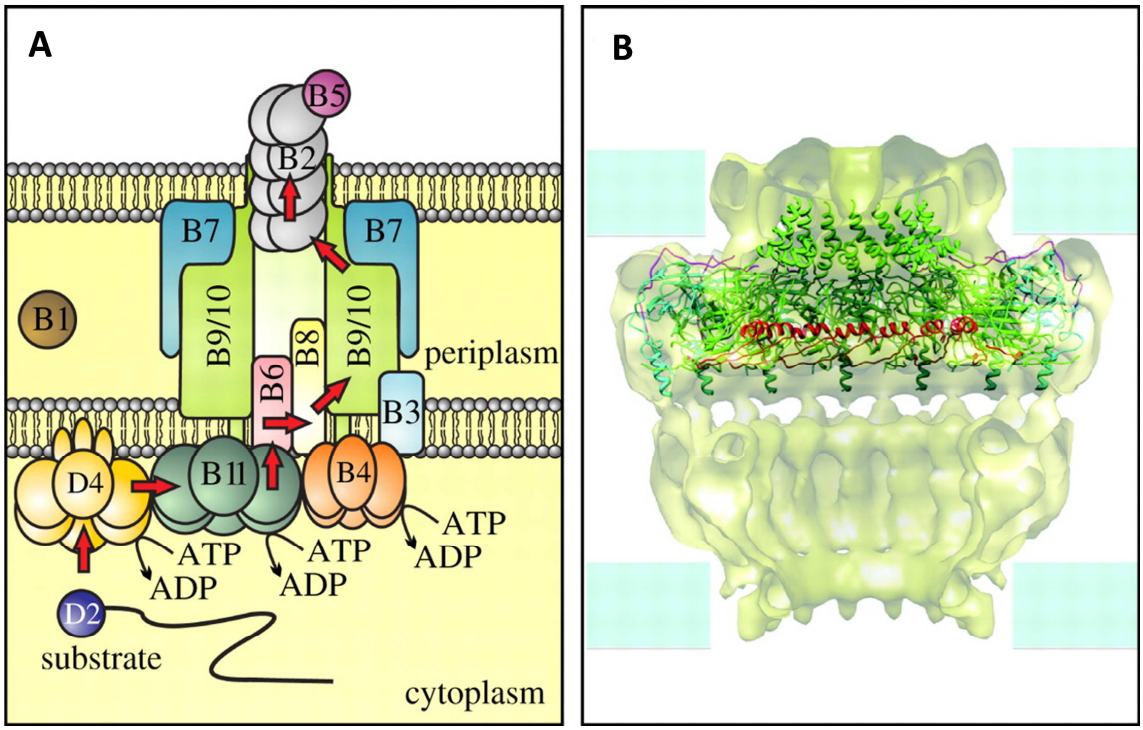

Figure 1.1. Model of the VirB/VirD4 type IV secretion system (T4SS) machinery of *Agrobaterium tumefaciens* [Zechner *et al.*, 2012]

(B) Pilus-associated extracellular components, T4SS components (pore complex and energizers), T4SS components and T4SS substrates are presented in yellow, blue, pink and green, respectively. (B) A cutout of Type IV secretion core complex structure.

1.3.3 Components of the Cag-T4SS

The complete *cag*-PAI is flanked by the same chromosomal genes and 31 bp repeats in all strains analyzed. However, the *cag*-PAI may be split into two regions originally termed cagI and cagII as a result of insertion of an IS605 sequence and an associated genome rearrangement [Akopyants *et al.*, 1998; Censini *et al.*, 1996]. However, comparative sequence analyses of *cag* islands among *H. pylori* strains suggested that this rearrangement is rare (reviewed in [Fischer, 2011]). Comparison of the complete *cag*-PAI sequences for 38 representative *H. pylori* isolates from various geographic populations showed that the content and the order of genes on the *cag*-PAI are mostly conserved [Olbermann *et al.*, 2010]. Systematic studies of 27 putative genes on the *cag*-PAI in *H. pylori* 26695 revealed that 17 genes are absolutely essential for CagA translocation into host cells and 14 genes are required for full IL-8 induction by epithelial cells [Fischer *et al.*, 2001b] (Figure 1.2).

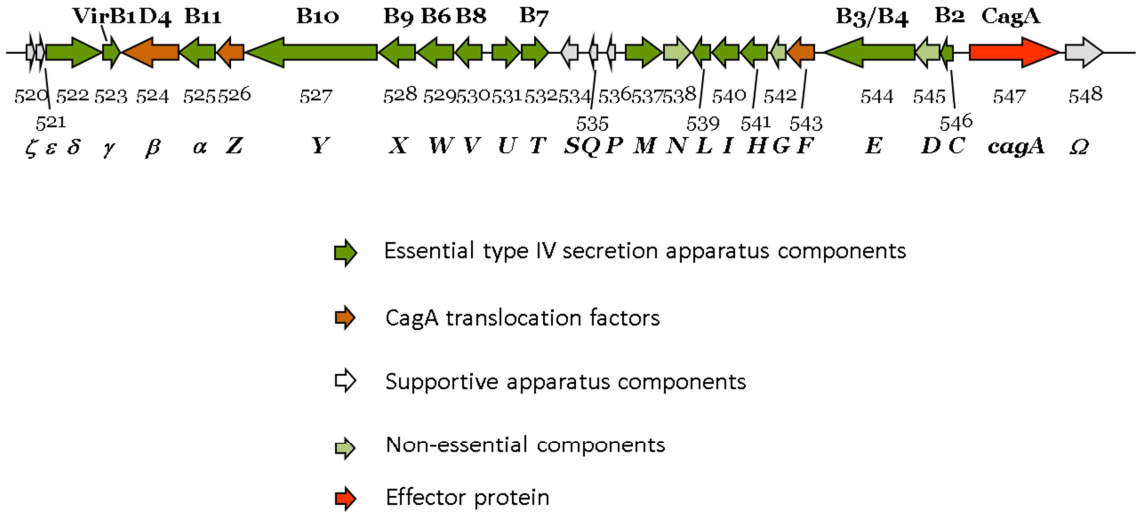

Figure 1.2. Features of CagH, CagI and CagL (Wolfgang Fischer, unpublished)

Genetic organization of the *cag* pathogenicity island in strain 26695. Gene designations and putative homologies to components of the *A. tumefaciens* T-DNA transfer system are indicated. Each gene is shown as a thick arrow with the orientation of transcription. The length and spacing of each annotated gene are shown in proportion to gene and intergenic spacing.

The Cag type IV secretion system is a multi-component transporter which is responsible for injection of CagA across the bacterial membranes into host epithelial cells [Backert and Selbach, 2008]. Although the Cag-T4SS is evolutionarily related to other T4SSs, there are only some *cag*-encoded proteins with high sequence similarities to components of other T4SSs [Francesco *et al.*, 2011]. By comparison with the prototypical T4SS VirB/VirD4 machinery in *A. tumefaciens*, clear similarities were found only for CagE (to VirB4), CagX (to VirB9), CagY (to VirB10), Cagα (to VirB11) and Cagβ (to VirD4). Moreover, three VirB-like protein components have been identified by other features, such as CagC (topological similarity to VirB2), CagL (functional analogy to VirB5), and CagT (lipoprotein like VirB7), (reviewed in [Cendron and Zanotti, 2011]. Additionally, CagW (VirB6) and CagV (VirB8) were found to be topologically comparable and to show weak sequence similarities to the respective VirB proteins as well (reviewed in [Fischer, 2011]).

Based on systematic studies of isogenic mutants in each *cag* gene, the Cag proteins can be divided into 4 groups according to their functions (reviewed in [Fischer, 2011]). An overview of characteristics and functions of *cag*-encoded proteins is shown in Table 1.1.

- **Essential secretion apparatus components**: These proteins are required for CagA translocation and IL-8 induction in AGS cells.
- **Supporting components**: These *cag* gene products are not absolutely required for Cag-T4SS functionality, but result in a reduced efficiency of both phenotypes when absent.
- **Translocation factors** include Cagβ, CagZ, CagF and possibly CagD [Cendron *et al.*, 2009]. They are necessary components for CagA translocation, but not for IL-8 induction.
- **Non-essential components**: These proteins are apparently not required for any effects on Cag-T4SS functionality. The exact function of these proteins is still unknown.

Table 1.1. Overview of characteristics and functions of *cag*-encoded proteins (modified after [Fischer, 2011])

Gene	Protein	VirB homologues	(Putative) Functions	IL-8 requirement	CagA translocation requirement
hp0520	Cagζ/Cag1				
hp0521	Cagε/Cag2				
hp0522	Cagδ/Cag3		OM complex	+	
hp0523	Cagγ/Cag4	VirB1	PG hydrolase	+	
hp0524	Cagβ/Cag5	VirD4	Coupling protein		+
hp0525	Cagα	VirB11	ATPase	+	
hp0526	CagZ		Cagβ stabilization		+
hp0527	CagY	VirB10	Core complex, integrin binding	+	
hp0528	CagX	VirB9	Core complex	+	
hp0529	CagW	VirB6	IM channel	+	
hp0530	CagV	VirB8	Core complex	+	
hp0531	CagU		Core complex, OM lipoprotein	+	
hp0532	CagT	VirB7		+	
hp0534	CagS				
hp0535	CagQ				
hp0536	CagP				
hp0537	CagM		OM complex	+	
hp0538	CagN				
hp0539	CagL	VirB5	Integrin binding		+
hp0540	CagI			+/-	+
hp0541	CagH			+	
hp0542	CagG				+
hp0543	CagF		Secretion chaperone		+
hp0544	CagE	VirB3/4	ATPase	+	
hp0545	CagD				+
hp0546	CagC	VirB2	Pilus subunit	+	
hp0547	CagB				
hp0548	CagA		Effector protein		

1.3.4 CagA translocation mechanism

The translocation process requires both N-terminal and C-terminal regions of CagA [Hohlfeld *et al.*, 2006]. As mentioned before, the N-terminal region was shown to bind to β1 integrin, and this binding plays a critical role in CagA translocation [Fischer, 2011; Jimenez-Soto *et al.*, 2009; Kaplan-Turkoz *et al.*, 2012]. Apart from this interaction, CagA was shown to bind to phosphatidylserine present in the outer leaflet of the host cell cytoplasmic membrane, which might induce its uptake into the cells (Murata-Kamiya, 2010). The C-terminal 20 amino acids were also demonstrated to be critically important for CagA translocation [Hohlfeld *et al.*, 2006]. Two functional motifs found in CagA, the EPIYA motifs, and a microtubule affinity-regulating kinase (MARK) inhibitor (MKI) motif, which is adjacent to the EPIYA motifs, are not necessary for CagA translocation [Fischer, 2011]. In the bacterial cytoplasm, CagA is recognized by several recognition factors such as CagF, CagZ and Cagβ, in which Cagβ and CagZ form a stable complex at the bacterial cytoplasmic membrane [Jurik *et al.*, 2010]. CagF acts as a chaperone-like protein which binds close to the carboxy-terminal secretion motif of CagA [Fischer, 2011]. Additionally, CagD was also found to be involved in CagA translocation. Since CagD was observed to be localized in the cytosolic fraction, in the inner membrane, as well as released into the supernatant during host cell infection, CagD was proposed to act as a multifunctional component involved in CagA translocation [Cendron *et al.*, 2009; Smith *et al.*, 2007].

The observation of CagA at the tips of the pili suggests that CagA might be delivered through these surface structures [Kwok *et al.*, 2007]. Likewise, the presence of CagA on the surface of bacteria [Murata-Kamiya *et al.*, 2010] raised the question whether pilus- or surface-associated CagA represents a translocation intermediate. However, the strong binding of CagA to integrins argues against pilus tip CagA as a translocation intermediate [Jimenez-Soto *et al.*, 2009]. The uptake process of CagA into the host cell cytoplasm is still poorly understood.

1.3.5 Architecture of the Cag Type IV secretion system

Numerous studies have shown that the Cag-T4SS forms needle-like appendages (also called T4SS pili), which are induced by cell contact at the interface between bacteria and gastric epithelial cells [Jimenez-Soto *et al.*, 2009; Johnson *et al.*, 2014; Kwok *et al.*,

2007; Shaffer *et al.*, 2011] (Figure 1.3). However, these structures were also sporadically found on the surface of bacteria in the absence of cell contact [Kumar *et al.*, 2013; Tanaka *et al.*, 2003].

Figure 1.3. Pilus formation [Rohde *et al.*, 2003]

Pili were formed at the interface between *H. pylori* and host cell when co-cultured with AGS cells analyzed by SEM.

Based on studies of function, localization and interaction of individual Cag protein components, different models of Cag-T4SS assembly which are similar to that of *A. tumefaciens* were proposed [Backert *et al.*, 2011; Fischer, 2011; Kutter *et al.*, 2008; Tegtmeyer *et al.*, 2011; Terradot and Waksman, 2011]. According to these models the *H. pylori* Cag-T4SS consists of a cytoplasmic complex, a translocation channel and an external pilus [Fischer, 2011; Tegtmeyer *et al.*, 2011; Terradot and Waksman, 2011] (Figure 1.3).

The cytoplasmic complex:

The cytoplasmic complex of the Cag apparatus is composed of three ATPases, CagE (VirB4), Cagα (VirB11) and possibly Cagβ (VirD4), all of which provide energy required for Cag apparatus assembly and/or for CagA transport [Terradot and Waksman, 2011]. Cagβ is a CagA translocation factor [Fischer, 2011] and probably acts as a coupling protein, which can bind and recruit CagA into the Cag apparatus [Jurik *et al.*, 2010; Schroder *et al.*, 2002]. The Cagα protein acts as an ATPase with an N-terminal domain and a RecA-like C-terminal domain [Fronzes *et al.*, 2009].

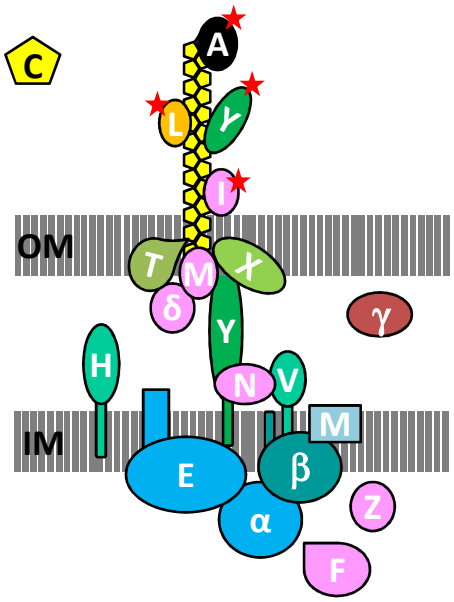

Figure 1.4. Architechture of the *H. pylori* Cag-T4SS (modified after [Terradot and Waksman, 2011])

Proteins forming the cytoplasmic complex, translocation pore and external pilus are presented in blue, green and yeallow/orange, respectively. CagA is located at the tip of the pilus. Others components, which have been shown to take part in the Cag apparatus, are shown in pink and red. OM: Outer membrane, IM: inner membrane.

The translocation pore:

In the last decade, the structures of several conserved T4SS proteins or protein fragments, either alone (VirB8, VirB9 [Terradot *et al.*, 2005]), or in complexes (VirB9:VirB7 [Bayliss *et al.*, 2007]; VirB7-VirB9-VirB10 [Chandran *et al.*, 2009; Fronzes *et al.*, 2009], VirB3-VirB10 [Low *et al.*, 2014]), have been published and provided also valuable information about the structure of the core complex of the Cag-T4SS, which spans the inner membrane and the outer membrane. In an earlier study [Busler *et al.*, 2006], the core complex was proposed to be composed of CagT (VirB7), CagV (VirB8), CagX (VirB9) and CagY (VirB10). These Cag proteins were found to interact with each other by Yeast Two Hybrid (YTH) and other protein-protein interaction studies. Apart from the interactions with each other, these four proteins also showed interactions with other Cag proteins such as Cagδ, CagM, CagI, CagG and CagF, which are not homologous to components of other T4SSs or to any known bacterial proteins [Busler *et al.*, 2006]. However, the data obtained from stabilizing effects, protein-protein interaction and localization studies strongly suggested that the

core complex consists of Cagδ, CagX, CagT and CagM at the outer membrane, and of CagY, CagV, CagW, CagU, and possibly others, at the inner membrane [Kutter *et al.*, 2008; Pinto-Santini and Salama, 2005].

The external pilus

The CagC [Akopyants *et al.*, 1998; Kalkum *et al.*, 2002; Kutter *et al.*, 2008], and CagL proteins [Kwok *et al.*, 2007] (VirB2 and VirB5-like, respectively) are considered as pilus-associated components. Additionally, pili may also contain the CagY, CagX and CagT proteins, as detected by immunogold-labelling studies [Rohde *et al.*, 2003; Tanaka *et al.*, 2003]. The surface protein CagC [Akopyants *et al.*, 1998] was proposed as a VirB2 homologue based on weak sequence similarities, however there is no direct evidence for the localization of CagC on the pili [Andrzejewska *et al.*, 2006; Rohde *et al.*, 2003]. Recently, a study to identify *cag* genes that are required for pilus formation showed that *cagT*, *cagX*, *cagV*, *cagM* or *cagδ* deletion caused a defect in pilus formation. In contrast, the *cagY* and *cagC* mutants were defective in T4SS function but not pilus formation [Johnson *et al.*, 2014], arguing against a role of CagC as a major pilin subunit.

1.3.6 The CagH, CagI and CagL proteins: Unique components of the Cag-T4SS

A systematic mutagenesis study clearly demonstrated that *cagH* and *cagL* genes are essential for translocation of CagA and IL-8 induction. In the same study, the *cagI* gene was reported to be required for CagA translocation, but not for IL-8 induction into host cells [Fischer *et al.*, 2001b]. However, two other publications reported conflicting results, showing the involvement of CagI in IL-8 secretion as well [Censini *et al.*, 1996; Selbach *et al.*, 2002].

The CagH and the CagI proteins had not been studied in detail so far. The prediction analysis of CagH and CagI showed that CagI (39 kDa) is a secretory protein as a result of a N-terminal signal sequence [Kutter *et al.*, 2008]. In contrast, CagH (41.5 kDa) is rather anchored in the inner membrane via a N-terminal hydrophobic helix. It had been suggested that CagI may not be a component of the Cag-T4SS but rather a putative effector protein [Kutter *et al.*, 2008]. Interestingly, CagI, like the CagA, CagY and CagL proteins has been shown to bind to β1 integrin by the YTH assay, suggesting a surface-exposed localization of CagI [Jimenez-Soto *et al.*, 2009]. Bacterial interaction

partners of CagI have been investigated in a YTH assay and pull-down assays, indicating that CagI might interact with CagZ and CagG. Besides, an interaction between CagI and Cagβ was observed as well, but it was rather weak [Busler *et al.*, 2006].

Unlike CagH and CagI, CagL has been studied more in detail recently. CagL (26 kDa) is a VirB5-like protein with an N-terminal, Sec-dependent signal sequence [Kutter *et al.*, 2008]. It is considered as a pilus associated component [Jimenez-Soto *et al.*, 2009; Kwok *et al.*, 2007] and a ligand binding to several integrin heterodimers, such as α5β1, αvβ5 and αvβ3 integrins, in an RGD (arginine-glycine-aspartate) motif-dependent manner [Conradi *et al.*, 2012; Jimenez-Soto *et al.*, 2009; Kwok *et al.*, 2007; Wiedemann *et al.*, 2012]. This motif, that was proposed as a common integrin binding motif [Kwok *et al.*, 2007; Takada *et al.*, 2007], is atypically located within a long alpha helix (Barden 2013). There are conflicting results concerning the importance of this RGD motif for T4SS functionality *in vitro*. In one study, the RGD motif was shown to be critical for integrin β1 binding [Kwok *et al.*, 2007]. In another study, however, the mutation of the CagL RGD motif caused no effect on Cag-T4SS functionality [Jimenez-Soto *et al.*, 2009]. Localization of CagL has been investigated using different techniques. By the total membrane fractionation method, CagL was detected in the soluble fraction [Kutter *et al.*, 2008]. Immunofluoresence staining suggested the presence of CagL on the T4SS pili [Kwok *et al.*, 2007] as well as on the surface of bacteria after cell contact [Tegtmeyer *et al.*, 2010].

1.4 Aim of this thesis

H pylori causes multiple alterations in gastric epithelial cells through processes which are dependent on the activity of the Cag-T4SS, and particularly on translocation of the only known effector CagA protein. Although much research interest worldwide focused on the CagA translocation mechanism, it remains until now unclear how the Cag-T4SS assembles to translocate CagA across the bacterial membrane, and how CagA is taken up into the host cell cytoplasm. To better understand the mechanism of action of this important virulence factor, characterization of the function of each *cag*-encoded protein, and the relationships between them during Cag-T4SS assembly and CagA translocation, is required.

The aim of this work was to focus on three essential, but unique, components of the Cag-T4SS, CagH, CagI and CagL. One major aim of this thesis was to clarify the individual importance of the CagH, CagI and CagL proteins for Cag-T4SS functionality. Another aim was to identify and characterize interaction partners of these proteins, and possibly the functional role of these interactions. Possible functional domains of these proteins for secretion system activity, or for protein interactions, were planned to be characterized. Furthermore, the localization of these proteins in *H. pylori* should be characterized in order to gain more insight into the assembly mechanism of the Cag-T4SS. Finally, the influence of a small regulatory RNA that has been identified within the *cag*-PAI, on the functionality of the T4SS was intended to be analyzed.

2 MATERIALS AND METHODS

2.1 Materials

2.1.1 Bacterial strains

2.1.1.1 *Helicobacter pylori*

Table 2.1. List of *Helicobacter pylori* (*H. pylori*) strains used in this study

Name	Genotype, Description and Reference
P12	Klinisches Isolat (888-0) der Abteilung ''Medizinische Mikrobiologie und Immunologie''der Universität Hamburg [Schmitt and Haas, 1994]
P12 strep	P12 transformed with NCTC 11637 ($strep^R$)
PT-H005 (P12Δ*cagIL*)	*cagI* and *cagL* deletion mutant (double mutant), P12 transformed with pPT2 (cat^R) [this work]
PT-H009 (P12Δ*cagIL/L*)	*cagI* and *cagL* deletion mutant complemented *cagL,* PT-H005 transformed with pWS255 (kan^R) [this work]
PT-H011 (P12Δ*cagIL/I*)	*cagI* and *cagL* deletion mutant complemented *cagI,* PT-H005 transformed with pWS322 (kan^R) [this work]
PT-H012 (P12/Δ*cagIL/IL*(pPT3))	*cagI* and *cagL* deletion mutant complemented *cagI* and *cagL,* PT-H005 transformed with pPT3 (cat^R) [this work]
PT-H014 (P12Δ*cagIL/*I_{Myc}*L*)	*cagI* and *cagL* deletion mutant complemented *cagI* and *cagL* (N-terminal Myc tagged-CagI), PT-H005 transformed with pPT4 (cat^R) [this work]
PT-H023 (P12*cagP*$_{M45}$)	*cagP* replaced by C-terminal M45 tagged-CagP, P12 transformed with pPT7 (cat^R) [this work]
PT-H030 (P12/Δ*cagP/cagP*$_{M45}$)	*cagP* deletion mutant complemented *cagP* (C-terminal M45 tagged-CagP), WSP543 transformed with pPT20 (kan^R) [this work]
PT-H047 (P12/Δ*cagIL/IL*(pPT9) or P12/Δ*cagIL/IL*$_{\Delta C}$)	*cagI* and *cagL* deletion mutant complemented *cagI* and *cagL* ($CagL_{\Delta C}$), PT-H005 transformed with pPT9 (kan^R) [this work]
PT-H054 (P12/Δ*cagIL/IL*(pPT10))	*cagI* and *cagL* deletion mutant complemented *cagI* and *cagL* ($CagL_{\Delta C+CC}$), PT-H005 transformed with pPT10 (kan^R) [this work]
PT-H058 (P12Δ*cagIL/*$I_{\Delta C}$*L*(pPT11))	*cagI* and *cagL* deletion mutant complemented *cagI* and *cagL* ($CagI_{\Delta C}$), PT-H005 transformed with pPT11 (kan^R) [this work]
PT-H061 (P12Δ*cagIL/*$I_{\Delta C}$*L*(pPT12))	*cagI* and *cagL* deletion mutant complemented *cagI* and *cagL* ($CagI_{\Delta C+CC}$), PT-H005 transformed with pPT12 (kan^R) [this work]
PT-H084 (P12Δ*cagIL/*$I_{\Delta C}$*L*(pPT13))	*cagI* and *cagL* deletion mutant complemented *cagI* and *cagL* (C-terminus deletion CagI), PT-H005 transformed with pPT13 (kan^R)

	[this work]
PT-H093 (P12Δ*cagH/H*)	*cagH* deletion mutant complemented *cagH,* WSP696 transformed with gene bank plasmid HP2kb05G17 (erm^S, $strep^R$) (*in cis*) [this work]
PT-H095 (P12Δ*cagIL/IL*$_{C128S}$)	*cagI* and *cagL* deletion mutant complemented *cagI* and *cagL* (CagL $_{C128S}$), PT-H005 transformed with pPT24 (kan^R) [this work]
PT-H109 (P12Δ*cagIL/IL*$_{D132A}$)	*cagI* and *cagL* deletion mutant complemented *cagI* and *cagL* (CagL $_{D132A}$), PT-H005 transformed with pPT25 (kan^R) [this work]
PT-H101 (P12Δ*cagH/H*$_{D265A}$)	*cagH* deletion mutant complemented *cagH* (CagH$_{D265A}$), WSP696 transformed with pPT28 (erm^S, $strep^R$) [this work]
PT-H099 (P12Δ*cagH/H*$_{C265S}$)	*cagH* deletion mutant complemented *cagH* (CagH$_{C265S}$), WSP696 transformed with pPT29 (erm^S, $strep^R$) [this work]
PT-H110 (P12Δ*cagIL/IL*$_{\Delta CPISD}$)	*cagI* and *cagL* deletion mutant complemented *cagI* and *cagL* (CagL $_{\Delta CPISD}$), PT-H005 transformed with pPT32 (kan^R) [this work]
PT-H112 (P12Δ*cagH/H*$_{\Delta CPIGD}$)	*cagH* deletion mutant complemented *cagH* (CagH$_{\Delta CPIGD}$), WSP696 transformed with pPT33 (erm^S, $strep^R$) [this work]
WSP128 (P12ΔPAI)	*cag*-PAI deletion mutant, P12 transformed with pJP46 (kan^R) (Wolfgang Fischer) [Fischer *et al.*, 2001b]
WSP498 (P12Δ*cagL*)	*cagL* deletion mutant, P12 transformed with pWS290 (cat^R) (Wolfgang Fischer) [this work]
WSP500 (P12/Δ*cagL/L*)	*cagL* deletion mutant complemented *cagL,* WSP498 transformed with pWS255 (kan^R) (Wolfgang Fischer) [Jimenez-Soto *et al.*, 2009]
WSP543 (P12Δ*cagP*)	*cagP* deletion mutant, P12 transformed with pWS316 (cat^R) (Wolfgang Fischer) [this work]
WSP597 (P12Δ*cagI/I*(320))	5' *cagI* deletion mutant, P12 $Strep^R$ transformed with pWS320 (erm^R) (Wolfgang Fischer) [this work]
WSP629 (P12Δ*cagI* (320/326))	5' *cagI* deletion mutant, marker-free, WS597 transformed with pWS326 ($strep^R$) (Wolfgang Fischer) [this work]
WSP639 (P12Δ*cagI/I*(320//322))	5' *cagI* deletion mutant (marker-free) complemented *cagI,* WS629 transformed with pWS322 (kan^R) (Wolfgang Fischer) [this work]
WSP644 (P12P12Δ*cagI/I*(320/326/322))	5' *cagI* deletion mutant complemented *cagI,* WS597 transformed with pWS322 (kan^R) (Wolfgang Fischer) [this work]
WSP645 (P12Δ*cagI/I*(320/327))	*cagI* deletion mutant, marker-free, WS597 transformed with pWS327 (kan^R) (Wolfgang Fischer) [this work]

WSP692 (P12ΔsRNA)	sRNA deletion mutant, P12 transformed with pWS426 (cat^R) (Wolfgang Fischer) [this work]
WSP696 (P12Δ*cagH*)	*cagH* deletion mutant, P12 $Strep^R$ transformed with pWS423 (erm^R) (Wolfgang Fischer) [this work]
WSP717 (P12Δ*cagP*+sRNA)	*cagP* and sRNA deletion mutant, P12 transformed with pWS433 (cat^R) (Wolfgang Fischer) [this work]
WSP736 (P12Δ*cagP/P*+sRNA)	*cagP* mutant complemented *cagP* and sRNA, WSP543 transformed with pWS338 (kan^R) (Wolfgang Fischer) [this work]
WSP912 (P12Δ*cagH/H* (pWS534))	*cagH* mutant complemented *cagH* WSP696 transformed with pWS534 (*in trans*) (Wolfgang Fischer) [this work]

C: C-terminal motif coding DNA sequence

CC: coiled-coil structure coding DNA sequence

2.1.1.2 *Escherichia coli*

Table 2.2. List of *Escherichia coli* (*E. coli*) strains used in this study

Name	Genotype and Reference
TOP10	F-*mcr*A Δ(*mrr-hsd*RMS-*mcr*BC) Φ80*lac*ZΔM15 Δ*lac*O74 *rec*A1 *ara*Δ139 Δ(*ara-leu*)7697 *gal*U *gal*K *rps*L (StrR) *end*A1 *nup*G (Invitrogen, Karlsruhe)
DH5α	F-Φ80d *lac*Z Δ*M15* Δ(*lac*ZYA-*arg*F) U169 *deo*R *rec*A1 *end*A1 *hsd*R17 (*rK*-, *mK*+) *pho*A *sup*E44 λ- *thi-l gyr* A96 *rel*A1 (Invitrogen, Karlsruhe)
BL21(DE3)	Genotype: F-, ompT, hsdS($_{r^-B}$, $_{m^-B}$), gal, dcm, _DE3 (lacI, lacUV5-T7 gene 1, ind1, sam7, nin5) This *E. coli* strain was used for the overexpression of the GST- and MBP- fusion proteins

2.1.3 Broth and culture media

Table 2.3. List of broth and culture media used in this study

Culture media and nutrients	Production and Source
LB liquid medium	20 g/l Lennox medium (Gibco/Invitrogen, Carlsbad, USA), autoclaved
LB-plates	32 g/l Lennox-L-Agar (Gibco/Invitrogen, Carlsbad, USA), autoclaved
SOC Medium	20 g/l tryptone, 5 g/l yeast extract, 10 mM NaCl, 2.5 mM KCl, 10 mM MgCl2, 10 mM MgSO4, 20 mM glucose (Invitrogen, Carlsbad, USA), autoclaved
Brucella-Broth (BB)	28 g/l Brucella Broth (Falcon BD, Franklin Lakes, USA), autoclaved
Serum plates	36 g/l GC-Agar-Base (Oxoid, Darmstadt, Germany), autoclaved and subsequently added 10 ml/l Vitamin-Mix, 80 ml/l Horse serum, 5 mg/l Trimethoprin, 1 mg/l Nystatin
Cholesterol plates	36 g/l GC-Agar-Base (Oxoid, Darmstadt, Germany), autoclaved and subsequently added 0,4% cholesterol, 10mg/l Vitamin-Mix, 5 mg/l Trimethoprin, 1 mg/l Nystatin
Vitamin mix	100 g/l α-D-Glucose, 10 g/l L-Glutamin, 26 g/l L-Cystein, 0.1 g/l Cocarboxylase, 20 mg/l Fe(III)-Nitrate, 333 mg/l Thiamine, 13 mg/l p-aminobenzoic acid, 0.25 g/l Nicotinamidadeninindinucleotid (NAD), 10 mg/l Vitamin B12, 1.1 g/l L-Cystine, 1 g/l Adenine, 30 mg/l Guanine, 0.15 g/l L-Arginine, 0.5 g/l Uracil

2.1.4 Cell lines

AGS (Human Adenogastric carcinoma cell line (ATCC CRL-1739))

2.1.5 Inhibitors and media supplements

Table 2.4. List of inhibitors and media supplements used in this study

Media supplements	Solvents	Concentrations
Ampicillin (Amp)	Water	100 µg/ml
(Sigma-Aldrich, St. Louis, USA)		
Chloramphenicol (Cat)	Ethanol	30 µg/ml (*E. coli*)
(Merck, Darmstadt, Germany)		6 µg/ml (*H. pylori*)
Erythromycin (Erm)	Ethanol	250 µg/ml (*E. coli*)
		10 µg/ml (*H. pylori*)
Kanamycin (Kan)	Water	50 µg/ml (*E. coli*)
(Merck, Darmstadt,Germany)		8 µg/ml (*H. pylori*)
Streptomycin (Strep)	Water	250 µg/ml (*E. coli*)

(Life Technologies)		250 µg/ml (*H. pylori*)
Trimethoprim	DMF	5 µg/ ml
(Sigma-Aldrich, St. Louis, USA)	Dimethylformamid	
Nystatin (Nys)	DPBS	440 µl/l (*H. pylori*)
(Merck, Darmstadt, Germany)		
β-D-thiogalactopyranosid (IPTG)	Water	
5-Brom-4-chlor-3-	DMSO	40 µg/ml (*E. coli*)
indoxyl-β-Dgalactopyranosid (X-Gal)	Dimethylsulfoxid	

2.1.6 Plasmids

Table 2.5. List of of plasmids and vectors used in this study

Plasmid/Vector	Description and references
pPT2	pBluescript II SK (+), cat^R, *H. pylori* P12 *cagI::cat; cagN* and *cagL* flanking regions [this work] pWS290 digested with *Sal*I and *Bam*HI (*cagN*); pWS325 digested with *Eco*RV/*Bam*HI (*cat* cassette and *cagH*); and ligated to pBluescript II SK (+) (*Sal*I/*Eco*RV)
pPT3	*H. pylori* shuttle-plasmid, pWS241, kan^R, *cagA* promoter region, *H. pylori* P12 *cagI* and *cagL* [this work] Constructed by PCR from P12 genomic DNA using primers WS311 and WS304 (*cagI* and *cagL*), digested with *Spe*I and *Kpn*I; and ligated to pWS241(*Spe*I/*Kpn*I)
pPT4	*H. pylori* shuttle-plasmid, pWS241, kan^R, *cagA* promoter region, *H. pylori* P12 N-terminal *myc-cagI* and *cagL* [this work] constructed by PCR from P12 genomic DNA using primers WS311 and PT1 (*cagI* (3')), digested with *Spe*I and *Bam*HI; and primers PT2 and WS308 (*cagI* (5') and *cagL*), digested with *Kpn*I and *Bam*HI; and ligated to pWS241 (*Spe*I/*Kpn*I)
pPT6	*H. pylori* shuttle-plasmid, pWS241, kan^R, *cagA* promoter region, *H. pylori* P12 N-terminal *M45-cagI* and *cagL* [this work] Constructed by PCR from P12 genomic DNA with primers WS311 and WS552 (*cagI* (3')), digested with *Spe*I and *Bam*HI, and PT2 and WS304 (*cagI* (5') and *cagL*) (*Bam*HI/*Xho*I); and ligated to pWS241 (*Spe*I/*Sal*I)
pPT7	pSMART, cat^R , *H. pylori* P12 N-terminal M45 tagged-*cagP*; *cagQ* and *cagM* flanking regions [this work] constructed by inverse PCR from gene bank plasmid pHP2kb04P16 using primers

	WS461 and WS550, digested with *Bam*HI and *Sal*I; and ligated to *cat* cassette (*Bam*HI/*Sal*I)
pPT8	pGEX4T3, amp^R, *H. pylori* P12 *cagL* lacking DNA sequence encoding for the C-terminal motif [this work]
	constructed by PCR from P12 genomic DNA using primers WS435 and JP52 (*cagL*), digested with *BamH*I and *Xho*I; and ligated to pGEX4T (*BamH*I/*Xho*I)
pPT9	*H. pylori* shuttle-plasmid, pWS241, kan^R, *cagA* promoter region, *H. pylori* P12 *cagL* lacking DNA sequence encoding for the C-terminal motif (*Spe*I/*Xho*I) [this work].
	constructed by PCR from P12 genomic DNA using primers WS311 and WS559 (*cagI* and *cagL*), digested with *Spe*I and *Xho*I; and ligated with pWS241(*Spe*I/*Sal*I)
pPT10	*H. pylori* shuttle-plasmid, pWS241, kan^R, *cagA* promoter region, *H. pylori* P12, *cagL* lacking DNA sequence encoding for the C-terminal motif and the coiled-coil structure, and *cagI* [this work]
	constructed by PCR from P12 genomic DNA using primers WS311 and WS560 (*cagI* and *cagL*), digested with *Spe*I and *Xho*I; and ligated to pWS241(*Spe*I/*Sal*I)
pPT11	*H. pylori* shuttle-plasmid, pWS241, kan^R, *cagA* promoter region, *H. pylori* P12, *cagI* lacking DNA sequence encoding for the C-terminal motif, and *cagL* [this work]
	constructed by PCR from P12 genomic DNA using primers WS311 and WS561 (*cagI*), digested with *Spe*I and *Xho*I; and primers WS304 and WS564 (*cagL*), digested with *Kpn*I and *Xho*I; and ligated to pWS241(*Spe*I/*Kpn*I)
pPT12	*H. pylori* shuttle-plasmid, pWS241, kan^R, *cagA* promoter region, *H. pylori* P12, *cagI* lacking DNA sequence encoding for the C-terminal motif and the coiled-coil structure [this work]
	constructed by PCR from P12 genomic DNA using primers WS311 and WS562 (*cagI*), digested with *Spe*I/*Xho*I; and primers WS304 and WS564 (*cagL*), digested with *Kpn*I and *Xho*I; and ligated to pWS241(*Spe*I/*Kpn*I)
pPT13	*H. pylori* shuttle-plasmid, pWS241, kan^R, *cagA* promoter region, *H. pylori* P12, *cagI* lacking DNA sequence encoding for the C-terminal part containing *cagL* transcriptional start site, and *cagL* [this work]
	constructed by PCR from P12 genomic DNA using primers WS311 and WS563 (*cagI* and *cagL*), digested with *Spe*I and *Xho*I; and primers WS304 and WS564 (*cagI* and *cagL*), digested with *Kpn*I/*Xho*I; and ligated to pWS241(*Spe*I/*Kpn*I)
pPT14	pGEX4T3, amp^R, *H. pylori* P12 *cagI* lacking DNA sequence encoding for the C-terminal motif [this work]
	constructed by PCR from P12 genomic DNA using primers WS307 and WS561

	(*cagI*), digested with *Bam*HI and *Xho*I; and ligated to pGEX4T (*Bam*HI/*Xho*I)
pPT15	pGEX4T3 amp^R, *H. pylori* P12 *cagI* lacking DNA sequence encoding for the C-terminal motif and the coiled-coil structure and [this work]
	constructed by PCR from P12 genomic DNA using WS307 and WS562 (*cagI*), digested with *Bam*HI/*Xho*I; and ligated to pGEX4T (*Bam*HI/*Xho*I)
pPT16	pGEX4T3, amp^R, *H. pylori* P12 *cagI* lacking DNA sequence encoding for the C-terminal region containing *cagL* transcriptional start site [this work]
	Constructed by PCR from P12 genomic DNA using primers WS307 and WS563 (*cagI*), digested with *Bam*HI and *Xho*I; and ligated to pGEX4T (*Bam*HI/*Xho*I)
pPT17	pGEX4T3, amp^R, *H. pylori* P12 *cagL* lacking DNA sequence encoding for the C-terminal motif [this work]
	constructed by PCR from P12 genomic DNA using primers WS435 and WS559 (*cagL*), digested with *Bam*HI and *Xho*I; and ligated to pGEX4T (*Bam*HI/*Xho*I)
pPT18	pGEX4T3, amp^R, *H. pylori* P12 *cagL* lacking DNA sequence encoding for the C-terminal motif and coiled coil structure and (*Spe*I/*Xho*I) [this work]
	Constructed by PCR from P12 genomic DNA using primers WS435 and WS560 (*cagI*), digested with *Bam*HI and *Xho*I; and ligated to pGEX4T (*Bam*HI/*Xho*I)
pPT19	pWS311, kan^R, *H. pylori cagA* promoter, (*Xpa*I to *Kpn*I) containing *Sal*I exchanged to pWS311 (*Kpn*I to *Xpa*I) [this work]
pPT20	*H. pylori* shuttle-plasmid, pWS311, kan^R, *cagA* promoter, *H. pylori* P12 C-terminal M45 tagged-*cagP* [this work]
	Constructed by PCR from P12 genomic DNA using primers WS568 and WS550 (*cagP*), digested with *Nde*I and *Sal*I; ligated to pPT19 (*Nde*I/*Sal*I)
pPT24	*H. pylori* shuttle-plasmid, kan^R, pWS241, *cagA* promoter, *H. pylori* P12 *cagL* (C128S), and *cagI* [this work]
	Constructed by inverse PCR from pPT3 using primers WS617 and WS616; and religated
pPT25	*H. pylori* shuttle-plasmid, kan^R, pWS241, *cagA* promoter, *H. pylori* P12 *cagL* (D132A), and *cagI* [this work]
	constructed by inverse PCR from pPT3 using primers WS617 and WS615; and religated
pPT28	pSMART-hc Kan, kan^R, *H. pylori* P12 *cagH* (D265A); *cagI* and *cagG* flanking regions [this work]

	constructed by inverse PCR from gene bank plasmid pHP2kb05G17 using primers WS620 and WS619; and religated
pPT29	pSMART-hc Kan, kan^R, *H. pylori* P12 *cagH* (C261S); *cagI* and *cagG* flanking regions [this work]
	constructed by inverse PCR from gene bank plasmid pHP2kb05G17 using primers WS620 and WS618; and religated
pPT31	pSMART-hc Kan, Kan^R, *H. pylori* P12 *cagH* lacking DNA sequence encoding for the C-terminal motif; *cagI* and *cagG* flanking regions [this work]
	constructed by inverse PCR from gene bank plasmid pHP2kb05G17 using primers PT4 and PT5; and religated
pPT32	*H. pylori* shuttle-plasmid, kan^R, *cagA* promoter, *H. pylori* P12 *cagL* lacking DNA sequence encoding for CGISD, and *cagI* [this work]
	constructed by inverse PCR from pPT3 using primers WS617 and PT8, religated
pPT33	pSMART-hc Kan, kan^R, *H. pylori* P12 *cagH* lacking DNA sequence encoding for CPIGD; *cagI* and *cagG* flanking regions [this work]
	constructed by inverse PCR from gene bank plasmid pHP2kb05G17 using primers WS620 and PT9; and religated
pWS241	*H. pylori* shuttle-plasmid, kan^R, *cagA* promoter, *H. pylori* P12 *cagA* (Wolfgang Fischer) [Hohlfeld *et al.*, 2006]
pWS255	*H. pylori* shuttle-plasmid, kan^R, *cagA* promoter, *H. pylori* 26695 *cagL* (Wolfgang Fischer) [Jimenez-Soto *et al.*, 2009]
pWS290	pBluescript II SK(+), cat^R; *H. pylori* P12 *cagL*::*cat*; *cagI* and *cagH* flanking regions [Jimenez-Soto *et al.*, 2009]
pWS311	*H. pylori* shuttle-plasmid, kan^R, *cagA* promoter, *H. pylori* P12 *cagA* (Wolfgang Fischer)
pWS316	pSMART-hc Kan; kan^R*;H. pylori* P12 *cagP::cat* with *cagQ* and *cagM* flanking regions (Wolfgang Fischer) [this work]
	constructed by inverse PCR from gene bank plasmid pHP2kb04P16 using primers WS406 and WS407; ligated with *Bam*HI/*Sal*I; and ligated to *cat* cassette (*Bam*HI/*Sal*I)
pWS320	pSMART-hc Kan; kan^R; erm^R*; H. pylori* P12 *cagI(5')::rpsl-erm* with *cagI(3')* and *cagH* flanking regions (Wolfgang Fischer) [this work]
	constructed by inverse PCR from gene bank plasmid pHP2kb05N02 using primers WS418 and WS419, ligated with *Bam*HI/*Sal*I; and ligated to *rpsL-erm* gene cassette

	(*Bam*HI/*Sal*I)
pWS322	*H. pylori* shuttle-plasmid, kan^R, *cagA* promoter, *H. pylori* P12 *cagI* (Wolfgang Fischer) [this work]
	constructed PCR from P12 genomic DNA using primers WS311 and WS308, digested with *Spe*I and *Xho*I; and ligated to pWS241 (*Spe*I/*Sal*I)
pWS325	pSMART-hc Kan, cat^R, *H. pylori* P12 *cagI::cat*, *cagI(3')* and *cagH* flanking regions (Wolfgang Fischer) [this work]
	constructed by inverse PCR from gene bank plasmid pHP2kb05N02 using primers WS418 and WS419, digested with *Bam*HI and *Sal*I, and ligated to *cat* gene cassette (*Bam*HI/*Sal*I)
pWS326	pSMART-hc Kan, kan^R, erm^R, *H. pylori* P12 *cagI::rpsL-erm*, *cagI(3')* and *cagH* flanking regions (Wolfgang Fischer) [this work]
	constructed by inverse PCR from gene bank plasmid pHP2kb05N02 using primers WS418 and WS419, digested with *Sal*I, and religated
pWS327	pSMART-hc Kan; kan^R; erm^R; *H. pylori* P12Δ*cagI* marker-free, *cagL* and *cagH* flanking regions (Wolfgang Fischer) [this work]
	constructed by inverse PCR from gene bank plasmid pHP2kb05N02 using primers WS420 and WS421; and blunt-end religated
pWS337	*H. pylori* shuttle-plasmid, kan^R, *cagA* promoter, *H. pylori* P12 *cagP* (Wolfgang Fischer) [this work]
	Constructed by PCR from P12 genomic DNA using primers WS371 and WS439 (*cagP*), digested with *Kpn*I and *Spe*I; and ligated to pWS241 (*Kpn*I /*Spe*I)
pWS338	*H. pylori* shuttle-plasmid, kan^R, *cagA* promoter, *H. pylori* P12 *cagP* [this work]
	Constructed by PCR from P12 genomic DNA using primers WS371 and hp537r (*cagP* and sRNA), digested with *Kpn*I and *Nde*I; and ligated to pWS311 (*Kpn*I/*Nde*I)
pWS423	pSMART-hc Kan; erm^R; *H. pylori* P12Δ*cagI* marker-free, *cagI* and *cagG* flanking regions (Wolfgang Fischer) [this work]
pWS426	pBluescript II SK(+), cat^R, *H. pylori* P12 *sRNA::cat* (Wolfgang Fischer) [this work]
	constructed by PCR from P12 genomic DNA using primers RB19 and WS439 (*cagQ, cagP* flanking regions), digested with *Xho*I and *Spe*I; and primers WS438 and WS155 (*cagM* flanking region), digested with *Sal*I and *Bam*HI; ligated to *cat* cassette (*Bam*HI/*Sal*I) and pBluescript II SK(+) (*Bam*HI/*Spe*I)
pWS433	pBluescript II SK(+), cat^R, *H. pylori* P12 *cagP+sRNA::cat*, *cagQ* and *cagM* flanking

	regions (Wolfgang Fischer) [this work]
	constructed by PCR from P12 genomic DNA using primers WS524 and WS461 (*cagP* and sRNA) digested with *Kpn*I and *BamH*I; and ligated to pWS426 (*Bam*I/*Kpn*I)
pWS534	Plasmid, kan^R, *alpA* promoter, *H. pylori* P12 *cagH* (Wolfgang Fischer) [this work]
	Constructed by PCR from P12 genomic DNA using primers WS638 and WS198 (*cagH*); digested with *Nde*I and *Not*I, digested with pLH2 (*Nde*I/*Not*I)
pHP2kb05G17	pSMART-hc Kan, kan^R, *cagG*, *cagH, cagI*
pHP2kb04P16	pSMART-hc Kan, kan^R, containing *cagM, cagP* and *cagQ*
pHP2kb05N02	pSMART-hc Kan, kan^R, containing *cagH, cagI* and *cagL*
pBluescript® II SK(+)	Cloning vector
pMal (g)	Expression MBP fusion protein, amp^R
pMal-*cagH*	pMal(g), amp^R, *H. pylori* P12 *cagH* (Wolfgang Fischer)
pGEX4T3	Expression GST fusion protein, amp^R

2.1.7 Oligonucleotides

Table 2.6. List of oligomucleotides used in this study

Oligo	Sequence (5'-3')	Description
PT1	GC **GGA TCC** CAG ATC CTC TTC TGA GAT GAG TTT TTG TTC AGA ACC AGC TTT TAA TTC GGC TTG AGC	Sense primer containing *Bam*HI for introducing epitope-Myc tagged-CagI
PT2	GC **GGA TCC** ATA GAA GCT CAA TCT AAT GCC AAA G	Antisense primer containing *Bam*HI for *cagI* amplification
PT4	G ATC **GGATCC** AAA CGA CCG ATT AGC AAA TT	Sense primer containing *Bam*HI for *cagI* amplification
PT5	GG **GGA TCC** AAG ATC ATT GTC AAA TGA TTT TCT	Sense primer containing *Bam*HI for *cagI* amplification
PT6	G GAA AGA GAT ATG AAA TGT TTT TTA AGC ATA TTT TC	Antisense primer for *cagH* mutagenesis ($CagH_{\Delta C}$)
PT7	TCA TTG CAC CCT TTC TGT TAA GTA GCT	Sense primer for *cagH*

	ATC	mutagenesis ($CagH_{\Delta C}$)
PT8	TTG CTG TTC AGC AGT CTT TTG G	Sense primer for *cagL* mutagenesis ($CagL_{\Delta CPISD}$)
PT9	AAA GTT CTT GCC GTT TAT TGC TAT GC	Antisense primer for *cagH* mutagenesis ($CagH_{\Delta CPIGD}$)
WS155	CG **GGA TCC** GAC TAT TCA AAG GGA TTA TTC	Antisense primer containing *Bam*HI for *sRNA* deletion
WS158	CCA TCG ATG GTA AAA ATG TGA ATC GT	*cagA* promoter for sequencing
WS198	A CCG **CTC GAG** CTT TAA GAA GGA GAT ATA CAT ATG GCA GGT ACA CAA GCT A	Antisense primer containing *Xho*I for *cagH* amplification
WS268	GCG ATA TCT TCT ATA TAA GC	Kanamycin resistance cassette for sequencing
WS303	GG**ACT AGT** TCT AAA GTT ATT GTC AAA TG	Antisense primer containing *Spe*I for *cagL* amplification
WS304	GG **GGT ACC** TCA TTT AAC AAT GAT CTT AC	Sense primer containing *Kpn*I for *cagL* amplification
WS307	TA **GGA TCC** CCG GTA ATA ACG CTT GAA CCC G	Antisense primer containing *Bam*HI for *cagI* amplification
WS308	ACC **GCT CGA** GTC ATT TGA CAA TAA CTT TAG	Sense primer containing *Xho*I for *cagI* amplification
WS311	GG **ACT AGT** GAA GTG AGG AAA GAG ATG TG	Antisense primer containing *Spe*I for *cagI* amplification
WS313	GG **ACT AGT** GAA TAA AGG AGT CAA AAA TAT G	Antisense primer containing *Spe*I for *cagG* amplification
WS371	CG **GGT ACC** TCA TAA GAA CCA ATT TTG CC	Antisense primer containing *Kpn*I for *cagP* amplification
WS406	GC **GGA TCC** CAA AAT TGG TTC TTA TGA TTC	Antisense primer containing *Bam*HI for *cagP* deletion
WS407	A CGC **GTC GAC** AAT CGG TCG TTT CAT TTT GG	Sense primer containing *Sal*I for *cagP* deletion,
WS418	A CCG **GTC GAC** TAA AAA ACA T TT CAT ATC TC	Sense primer containing *Sal*I for *cagI* deletion, phosphorylated
WS419	A CCG **GTC GAC** **GGA TCC** GAC AAC GCT CAA TAC ATC G	Antisense primer containing *Sal*I, *Bam*HI for *cagI* deletion, phosphorylated
WS420	CAT ATC TCT TTC CTC ACT TC	Sense primer for *cagI*

		deletion, phosphorylated
WS421	AAA ACA CTC GTG AAA AAT ACC	Antisense primer for *cagI* deletion, phosphorylated
WS435	CG **GGA TCC** GAA GAT ATA ACA AGC GGC TTA AAG	Antisense primer containing *Bam*HI for *cagL* truncation
WS438	A CCG **GTC GAC** GTT TCT ATC CAA AAA ACA CAG G	Sense primer containing *Sal*I for *sRNA* deletion
WS439	GC **GGA TCC** A AGT AGG GTA TCT TGG	Antisense primer containing *Bam*HI for sRNA amplification
WS461	GC **GGA TCC** TTC GTC CAA AAA TTT CTC AAG AC	Antisense primer containing *Bam*HI for *cagQ* amplification
WS524	GC **GGT ACC** TAG AGT CTT ACT TGA GAG AC	Sense primer containing *KpnI* for *cagQ* amplification
WS550	A CGC **GTC GAC** TTA TAA GAT CCT GGT TTC TGT TTC AAA AGG CGG CAA ACG ATC CCT GCT CCT GTC TAA GAA CCA ATT TTG CCA TTG	Sense primer containing *Sal*I for introducing M45 tagged-CagP
WS552	GC**GGA TCC** TAA GAT CCT GGT TTC TGT TTC AAA AGG CGG CAA ACG ATC CCT GCT CCT GTC AGC TTT TAA TTC GGC TTG AGC	Sense primer containing *Bam*HI for M45 tagged-CagI
WS559	A CCG **CTC GAG** TTA CCT TTC TTG TAA GTA TTG TCG	Sense primer containing *Xho*I for *cagL* truncation
WS560	A CCG **CTC GAG** TTA ATT CTT TAG GCT TTC TAC AAG	Sense primer containing *Xho*I for *cagL* truncation
WS561	A CCG **CTC GAG** TTA AGC AAT GTT TCT TGC TGT CG	Sense primer containing *Xho*I for *cagI* truncation ($CagI_{\Delta C}$)
WS562	A CCG **CTC GAG** TTA TAA GGT TTT GAT TTC TCC ATT G	Sense primer containing *Xho*I for *cagI* truncation ($CagI_{\Delta C+CC}$)
WS563	A CCG **CTC GAG** TTA TTG GGT ATT AAT TTT TTG TTT TTC	Sense primer containing *Xho*I for 3' *cagI* truncation
WS564	A CCG **CTCGAG** ACA GCA AGA AAC ATT GCT AGC TC	Antisense primer containing *Xho*I for *cagL* amplification
WS568	ACG CTA **CAT ATG** AAA CGA CCG ATT AGC	Antisense primer containing *Nde*I for introducing *cagP* amplification
WS615	ATC GGA TAT TCC GGA TTG CTG TTC	Sense primer for *cagL*

		mutagenesis ($CagL_{C128S}$)
WS616	AGC GGA TAT TCC GCA TTG CTG TTC	Sense primer for *cagL* mutagenesis ($CagL_{D132A}$)
WS617	AAT TTT AGT TCT TTA TTG TGA GGG GAA G	Antisense primer for *cagL* mutagenesis (general primer, phosphorylated)
WS618	TGC CCT ATT GGG GCC AAA GTT CTT G	Antisense primer for *cagH* mutagenesis ($CagH_{D265A}$)
WS619	TCC CCT ATT GGG GAC AAA GTT CTT G	Antisense primer for *cagH* mutagenesis ($CagH_{C261S}$)
WS620	TGC AGG AGT GGT CAT AGG ATT AGT G	Sense primer for *cagH* mutagenesis (general primer, phosphorylated)
WS638	A TG **CGG CCG** CTC ACT TCA CGA TTA TTT TAG TTT G	Sense primer containing *Not*I for *cagH*
JP52	A CCG **CTC GAG** TAA AAT TGT GCTTT TTT G	Sense primer containing *Xho*I for *cagL*
HP537r	A CGT **CTC GAG** GAT TTT TGC AAG CAT CTT A	Antisense primer containing *Xho*I for *cagM*
RB19	CCG **CTC GAG** CTA GAG TCT TAC TTG AGA	Sense primer containing *Xho*I for *cagQ*
UB023	AGC GCT CAT AGT TGC AAG CT	Antisense primer for *cagI* qPCR
UB024	GCT CAA TCT AAT GCC AAA GAA AAA GC	Sense primer for *cagI* qPCR
UB044	GAA AAC ACT CGT GAA AAA TAC CAT ATC T	Antisense primer for *cagL* qPCR
UB045	GAC GGT GAG CTG GTG ATA TGG	Sense primer for *cagL* qPCR

Restriction sites are underlined.

2.1.9 Antibodies

Table 2.7. List of antibodies used in this study

Antibodies	Description
Primary antibodies	
α-CagA (AK257)	Polyclonal antibody against the C-terminal part of CagA from *H. pylori* 185-144 (Rabbit) (1:5000) [Odenbreit *et al.*, 2000]
α-CagI (AK250)	Polyclonal antibody against the C-terminal part (peptide 327-345) of CagA from *H. pypori* (Rabbit) (1:1000) [this work]
α-CagH (AK294)	Polyclonal antibody against the MBP fusion protein (Rabbit) (Firma Gramsch) (1:1000) [this work]
α-CagL (AK271)	Polyclonal antibody against the *H. pylori* CagL protein (Rabbit) (1:1000) [Jimenez-Soto *et al.*, 2009]
α-CagX (AK290)	Polyclonal antibody against the *H. pylori* CagX protein (Rabbit) (1:2000)
α-RecA (AK263)	Polyclonal antibody against CagL protein from *H. pylori* (Rabbit) (1:1000) [Fischer and Haas, 2004]
α-AlpB (AK262)	Polyclonal antibody against the *H. pylori* AlpB fusion protein (Rabbit) (1:2000) [Odenbreit *et al.*, 2009]
α-P-Tyr (4G10)	Monoclonal antibody against the Tyrosine phosphorylated protein (Mouse) (Millipore, Schwalbach, Germany) (1:10000)
α-Myc tag	Monoclonal antibody against the Myc protein (Mouse) (Cell signaling Technology, USA) (1:1000)
α-His tag	Monoclonal antibody against the Myc protein (Mouse) (1:10000) (Antibodies online, USA)
α-GST	Monoclonal antibody against the Glutathion-S-Transferase GST protein (Mouse) (1:10000) (GenScript, USA)
α-MBP	Monoclonal antibody against the MBP protein (Mouse) (1:1000) (Sigma-Aldrich, St. Louis, USA)
Secondary antibodies	
α-Mouse IgG POX	Horseradish peroxidase-conjugated polyclonal antibody against mouse IgG (Goat) (1:10000) (Dianova, Sigma-Aldrich, St. Louis, USA)
α-Rabbit IgG POX	Horseradish peroxidase-conjugated polyclonal antibody against rabbit IgG (Goat) (1:10000) (Dianova, Sigma-Aldrich, St. Louis, USA)
α-Mouse IgG AP	Alkaline phosphatase-conjugated monoclonal against mouse IgG (Goat) (1:2000) (Dianova, Sigma-Aldrich, St. Louis, USA)
Protein A AP	Alkaline Phosphatase (AP) coupled to protein A (1:5000) (Sigma-Aldrich, St. Louis, USA)

2.1.10 Proteins and enzymes

Table 2.8. List of proteins and enzymes used in this study

Protein/Enzyme	Company
Fetal calf serum (FCS)	PAA, Pasching, Austria
Horse serum	Carlsbad, USA
Bovine serum albumin (BSA)	Sigma-Aldrich, St. Louis, USA
Takara-Ex Taq-Polymerase	TaKaRa Bio Inc., Otsu, Japan
Takara-LA Taq-Polymerase	TaKaRa Bio Inc., Otsu, Japan
PowerScript DNA Polymerase	Biotech, Germany
Phusion High-Fidelity DNA polymerase	Thermo Scientific, USA
Proteinase K	Roche, Germany
Lysozyme	Roche Grenzach-Wyhlen, Germany
T4 DNA ligase	Thermo Scientific, USA
Restriction enzymes	Roche, Grenzach-Wyhlen and NEB, Germany
	Fermentas, Germany
RNA free DNAse	Thermo Scientific, USA
Purified CagI and CagL	Terradot's lab, Baltimore, USA
Purified α5β1 (closed and open forms)	Lea Hostel

2.1.11 Standard buffers

SDS sample buffer (2X): 100 mM Tris-HCl pH 6.8, 4% (w/v) SDS, 20% (v/v) glycerol, 10% (v/v) β-mercaptoethanol, 0.2% (w/v) bromphenol blue

PBS: 27 mM KCl, 1.38 M NaCl, 15 mM KH_2PO_4, 80 mM Na_2HPO_4

TBS: 150 mM NaCl, 20 mM Tris-HCl, pH 7.5

An asterisk (*) denotes the addition of protease inhibitors into a buffer at the following concentrations: 1mM PMSF, 1 mM Sodium vanadate, 1 µM Leupeptin, 1 µM Pepstatin.

2.1.12 Consumables and Equipment

2.1.12.1 Consumables

X-Ray film (Fuji Film, Dussendorf, Germany), Dialysis membranes for small volumes (Pierce), PVDF membrane (Bio-Rad, Hercules, USA), BD Falcon 15 and 50 ml (BD Biosciences, Flanklin Lakes, USA), 0.2 µm- Sterilefilters (Millipore, Schwalbach, Germany), ELISA Maxisorp plates (Nunc), Cell scrappers (Falcon), FACS tubes (Becton Dickinson), Freezing Tubes 2 ml (Nalgene), Protein G agarose (Roche

Diagnostic, Germany), Double-distilled water (Roth, Germany), Amylose resin (Biolabs, Germany), Glutathione sepharose 4B (GE Healthcare, Sweden), Cholesterol (Gibco, Invitrogen).

2.1.12.2 Equipment

Voltage Units PowerPac 300 (BioRad, Hercules, USA), PAGE-Mini Gel System Mini-Protean IIITM (BioRad, Hercules, USA), Agarose Gel Electrophoresis chamber (BioRad, Hercules, USA), Anaerobic Incubator MI122C (Scholzen, Wittenbach, CH), Centrifuge Biofuge 15 R and Megafuge 3.0R (Heraeus, Hanau, Germany), Ultra-centrifuge Optima^{TM} TL (Beckman Coulter Inc., Fullerton, USA), Cell Disruptor; 450 Sonifier Analog (G. Heiermann, Germany), French press SIM AMINCO Spectronic (New York), Vacuum-centrifuge Savant SpeedVac DNA 110 (GMI, Ramsey, USA), Wettern blot-Apparature semi-dry (Biotech Fischer, Reiskirchen, Germany), Gel-documentation system Quantity One 4.4.0 (BioRad, Hercules, USA), FACS-Canto II (BD Biosciences, Germany), Fridge (Liebherr, Biberach a.d. Riss, Germany), ABI Prism 7000 Real-Time PCR (ABI, USA), Gene Pulser TM Electroporation (BioRad, Hercules, USA), Magnetic Stirrer MR 3001 (Heidolph, Schwabach, Germany), Scale (Biotech Fischer, Reiskirchen, Germany), Microwave (AEG, Nürnberg, Germany), Water bath 1012 (GFL, Burwedel, Germany), Eppendorf Thermomixer® comfort (Eppendorf, Hamburg, Germany).

2.1.13 Molecular markers

Figure 2.1. List of molecular markers used in this study

Molecular marker	Company
DNA- Gel electrophoresis	GeneRulerTM 1 kb DNA Ladder (MBI Fermentas, St. Leon-Roth, Germany)
Protein Electrophoresis	Prestained Protein Molecular Weight Marker, 26612 (MBI Fermentas, St. Leon-Roth, Germany)

2.1.14 Commercial Kits

Table 2.9. List commercial kits used in this study

Kit	Company
illustra GFX PCR DNA and Gel Band Purification Kit	GE-Healthcare, Buckinghamshire, UK
QIAprep Spin Miniprep KitTM	Qiagen, Hilden, Germany
QIAamp DNA Mini KitTM	Qiagen, Hilden, Germany
TOPO-TA-CloningTM-Kits with pCR2.1-TOPOVector	Invitrogen, Carlsbad, USA
Alexa Fluor 647 Monoclonal Antibody Labeling Kit	Invitrogen, Carlsbad, USA
Wizard® Plus SV Minipreps DNA Purification System	Promega, Madison, USA
RevertAid First Strand cDNA Synthesis Kit	Thermo Scientific, Germany
Power SYBR® Green PCR Master Mix	Life Technology, USA

2.2 Methods

2.2.1 Microbiological methods

2.2.1.1 Cultivation and freezing of *E. coli*

E. coli strains were incubated and cultured either on LB agar plates or in liquid LB medium at 200 rpm in a shaking incubator at 37°C for normal growth with the corresponding antibiotics for selection.

The cultivation of *E. coli* strains for protein expression was done by growing bacteria at 37°C in the shaker at 200 rpm till the OD_{600} reached 0,4 and inducing with IPTG 1mM at 27°C for 3-4 h with appropriate antibiotics.

E. coli strains were stored by suspending bacteria from LB agar plates in the liquid LB medium supplemented with 20% glycerol, and frozen at -70°C in cryogenic tubes.

2.2.1.2 Cultivation and freezing of *H. pylori*

H. pylori strains were cultivated on supplemented GC agar plates (section 2.1.2) at 37°C under microaerobic conditions (5% O_2, 10% CO_2, 85% N_2) for 2-3 days from glycerol stock and 24 h before being recultured. For liquid culture, bacteria from GC agar plates were inoculated with an OD_{550} of 0.2 in a small BB medium (Oxoid, TFS) supplemented with 0.4% glycerol (Gibco) and agitated at 90 rpm for 24 h and transferred to the main culture with an OD_{550} of 0.05 for 24 h.

H. pylori strains were stored by suspending bacteria from GC agar plates in the liquid BB medium supplemented with 10% FCS, 20% Glycerol, and frozen at -70°C in cryogenic tubes.

2.2.1.3 Determination of optical density

Bacteria from agar plate were suspended in a desired medium or PBS. The suspension was then diluted to a appropriate dilution in plastic cuvettes. The optical density (OD) of bacteria was measured by spectrophotometer at a wavelength of λ550 (OD_{550}) for *H. pylori* and λ600 (OD_{600}) for *E. coli* against a respective blank.

2.2.1.4 Preparation of chemically competent *E. coli* cells

E. coli chemically competent cells were produced by the rubidium method. Briefly, an overnight liquid culture of *E. coli* was inoculated in 100 ml of LB medium and grown until it reached an OD_{550} of 0.5 to 0.6 at 37°C in a shaking incubator (180 rpm). The cultivated culture was chilled on ice for 30 min and centrifuged at 4000 rpm for 15 min at 4°C. The cell pellet was suspended in 40 ml of TFBI buffer. After 5 min incubation on ice, cells were centrifuged and followed by suspending in 4 ml of TFBII buffer. Competent cells were then aliquoted into 50 µl and frozen in liquid nitrogen. The cells were further stored at -70°C.

TFBI buffer: 30 mM potassium acetate CH_3COOH, 100 mM RbCl, 10 mM $CaCl_2$, 50 mM $MnCl_2$, 15% (v/v) glycerol, pH 5.2 adjusted with 0.2 M CH_3COOH, sterilized.

TFBII buffer: 10 mM MOPS, 75 mM $CaCl_2$, 10 mM RbCl, 15% (v/v) glycerol, pH 6.5 with KOH, sterilized.

2.2.1.5 Transformation of chemically competent *E. coli* cells

An aliquot of *E. coli* competent cells was thawed on ice for 30 min before adding DNA samples (500 mg of ligation and 5-10 mg of plasmid) and followed by 30 min on ice incubation. Heat shock was done by immersion in a pre-heated water bath at 42ºC for 60 seconds. After adding LB medium (1 ml), the cells were incubated in a 37°C shaking incubator at 200 rpm for 1 h and plated on appropriate antibiotic selective LB agar plates for overnight at 37°C.

2.2.1.6 Natural transformation into *H. pylori* (modified after [Haas *et al.*, 1993])

H. pylori strains from GC agar plates were suspended in PBS or BB medium supplemented with 10% FCS. Bacterial suspension was adjusted to an OD_{550} of 0,2 and added to a 24-well plate (1 ml). The plate was incubated at 37°C, 10% CO_2 for 1-2 h. The mobility of bacteria was checked under a microscope before adding DNA (500 ng) and incubated for another 4-6 h. Bacteria were collected by centrifugation at 1000 g for 5 min and resuspended in BB medium and plated on appropriate antibiotic selective GC agar plates for 3-5 days at 37°C under micro-aerobic conditions. The clones were restreaked on a fresh selective plate for further testing.

2.2.1.7 Electroporation of *H. pylori* (according to [Segal and Tompkins, 1993])

H. pylori strains from GC agar plates were suspended in PBS. bacterial suspension (1 ml) with an OD_{550} of 1 was washed once with PBS and followed by 2 times of washing with of electroporation buffer (500 µl). Bacteria were pelleted by centrifugation at 1000 g for 5 min. Bacteria were resuspended in EB buffer (40 µl) and transferred to a pre-chilled cuvette. After adding DNA (500 ng), an electroporation pulse at 2.5 kV, 200 Ω, 25 µF was applied. Subsequently, 1 ml of BB medium containing 10% FCS was added directly to bacterial suspension. This suspension was incubated for 4 h in a 24-well plate before being pelleted and plated on appropriate antibiotic selective GC agar plates for 3-5 days at 37°C under micro-aerobic conditions. The clones were restreaked on selective plates for further testing.

Electroporation buffer (EB): 272 mM saccharose; 15% (v/v) glycerin; 2.43 mM K_2HPO_4; 0.57 mM KH_2PO_4

2.2.1.8 Plate transformation of *H. pylori*

H. pylori strains from GC plates were transferred to a fresh GC plate. An amount of 500 ng DNA plasmid was suspended with bacteria in a small area of the circle with a diameter of 2 cm for 24 h. The bacteria were then recultured on a selective plate and incubated for 3-5 days at 37°C under micro-aerobic conditions. The clones were restreaked on fresh selective plates for further testing.

2.2.2 Genetic and micromolecular methods

2.2.2.1 Extraction of nucleic acids

2.2.2.1.1 Genomic DNA isolation from H. pylori

The isolation of chromosomal DNA from *H. pylori* was performed according to the manufacturer's instructions with the QIAamp Tissue Kit from Qiagen (Hilden, Germany). *H. pylori* cells were grown for overnight at 37°C under micro-aerobic conditions on a GC agar plate and then one fourth of the plate was suspended in Lysis buffer. The chromosomal DNA was eluted from the column by adding 100-200 µl of sterile distilled water. The DNA concentration in the eluate was measured on a NanoDrop ND-1000 spectrophotometer (PeqLab).

2.2.2.1.2 DNA plasmid isolation from E. coli

Plasmid preparation by boiling procedure

Bacteria on the plate was suspended in STET buffer (300 µl). After adding 15 µl of lysozyme solution, bacterial suspension was incubated on ice for at least 5 min and boiled for 1 min in order to lyse the cells and release DNA. The lysate was centrifuged for 30 min at room temperature and the supernatant was transferred in 1 V isopropanol and incubated at -20^{o}C for 10 min before being centrifuged at 20000 g for 10 min. The DNA containing pellet was washed with 70% ethanol and dried out by Speed Vac and resuspended in double-distilled water (50-100 µl).

STET-buffer: 8% glucose, 5% double-distilled water Triton X100, 50 mM EDTA, 50 mM Tris pH 8.0

Lysozyme: 10 mg/ml in STET buffer

QIA Prep Spin Miniprep Kit

Plasmid DNA was prepared from *E. coli* cells using the QIAprep Spin Miniprep Kit (Qiagen) according to the instructions of the manufacturer. DNA was eluted with 50-200 µl double-distilled water and DNA concentration in the eluate was measured with a NanoDrop ND-1000 spectrophotometer (PeqLab).

2.2.2.1.3 Extraction and isolation of DNA from agarose gel

After PCR amplification or restriction digestion, the DNA fragments were separated on 1% agarose gels and stained with solution containing 0.1% (w/v) methylene blue. The DNA bands of interest were excised and purified from agarose gel using illistra GFX PCR DNA and Gel band Purification Kit (GE Healthcare) according to the instructions of the manufacturer. The DNA was eluted from the column with an appropriate amount of double-distilled water and quantified with a NanoDrop ND-1000 spectrophotometer (PeqLab) for concentration.

2.2.2.1.4 RNA extraction from H. pylori

Total RNA was isolated from *H. pylori* strains grown in liquid cultures for 16-24 h by the hot phenol method [Sharma *et al.*, 2010]. Briefly, bacterial cells from 10 ml of liquid cultures (OD_{550} of 0.8-1.0) were mixed with a stop solution containing 95% ethanol and 5% phenol and collected by centrifugation. Pellets were resuspended in 600 µl of TE buffer (pH 8.0) containing 0.5 mg/ml lysozyme and added with 60 µl of 10% SDS. The suspension was incubated at 64°C for 2 min, mixed with 66 µl of 1M sodium acetate (pH 5.2), and extracted with 750 µl of phenol at 64°C. Traces of phenol were removed from the aqueous phases by extraction with 750 µl chloroform and centrifugation at 12000 g for 15 min. RNA was precipitated from the aqueous phases with ethanol/sodium acetate (30:1 (v/v)) (pH 6.5), redissolved in DEPC-treated water, and treated with RNase-free DNase I (Fermentas). Total RNA was analyzed on nondenaturing 1.0% agarose gels and quantified with a NanoDrop ND-1000 spectrophotometer (PeqLab).

TE buffer (Tris-EDTA): 10 mM Tris, 1 mM EDTA

2.2.2.2 DNA gel electrophoresis

The DNA and RNA molecules were separated by electrophoresis on agarose gel ranging from 1-2%, depending on the size of the molecules in TAE buffer at 80 V for 50 min. Before loading on the agarose gels, the DNA or RNA samples were mixed with one fourth volume of GEBS buffer. The gels were stained with either ethidium bromide (1 mg/ml) and observed under UV light at 260 nm using Molecular Imager Gel Doc XR system (Bio Rad) or stained with methylene blue (0.1% (w/v)) as described above (section 2.2.2.1.3).

1X TAE buffer: 40 mM Tris, 20 mM Acetic acid, 1 mM EDTA.

GEBS buffer: 20% (v/v) glycerol, 50 mM EDTA, 0.05% (w/v) bromophenol blue, 0.5% (w/v) N-Lauryl Sarcosyl.

2.2.2.3 Restriction digestion

Plasmid DNA and PCR fragments were purified using illistra GFX PCR DNA and Gel band Purification Kit (GE Healthcare) before being digested with restriction enzymes obtained from Thermo Fisher Scientific or Roche Applied Science and the corresponding buffers according to manufacters'instructions. The double digestion was conducted by determining the appropriate buffer which is compatible for both enzymes. Approximately 500 ng of DNA were used for diagnostic digests and up to 3 µg for preparative purposes with 0.5-1 U/µl enzyme in the reaction. To separate the digested vector from the small DNA fragment, the incubation time ranged from 1 h to overnight. The band of interest was excised and purified using preparative agarose gel electrophoresis as described above (section 2.2.2.1.3)

For cloning of PCR products with phosphorylated primers and increasing of the directed mutagenesis efficiency, the PCR phosphorylated fragments were subjected to *Dpn*I digestion for 2 hours before being ligated.

2.2.2.4 Ligation

For cloning of the DNA fragments into vectors, a ligation reaction was performed for ON in a 10 µl final volume, including T4 ligase (1 µl) , T4 ligase buffer (1 µl) (Roche or Fermentas) and digested vector and insert DNA. The ratio of vector to insert was 1:3, and calculated by formular:

$$\frac{ng\ of\ vector\ x\ kb\ size\ of\ insert}{kb\ size\ of\ vector}\ x\ molar\ ratio\ of\ \frac{insert}{vector}$$

The ligation was then heated up to 65^{o}C for 5 min to inactivate T4-ligase and added directly into the transformation of competent *E. coli* cells.

2.2.2.5 Reverse Transcription and cDNA synthesis

In order to get the full length mRNA transcripts encoding for proteins of interest, the synthesis of first strand cDNA was performed by using RevertAid™ First Strand cDNA

Synthesis Kit (Thermo Scientific). First, the amount of 1.0 µg of total RNA was treated with 1 U (1 µl) of DNAse I (Thermo Scientific) for removing the single and double stranded DNA at 37°C for 1 h. The RNA was used directly for cDNA synthesis after being inactivated by heating at 65°C for 10 min in the presence of 1M EDTA. A mixture of 1.0 µg DNA-free RNA, 1 µl random Hexamer primer (100 µM) and water with the final volume of 12 µl was incubated for 5 min at 65°C and chilled on ice. The reaction then was added 4 µl 5 x RT buffer, 1 µl Ribolock RNase Inhibitor (20 U/µl), 2 µl 10 mM dNTP, RevertAid M-MuLVRT (20 U/µL) with the final volume of 20 µL. The mixture was incubated for 5 min at 25°C followed by 60 min at 42°C and terminated by heating at 70°C for 5 min. The reverse transcription reaction product was directly used in PCR applications or stored at -20°C. For long-term storage, cDNA samples were stored at -80°C.

2.2.2.6 Polymerase chain reaction

The DNA fragments were amplified from genomic DNA, plasmid DNA or cDNA using Ex Taq (Takara), LA Taq (Takara) or PAN polymerase (Clontech) as instructions of manufacturer following the protocol presented in Table 2.10.

Table 2.10. Standard PCR protocol

Step	Temperature		Time	Cycles
Initial denaturation	94°C		1 min	1
Denaturation	94°C		30 sec	
Annealing	48-54°C		30 sec	30
Elongation	68 °C	Ex taq and LA Taq	30 sec/1 kb	
	72°C	PAN Taq		
Final elongation	68°C	Ex taq and LA Taq	10 min	1
	72°C	PAN Taq		

2.2.2.7 Colony PCR

Colony PCR is a quick method of screening for plasmid inserts directly from *E. coli* colonies. PCR components were mixed and kept on ice. A small amount of colony was added to the PCR reaction. PCR was done by standard protocol for PAN polymerase (section 2.2.2.6).

2.2.2.8 Site-directed mutagenesis PCR

Site-directed mutagenesis PCR was used for introducing the point mutations and deletions in the plasmid DNA using Phusion High-Fidelity DNA polymerase (Thermo Scientific) according to the protocol provided by the manufacturer (Table 2.11). The entire plasmid was amplified using phosphorylated primers. A small amount of 5 ng was used.

The linear PCR products containing desired mutations were digested with *Dpn*I restriction enzyme, which cleaves methylated DNA from the template for 1 h at 37^{o}C, and re-ligated using T4 Ligase (Fermentas).

Table 2.11. PCR mutagenesis protocol

Step	Temperature	Time	Cycles
Initial denaturation	98^{o}C	30 sec	1
Denaturation	98^{o}C	30 sec	
Annealing	48-54^{o}C	30 sec	25
Elongation	72^{o}C	30 sec/1 kb	
Final elongation	72^{o}C	10 min	1

2.2.2.9 qPCR

Quantitative PCR was carried out using the ABI 7700 of Applied Biosystems, according to the manufacturer's instructions. The first strand cDNA was synthesized using random hexamer primers. The cycle conditions for real-time PCR are shown in Table 2.12.

Table 2.12. Quantitative PCR protocol

Step	Temperature	Time	Cycles
Initial denaturation	95^{o}C	1 min	1
Denaturation	95^{o}C	30 sec	
Annealing	59 - 61^{o}C	30 sec	43
Elongation	72 ^{o}C	30 sec	

2.2.2.10 DNA sequencing

DNA sequencing was purchased from GATC (Kempten, Germany) with standard primers or specific primers for the corresponding DNA sequence. The analysis of the sequences was carried out by the DNAMAN program and CLC DNA Workbench 6.

2.2.3 Protein methods

2.2.3.1 Preparation of whole *H. pylori* bacterial lysates for SDS-PAGE

Whole bacterial lysates for SDS-PAGE were prepared by suspending the bacteria from a 24 h agar plate in PBS and adjusting to an OD of 7.0. The samples were mixed with 2 X SDS sample buffer (1:1) (v/v)) and incubated for 10 min at 95^{o}C and followed by centrifugation at 13000 rpm for 5 min.

SDS sample buffer (2 X): 100 mM Tris-HCl pH 6.8, 4% (w/v) SDS, 20% (v/v) glycerol, 10% (v/v) β-mercaptoethanol, 0.2% (w/v) bromphenol blue, and 10% (v/v) mercaptoethanol.

2.2.3.2 SDS-PAGE

Sodium dodecyl sulfate-polyacrylamide gel electrophoresis (SDS-PAGE) was performed using the Laemmli gel system. 10 µl of whole cell lysates with OD_{550} of 10 suspended in 2 X SDS sample buffer were loaded on a 6-15% SDS gel, depending on the size of the protein of interest, under denaturing condition. A pre-stained Protein Molecular Weight Marker was loaded in parallel for size-determination. Protein gels between 6-15% were made from a 30% acrylamide solution in a separating gel buffer (1.5 M Tris/HCl pH 8.8). The concentration of Stacking gel was always on 5% in a Stacking buffer (1.0 M Tris/HCl pH 6.8) is set (Table 2.13). The separation of proteins was carried out in an electrophoresis buffer at a voltage of 80-130 V for approximately 80 min to 120 min.

Table 2.13. Preparation of polyacrylamide gels

Components	Separating gels				Stacking gel
	6%	10%	12%	15%	
dH_2O	2.6 ml	1.9 ml	1.6 ml	1.1 ml	0.68 ml
Acrylamide 30%	1.0	1.7	2.0	2.5	0.17
1.5 M Tris HCl pH 8.0	1.3	1.3	1.3	1.3	

1.5 M Tris HCl pH 6.8					0.13
SDS 10%	0.05	0.05	0.05	0.05	0.01
10% APS	0.05	0.05	0.05	0.05	0.01
TEMED	0.004	0.02	0.02	0.02	0.001

Electrophoresis buffer: 250 mM glycine, 0.1% (w/v) SDS, 25 mM Tris-HCl pH 8.3

2.2.3.3 Detection of proteins on Polyacrylamide gel

The SDS-PAGE was stained with a Coomassie solution according to [Zehr *et al.*, 1989]. The gel was fixed for 20 min and then washed with a distaining solution on a shaker until all relevant bands were visible.

Coomassie solution: 0.275% (w/v) coomassie brilliant blue R250 (Biomol), 50% methanol, 10% acetic acid.

Destaining solution: 10% methanol, 10% ethanol, 7.5% acetic acid.

2.2.3.4 Western blotting

2.2.3.5 Transfer of proteins to PVDF membrane

For immunoblotting, the separated molecules from SDS-PAGE after electrophoresis, were transferred or blotted onto a methanol activated polyvinylidene difluoride (PVDF) membrane using semi-dry blotting chambers (Biotec-Fischer). The transfer sandwich was assembled with a stacking gel and pieces of filter paper on each side of the sandwich, which had been soaked in anode I/II and cathode buffers on the anode/cathode side of the gel and membrane, respectively. Electro-transfer proteins from the gel on the Membrane were done for 75 min at room temperature with a current of 1.2 mA/cm^2 for 60-70 min. After transfer, the membrane was either dried (1 h at 37°C or overnight at room temperture) or directly used for immunoblotting. The dried membrane was briefly reactivated with methanol before further purposes.

Anode I buffer: 300 mM Tris-HCl pH 10.4, 10% methanol

Anode II buffer: 25 mM Tris-HCl pH 10.4, 10% methanol

Cathode buffer: 25 mM Tris-HCl pH 9.6, 40 mM 6-amino caproid acid, 10% methanol

2.2.3.6 Detection of immobilized proteins with antibodies

In order to prevent any nonspecific bindings of antibodies to the surface of the membrane, the membranes were blocked with a blocking buffer for at least 1 h at room temperature. The primary antibodies against the target proteins with appropriate dilutions were applied to the blots for overnight at 4^{o}C or 2 h at room temperature. The blots were washed 3-5 times for 10 min each with TBS-T and followed by incubating with HRP-conjugated secondary antibody or protein A, alkaline phosphatase conjugate solution according to the manufacturer's recommended ratio for 1 h at room temperature. The blots were further washed 3-5 times for 10 min each with TBS-T. Upon addition of the primary antibody, either the chemiluminescent substrate (Immobilon Chemiluminescent HRP Substrate, Millipore) which is catalyzed by horseradish peroxidase (POX) bound to the secondary antibody, or AP substrate which forms an insoluble black-purple precipitate when reacted with alkaline phosphatase was applied to the blots. The chemiluminescence reaction was detected with X-ray films (Fuji Medical X-Ray Films Super RX, Fujifilm) or via a Bio-Rad ChemiDoc XRS.

Blocking buffer: 5% skim milk in TBS

Primary and secondary antibody solution: 1% skim milk in TBS-T buffer

AP substrate: 0.1 M Tris-HCl, pH 9.6; 7 mM $MgCl_2$; 0.1 mg/ml nitro-blue tetrazolium chloride in 0.1 M Tris-HCl, pH 9.6; 0.05 mg/ml 5-bromo-4-choloro-indolyl phosphate in dimethylformamide

2.2.3.7 Removal of immune complexes from PVDF

The blots were incubated in a stripping buffer (50 mM NaOH) for 30 min with some agitation. After 2 times washing with TBT-T, the blots were blocked with blocking buffer or dried and activated with methanol before further use.

2.2.3.8 Determination of protein concentration

A colorimetric assay, which based on an absorbance shift of the dye Coomassie Brilliant Blue G-250 was applied to determine the concentration of protein solutions. A series dilution of the standard BSA (0-0.6 mg/ml) and serial dilution of protein samples were prepared with Protein Assay Dye Reagent Concentrate (Bio-Rad) according to the instructions of the manufacturer. Absorbance shift of Coomassie Blue dye to 595 nm

was measured in 96-well plates (Costar EIA/RIA plate, flat well, medium binding, Corning) using a Tecan Sunrise microplate reader.

2.2.3.9 In vitro phosphorylation assay

The ability of the cells to phosphorylate CagA was checked by performing an infection assay using using total lysates of bacteria. AGS cells were grown in RPMI media supplemented with 10% Fetal Calf Serum (FCS) with a confluency of 70-80%. The infection (MOI of 60) was done in 6 well plates for for 3-4 h at 37^{o}C in 5% CO_2. After infection, cells were washed with PBS and harvested by scrapers in PBS*. After being centrifuged at 500g for 10 min at 4^{o}C, cells were resuspended in 25-30 µl PBS* and lysed in SDS sample buffer for Western blot detection of phosphorylated proteins.

2.2.3.10 ELISA for IL-8 quantification

An EILSA was performed to measure the concentrations of IL-8 protein produced by AGS cells during infection assays. An immunoabsorbent 96-well plate was coated with 50 µl diluted IL-8 antibody (3 µl/ml in coating buffer) and 50 µl of coating buffer per well at 4^{o}C for over night. The plate was washed 4 times with 200 µl wash buffer and followed by blocking with 200 µl blocking buffer. The plate was covered and incubated for 2-4 hours at room temperature or 4^{o}C overnight. After 3 times of washing, the dilution series of human IL-8 medium ranged from 0 to 800 pg/ml and appropriate dilutions of samples were added. Standard human IL-8 and samples were diluted in RPMI medium with 10% FCS with the final volume of 100 µl per well. The plate then was incubated at 4^{o}C for ON. Four time washing steps were repeated to remove unbound antigen. To detect the bound IL-8, 100 µl of a solution containing biotylated anti IL-8 antibody (0.5 µl/ml in washing buffer with 10% FCS) was added. The biotylated antibody was incubated at room temperature for 1-2 hours and followed by 6 times of washing and adding prepared conjugate solution (Streptavidin-Biotin-POX). After 1 h incubation, the plate was washed 6 times with washing buffer and added 100 µl TMB substrate solution (1:1) (Millipore) per well and incubated for 30 min at room temperature in the dark. The reaction was stopped with 50 µl 1M H_2SO_4 and measured using a wavelength of 450 nm with subtraction of a 570 nm wavelength in a Tecam Sunrise ELISA plate reader. The data analysis was done using Magellan 3 Software.

Coating-buffer: 100mM Na_2HPO_4 pH 9.0

Washing buffer: PBS with 0.05% Tween 20

Blocking buffer: PBS with 10% FCS

Conjugate solution: 200 µl 50mM Tris pH 7.6; 1.5 µl solution A; 1.5 µl solution B. Mix well and incubate for 30 min at room temperature then add 9.8 ml 50 mM Tris pH 7.6.

2.2.3.11 Immunoprecipitaion

Immunoprecipitation (IP) is one of the most commonly used methods for verification of protein-protein interactions. In this experiment, a protein antigen – a bait protein is captured from out of *H. pylori* lysate using an antibody that specifically binds to that particular protein and the interaction partners which have been bound to the bait protein are subsequently identified by Western blotting. In this work, IP experiments were performed for investigating possible interactions of CagH, CagI and CagL the Cag-T4SS.

H. pylori grown on 24 h GC agar plate were suspended and washed twice with PBS. The start bacterial lysates were prepared with the OD_{550} of 10. The bacterial pellets were resuspended in a pre-chilled RIPA buffer with an OD_{550} of 15 in 500 µl for one direction of IP and lysed by ultra-sonication treatment (20 sec intervals 20 sec of rest, output 2-4, duty cycle 20-30%) using Sonifier 250 (Branson). The intact cells were removed by low speed centrifugation for 10 min at 4°C and followed by 30 min at 20000 g at 4°C. To remove un-specifically reacting proteins, bacterial lysates were incubated with 50 µl prewashed G agarose beads (Roche Diagnostic) (3 times at 20000 g for 30 sec) for 2 h at 4°C and centrifuged at 20000 g for 10 min. The specific antibodies (5 µl) against proteins of interest were added into the supernatant after discarding the pellet and the samples were incubated for over night at 4°C. The prewashed G agarose beads (50 µl) were added to the samples and incubated for another 2 hours at 4°C. The antigen-antibody-protein G complexes were pulled down by centrifugation at 20000 g at 4°C for 10 min. After 3 times of washing with RIPA buffer for removing unspecific binding, proteins were eluted from the beads by adding 50 µl SDS sample buffer and boiling at 95°C for 10 min.

In this thesis, IP-CagI, -CagL and -Myc were done using CagI, CagL and Myc antibodies, respectively.

RIPA buffer: 150 mM NaCl, 1 mM EDTA, 0.5% Nornidet P40, 0.25% sodium deoxycholate, protease inhibitors (1% PMSF, 1%v, 0.1% leupeptin, 0.1% pepstatin).

2.2.3.12 Pull-down experiments

The pull-down experiments were carried out to confirm the interaction between CagI, CagL and CagH proteins. The method involves in the binding of GST/MBP fusion proteins coupled beads to proteins of interest.

For production and purification of GST/MBP fusion proteins, *E. coli* BL21 (DE3) containing plasmids listed in Table 2.14, overnight cultures were diluted in fresh LB medium and grown at 37°C and 200 rpm in LB medium supplemented with ampicillin/kanamycin for GST and MBP fusion proteins, respectively, until they reached an OD_{600} of 0.5-0.6 before inducing IPTG with a final concentration of 1 mM for 3 h. The cultures (50 ml) were centrifuged (4000 g, 10 min, 4°C) and the bacterial pellet was resuspended in one tenth volume of lysis buffer (5 ml). Bacterial lysates were prepared by ultra-sonication treatment (20 sec intervals 20 sec of rest, output 2-4, duty cycle 20-30%) using Sonifier 250 (Branson). Intact cells were removed by low speed centrifugation for 10 min at 4^oC and followed by 30 min at 20000 g at 4^oC. The lysates were incubated with Triton X100 with the final concentration of 1% for 30-60 min in order to reduce the amount of inclusion bodies. The lysates were then applied for centrifugation at 20000 g for 30 min at 4^oC.

Lysis buffer: 1X PBS, 0.5% Nornidet P 40, 1 mM EDTA, 1% PMSF, 1% vanadat, 0.1% leupeptin, 0.1% pepstain

Table 2.14. List of plasmids for expression of GST- and MBP- fusion proteins

GST constructs	MBP constructs
pWS258	H-MBP
pPT14	pMal(g) (control)
pPT15	
pPT16	
pPT8	

pPT17
pPT18
pGEX4-T3 (control)

2.2.3.12.1 GST pull-down

***Coupling*:** 1 ml bed volume of Glutathione Sepharose 4B beads (GE Healthcare) was prepared by washing 3 times with PBS* (spin at 5000 rpm for 5 min). The *E. coli* pellets containing unlysed bacteria were discarded and the supernatants were incubated with for at least 3 hours or overnight under gentle agitation in order for the bait proteins to be captured on beads. After 3 times of washing with PBS* (spin at 5000 rpm for 5 min), the beads were suspended in the 1 volume of PBS* (1 ml) PBS*. A 50 µl of suspension was used for Western blotting and for pull-down experiments.

***Elution*:** After triple washing of the matrix with 10 bed volumes each of PBS*, the GST-CagL fusion protein and GST control protein were eluted in three fractions with 10 volumes of elution solution for 10 min each at room temperature and then concentrated using Amicon Ultra 4 (10000 NMWL). The concentration of each protein was measured by Bradford assay (section 2.2.3.8).

Elution buffer: 50 mM Tris-HCl, pH 8.2, and 30 mM reduced Glutathione

***Pull-down*:** *H. pylori* lysates containing putative prey proteins were prepared as described in section 2.2.3.11. Bacterial lysates were pre-incubated for 2 hours with 50 µl MBP beads to avoid unspecific bindings. After 10 min centrifugation at 20000 g at 4^{o}C, the supernatant was collected and incubated with 50 µl bait proteins coupled Glutathione Sepharose beads suspension for overnight. The GST coupled beads were used as a negative control. The samples were centrifuged at 20000 g at 4^{o}C for 10 min and followed by 2 washing steps. The complexes were eluted from the beads by adding of SDS sample buffer (50 µl) and boiling at 95^{o}C for 10 min.

2.2.3.12.2 MBP pull-down

***Coupling*:** 1ml bed volume of the amylose resins (New England Biolabs) was prepared by washing 2 times with 5ml water and 2 times with 5 ml column buffer (spin at 3500 rpm for 3 min). The lysates containing MBP fusion proteins were prepared as mentioned in section 2.2.3.12.1 and mixed with equilibrated resin overnight at 4°C. After 5 times of wash with column buffer (spin at 3500 rpm for 3 min), 1 volume of PBS* (1 ml) was added and samples were stored at 4°C. 40 µl of suspension was used for Western blotting and for pull-down experiments.

Pull-down:

For investigating the possible direct interaction between CagH, CagI and CagL, the amount of 5 µg of each purified CagI or CagL proteins were added into a 50 µl CagH coupled beads and filled it up to 100 µl using PBS*. The samples were then incubated at 4°C for 3 hours and washed 3 times with PBS* by centrifugation at 20000 g for 30 s at 4°C. The complexes were eluted from the beads by adding 50 µl of SDS sample buffer and boiling at 95°C for 10 min.

For another strategy to check the interaction between CagH and CagL, 5 µg of GST-CagL was mixed with 50 µl of MBP-CagH coupled Amylose beads and incubated at 4°C for 2 hours and washed 3 times with PBS* by centrifugation at 20000 g for 30 s at 4°C. As controls, MBP coupled Amylose beads and GST alone were used.

Column buffer: 1 mM EGTA, pH 8.0; 200 mM KCl; 50 mM Tris-HCl, pH 8.0; 1 mM EDTA, pH 8.0; 10% (v/v) glycerol;

2 mM sodium metabisulfite (Na_2S_2O5), 0.5 mM DTT, 1 mM PMSF freshly added.

Lysis buffer for MBP fusion proteins: 1 mM EGTA, pH 8.0; 100 mM KCl; 50 mM Tris-HCl, pH 8.0; 1 mM EDTA, pH 8.0; 1 M NaCl;

00.5 mM DTT, 1 mM PMSF, protease inhibitors freshly added.

Lysis buffer for GST fusion proteins: PBS* supplemented with 0.5% Nonidet P40.

2.2.3.13 Membrane protein fractionation

H. pylori were grown in 200 ml BB medium supplemented with 4% cholesterol for 24 h. Bacteria were then harvested, washed, and resuspended in 3 ml Lysis buffer. Bacteria were lysed as above (section 2.2.3.11), and bacterial lysate was centrifuged for 10 min

at 7000 g to remove unbroken cells and cell debris. The supernatant was collected and separated by ultracentrifugation (60 min, 230000 g) into the soluble fraction containing cytoplasmic and periplasmic proteins and total membrane fraction.

Proteins in the soluble fractions were concentrated by chloroform-methanol precipitation [Wessel and Flugge, 1984]. Briefly, 300 µl of the sample were mixed carefully by hand with 600 µl methanol, 200 µl chloroform, and 200 µl of water. After centrifugation at 20000 g for 2 min, the upper organic phase was removed without disturbing interphase containing protein while the membrane fractions were washed with and resuspended in preparation buffer. For differential extraction, triton X-100 was added to the membrane suspension to a final concentration of 1% (w/v), and the mixture was incubated on ice for 30 min in order to isolate membrane proteins and then fractionated by ultracentrifugation (45 min, 230000 g). The pellet was then resuspended in in preparation buffer and the supernatant was concentrated as above.

Lysis buffer: 10 mM Tris-HCl, pH 8.0, 1 mM PMSF, 1 µM leupeptin, 1 µM pepstatin

2.2.3.14 Sucrose density gradients

Sucrose density gradients are based on the migration of inner and outer membrane vesicles according to their different densities when exposed to the elevated centrifugal force. A discontinuous sucrose gradient was prepared by loading the decreasing sucrose density solutions ranging 60% (w/v) to 25% (w/v) in M buffer upon one another in SW41 rotor tubes, followed by overnight equilibration at 4°C. Total membrane fractions resuspended in Triethanolamine buffer were layered on top of the density gradients and centrifuged at 4^{o}C for 17 h at 285000 g. The eight fractions were collected, and proteins were concentrated by precipitation described above (section 2.2.3.13).

M buffer: 50 mM triethanolamine, pH 7.5; 1 mM EDTA

2.2.3.15 Limited Proteinase K Digestion

This method was carried out in order to access the susceptibility of bacterial surface exposed proteins with proteinase K digestion. *H. pylori* were grown on GC agar plates for 24 hours, harvested and washed in PBS, and resuspended at a density of 6×10^7 cells per ml in proteinase K buffer. This suspension was incubated at room temperature for 30 min. To stop the reaction, PMSF was added to the reaction with the final

concentration of 5 mM. Bacterial cells were then washed twice with PBS and resuspended in PBS (1/10 v/v) and 2X SDS sample buffer.

Proteinase K buffer: 50 mM Tris-HCl, pH 7.4; 150 mM NaCl, 1 mM $CaCl_2$, 1 mM $MgCl_2$, 1 mM KCl containing 1 mg/ml proteinase K

2.2.3.16 Labeling of α5β1 integrin with Alexa Dye

The 2 forms of purified α5β1 integrin (active and inactive) were labeled with Alexa dye using Fluor 647 Monoclonal Antibody Labeling Kit obtained from Invitrogen according to the instructions of the manufacturer with some modifications. Briefly, the glycerol and Tris from the storage buffer of 100 µg proteins was removed from the sample by dialyzing against PBS (-KCl) in Slide-A-Lyzer dialysis cassettes (100K MWCO, Thermo Fisher Scientific) for 4 hours in dark at 4°C and followed by adding one tenth volume of 1M $NaHCO_3$. The samples were transferred to the vial of reaction dye (250 µg) then incubated at room temperature in the dark for 1 hour under agitation. To purify labelled integrins, the samples were loaded on the prepared spin column containing purification resin and centrifuged for 5 min at 1100g. Protein concentration and degree of labeling were measured by UV-VIS module of a NanoDrop ND-1000 spectrometer (PeqLab) at 280 n (A_{280}) and 650 nm (A) and stored at -20°C.

PBS(-KCl): 7.7 mM Na_2HPO_4, 2.5 mM NaH_2PO_4, 150 mM NaCl

2.2.3.17 Staining of *H. pylori* with integrin coupled Alexa Fluor 647

H. pylori strains were grown on cholesterol plates for at least two passages so that the serum proteins in bacteria which would cause a fault positive in binding assay were reduced. Bacteria were harvested and suspended in PBS (-Ca, -Mg) by pipetting. Bacterial suspension was adjusted to an OD of 0.4 and distributed in 100 µl aliquots on a 96 well plate. 100 µl aliquots which contained 0.4 µg of the active and in active integrins were added to the wells. After 1 h incubation, the plate was centrifuged at 3000 rpm for 10 min at 4°C and followed by washing with 200 µl PBS before adding 200 µl of PBS and measuring APC level fluorescent emission on a FACS-Canto II (BD Biosciences) with side scattering as a threshold for the events.

To induce the production of pili, bacteria were subjected to an infection with AGS cells (confluency of 70-80%) with OD_{550} of 0.2 (MOI of 60). After 1 h infection, unbound

bacteria were washed 1 time with PBS and centrifuged at 3000 rpm for 10 min at 4^{o}C. The bacterial pellets were resuspended by pipetting in PBS and used for binding assay as described above.

2.2.4 Statistical analysis

All values were mean values +/- standard errors. The data collected from at least 3 independent experiments and the significant difference were analyzed by One-way ANOVA (*P < 0.05, **P < 0.01, ***P < 0.001) using Graphpad Prism5 software.

3 RESULTS

3.1 Role of the CagH, CagI and CagL proteins for T4SS functionality

3.1.1 Features of the CagH, CagI and CagL proteins

The CagH (39 kDa), CagI (42 kDa) and CagL (29 kDa) proteins are components of the Cag Type IV Secretion System of *H. pylori.* In strain 26695, the genes encoding for CagH, CagI and CagL proteins were shown to be located in a putative operon, which may contain five genes (*cagF, cagG*, *cagH*, *cagI* and *cagL*) or even more genes [Sharma *et al.*, 2010]. One study on transcriptional units of the Cag-T4SS suggested a conserved existence of 11 operons in different strains, in which *cagI-cagL* and *cagG-cagH* were found to be organized in 2 different operons [Ta *et al.*, 2012]. By promoter-trap and reverse transcription PCR analyses of ORFs and intergenic transcripts, the *cagG* promoter was found to drive expression of the operon *cagG-cagH*, while the opreron *cagI-cagL* might be controlled by a promoter within the *cagG-cagH* genes [Ta *et al.*, 2012] (Figure 3.1A). A closer look on the putative *cagFGHIL* operon revealed that *cagH, cagI and cagL* have overlapping ORFs, in which the 3' end of *cagI* ovelaps with the start codon of *cagL* and the Shine-Dalgarno sequence of *cagI* overlaps with the stop codon of *cagH* (Figure 3.1A).

In order to characterize the CagH, CagI and CagL proteins, the amino acid sequences of these proteins were analyzed by the Phobius software. CagI and CagL are characterized by a predicted N-terminal signal peptide for being exported into the periplasmic space, whereas CagH is predicted to have one single transmembrane helix and is thus most likely a cytoplasmic membrane protein (Figure 3.1B). Interestingly, analysis of the C-terminal amino acid sequences of these 3 proteins showed a high identity of 6 amino acids from each protein (CagH (TKIIVK), CagI (SKVIVK) and CagL (SK(I/V)IVK)) (Figure 3.1C).

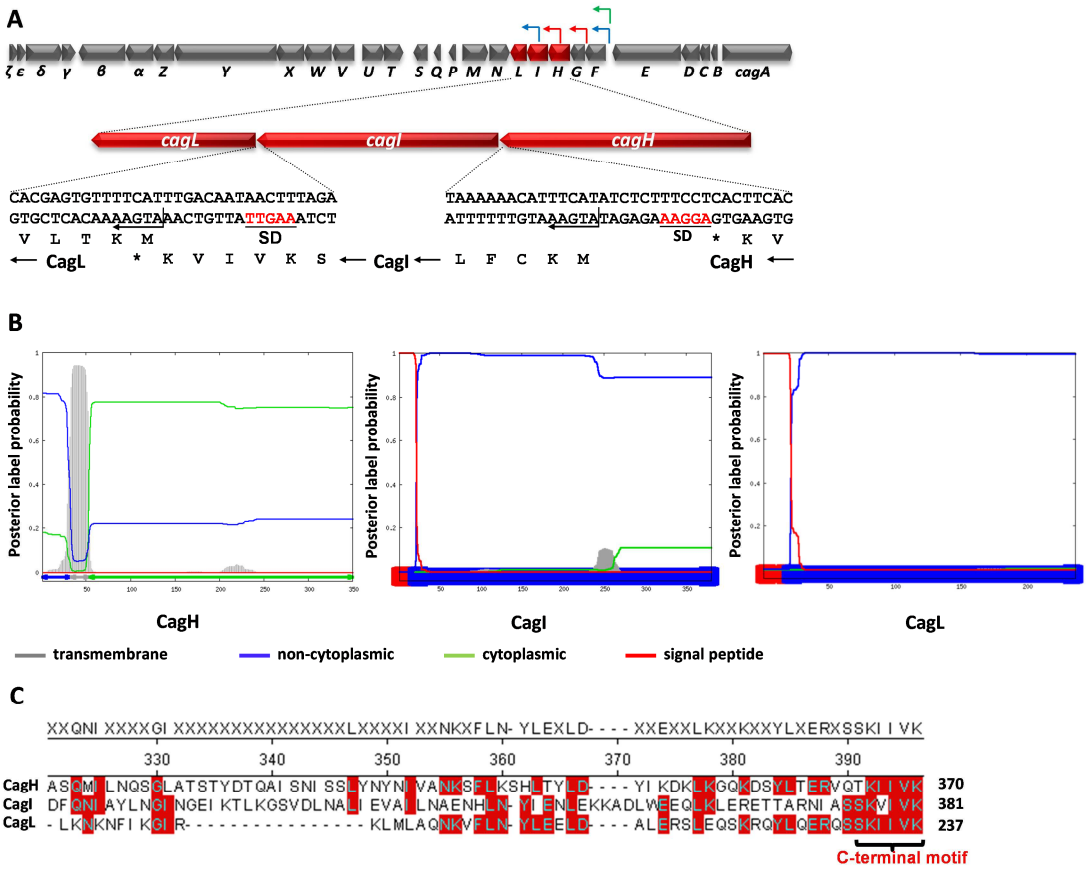

Figure 3.1. Features of CagH, CagI and CagL

(A) Genetic organization of the *cag* pathogenicity island in strain P12. Each gene on the *cag*-PAI is shown as a thick arrow with the orientation of transcription. The length and spacing of each annotated gene are shown in proportion to the real sizes. The genes of interest, *cagH*, *cagI* and *cagL* (denoted in red arrows) have overlapping open reading frames. The identified transcriptional start sites are represented by bent arrows (blue according to [Sharma *et al.*, 2010], green according to [Vannini *et al.*, 2014]; red according to [Ta *et al.*, 2012]). SD: Shine-Dalgarno sequence. (B) The prediction software analysis (Phobius) suggested that CagI and CagL are secreted across the inner membrane as a result of an N-terminal signal peptide denoted by a red line, whereas CagH is predicted to be a cytoplasmic membrane protein with a transmembrane region indicated by a gray peak. The predicted non-cytoplasmic region is presented in blue. (C) The sequence comparison of CagH, CagI and CagL using the MegAlign software reveals a conserved C-terminal motif. The C-terminal motif containing 6 amino acids of each protein is highlighted in red, (CagH (TKIIVK), CagI (SKVIVK) and CagL (SK(I/V)IVK)).

3.1.2 Deletion and complementation of the *cagH, cagI* and *cagL* genes

3.1.2.1 The CagH, CagI and CagL proteins are required for Cag-T4SS functionality

With the aim of investigating the role of CagH, CagI and CagL in functionality of the Cag-T4SS, a set of mutants and complemented strains were constructed (Figure 3.2A). In order to avoid polar effects of the mutations, we constructed marker-free deletion mutants for the analysis of gene function. The principle of the system for generating maker-free deletion mutants was described earlier [Dailidiene *et al.*, 2006] and is shown in Figure 3.2B. The P12Δ*cagH* deletion mutant was constructed by replacement of the *cagH* gene with an *rpsL-erm* cassette using plasmid pWS423[1]. The P12Δ*cagI* marker-free deletion mutant was constructed in such a way that the 3' region of *cagI* was kept to avoid a transcriptional effect on *cagL* by deletion of a transcriptional start site located in the 3' part of *cagI* (constructed using plasmid pWS320). These plasmids were constructed as described in section 2.1.5. The *cagL* gene was deleted from P12 by transforming with plasmid pWS290 [Jimenez-Soto *et al.*, 2009]. The presence of CagH, CagI and CagL proteins in the deletion and complemented mutants were checked by Western blotting using the corresponding antibodies. As shown in Figure 3.3A, CagI and CagL were absent in the corresponding mutants and could be restored by genetic complementation. In the absence of CagI, CagL levels were considerably reduced, and the same effect was observed for CagI in the P12Δ*cagL* mutant. Since the *cagL* gene is the last gene of the putative operon *cagGHIL*, the absence of CagI in the P12Δ*cagL* mutant background cannot be caused by insertion of the *cat* cassette, but was rather due to the lack of the *cagL* gene product.

In the case of CagH, the P12Δ*cagH* mutant was defective in production of full levels of CagI and CagL as shown in Figure 3.3A. Both phenotypes were rescued by complementation *in cis* using the gene bank plasmid pHP2kbG17. Unfortunately, we were not able to construct an unmarked deletion mutant to exclude a polar effect caused by insertion of the *rpsL-erm* cassette (data not shown). Likewise, we could not

[1] Was performed by Evelyn Weiss

complement the P12Δ*cagH* mutant using a standard chromosomal integration vector because *E. coli* cells seemed not to tolerate of *cagH* (data not shown). Nevertheless, we were able to complement this mutant *in trans* using plasmid pWS534, in which the *cagH* gene is not integrated into the chromosome, but into the naturally occurring plasmid pHel12 (Lea Holsten), and expressed under the control of the *alpA* promoter. The resulting strain (P12Δ*cagH/H*(pWS534) recovered CagI and CagL production[2] (Figure 3.3A). These results indicated that insertion of the *rpsl-erm* cassette did not influence the expression of downstream genes *cagI* and *cagL*, or at least did not cause a strong reduction of transcription. The reduced levels of CagI and CagL observed in this mutant are thus more likely due to the absence of CagH, suggesting a stabilizing effect of CagH on CagI and CagL. Taken together, these observations suggest that the stability of each protein in this putative complex depends on the presence of the others.

To determine the requirement of these 3 proteins for CagA translocation and IL-8 induction, infection experiments of AGS cells with strain P12 and the deletion and complemented strains were performed. Tyrosine phosphorylation of the CagA protein was examined by Western blotting, and IL-8 induction was analyzed by a sandwich ELISA. Figure 3.3B shows that in comparison to the P12 wild-type strain, the mutants failed to translocate CagA into AGS cells and were completely abolished in IL-8 induction. The complementation of the deletion mutants restored both CagA translocation and IL-8 secretion after AGS cells infection. Additionally, in the case of CagH, the complementation of the P12Δ*cagH* mutant not only *in cis* but also *in trans* rescued all of the defects observed in the absence of this protein (Figure 3.3B), suggesting an important role of CagH in functionality of the Cag-T4SS. However, it remained unclear whether the deficiency of the *cagH* mutants in CagA translocation and IL-8 induction are absolutely due to CagH itself or rather due to the reduction of CagI.

To sum up, we conclude that CagH, CagI and CagL are required for CagA translocation and IL-8 induction. They are thus essential components of the Cag-T4SS.

[2] was performed by Evelyn Weiss

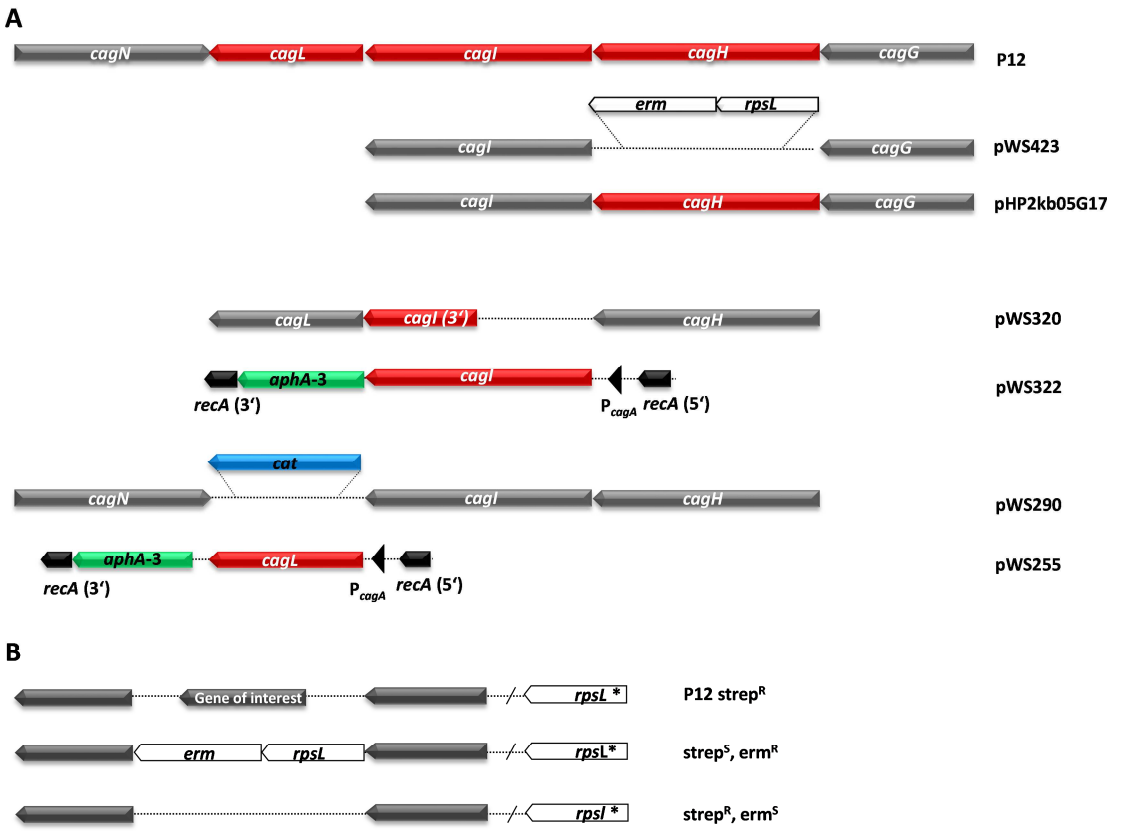

Figure 3.2. Schematic representation of constructs used for *cagH, cagI,* and *cagL* deletion and complementation

(A) The *cagH, cagI* and *cagL* deletion mutants were generated from strain P12 by transforming with plasmids pWS423, pWS320 and pWS290, respectively. For complementation *in trans*, *cagI* and *cagL* were introduced into the *recA* locus of the P12Δ*cagI* and P12Δ*cagL* strains using plasmids pWS322 and pWS255, containing a kanamycin resistance cassette, respectively, whereas *cagH* was complemented in the *cagH* locus of the P12Δ*cagH* strain replacing the *rpsL-erm* cassette using the gene bank plasmid HP2kb05G17. (B) Principle of the system for generating a marker-free deletion mutant. In the first step, the P12 wild-type strain carrying a point mutation in the *rpsL* gene (*rpsL**, strep^R) was transformed with plasmid containing an *rpsL-erm* cassette which confers dominant streptomycin susceptibility and selectable erythromycin resistance. The resulting strain was used for the second step to remove the *rpsL-erm* cassette by transforming with a plasmid containing no insertion and selecting for streptomycin resistance and erythromycin susceptibility.

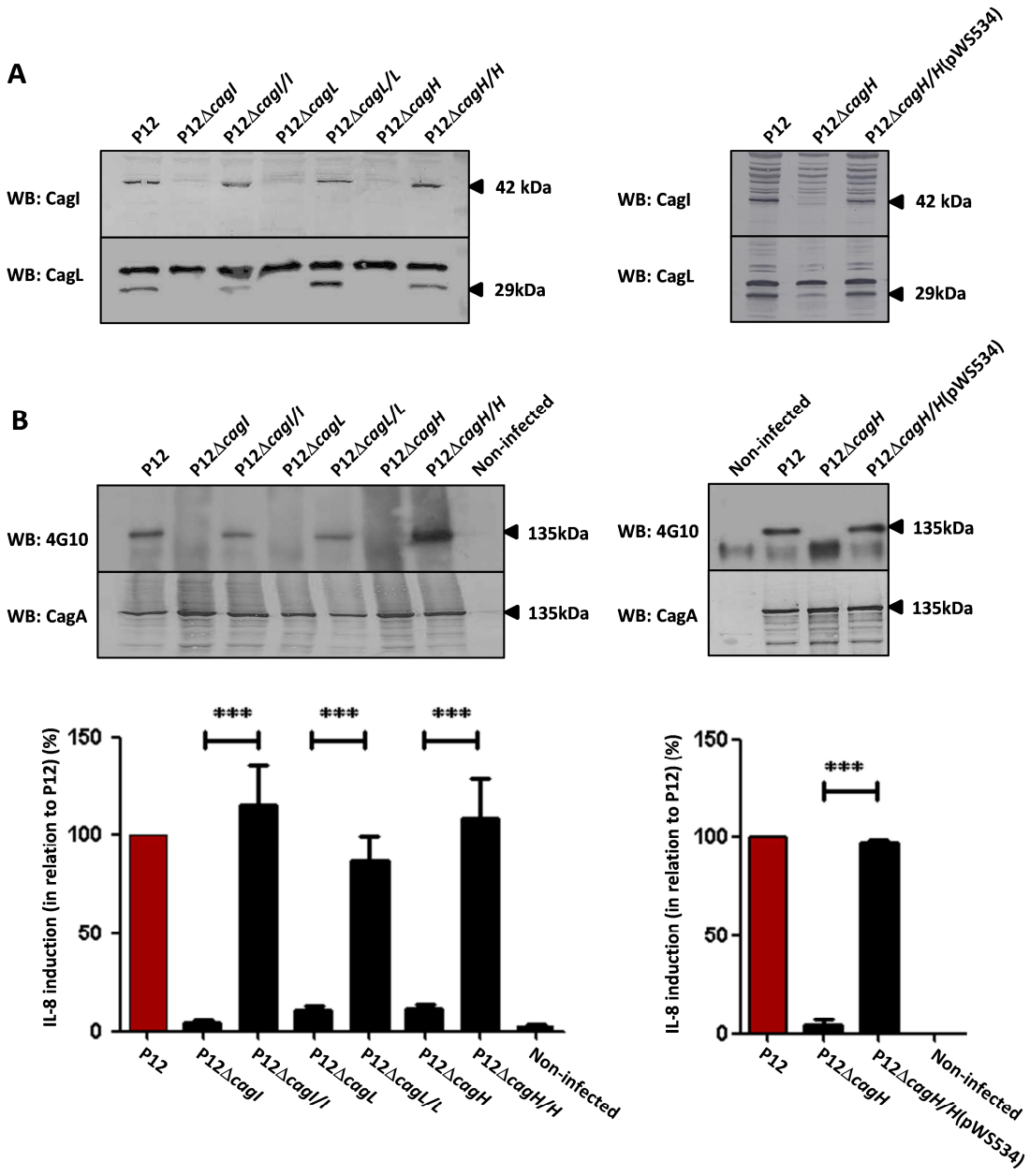

Figure 3.3. Functional analysis of the Cag-T4SS components CagH, CagI and CagL

(A) Whole cell lysates of the P12 wild-type strain and the indicated mutants as well as complemented strains were immunoblotted using CagI and CagL antibodies. (B) Functionality of the Cag-T4SS in strain P12 and the indicated mutants was tested by performing infection assays of AGS cells to determine CagA tyrosine phosphorylation. The IL-8 values induced by the P12 wild-type strain were set to 100% and other values were normalized to these values (%). The data collected from at least 3 independent experiments were statistically analyzed by One-way ANOVA (***$P < 0.001$).

3.1.2.2 CagI is not absolutely required for CagL production

As mentioned above, *cagI* and *cagL* genes are located in a putative operon and they have overlapping open reading frames (Figure 3.1A). Furthermore, they were shown to be transcribed into one transcriptional unit (mRNA) [Ta *et al.*, 2012]. For further investigation of the role of CagL in the absence of CagI, a set of *cagI* mutants was constructed (Figure 3.4). The 5' part of *cagI* was either deleted and replaced by a streptomycin sensitivity/erythromycin resistance gene cassette in the mutant P12Δ*cagI*(320) or deleted without insertion for generating a marker-free deletion mutant P12Δ*cagI*(320/326). Since the 3' part of *cagI* has been predicted to harbor an alternative transcriptional start site of *cagL* [Sharma *et al.*, 2010], *cagI* was deleted completely in the mutant P12Δ*cagI*(320/327) in such a way that the Shine-Dalgarno sequence of *cagH* is used as a ribosome binding site for *cagL* allowing the transcription directly from *cagH* to *cagL* (Figure 3.4). As expected, the production of CagI was lost in all the *cagI* mutant individuals. The presence of the CagL protein was analyzed by Western blotting and the results showed that deletion of *cagI* led to a strong reduction of CagL with different levels. The complementation of *cagI* into the chromosomal *recA* locus was done for these mutants by transforming with plasmid pWS322 containing *cagI* under the control of the *cagA* promoter. CagI and CagL immunoblots of whole bacterial lysates from these complemented strains in comparison to the P12 wild-type strain and deletion mutants indicated that the complementation restored not only CagI but also CagL production. Surprisingly, in the precise deletion of the *cagI* gene, the P12Δ*cagI*(327) strain produced normal levels of CagL, suggesting that CagI is not absolutely required for CagL production (Figure 3.5A). Unfortunately, our attempts to complement this mutant with a chromosomal integration vector containing the *cagI* gene were not successful (data not shown). Nevertheless, the results provided evidence that deletion of the *cagI* gene and its replacement by a resistance gene cassette does not cause any polar effects on the expression of downstream the *cagL* gene but rather that CagI has a direct stabilizing effect on CagL.

As shown before, CagL itself is important for CagA translocation and IL-8 secretion. However, to definitively determine whether the varying CagL levels caused by deletion of the *cagI* gene are involved in Cag-T4SS functionality, or whether CagI itself is responsible for the deficiency in CagA phosphorylation and IL-8 induction, infection

experiments of AGS cells were performed with the P12 wild-type strain, the deletion and complemented strains. As shown in Figure 3.5B, all the *cagI* mutant strains were unable to phosphorylate CagA and induce IL-8 by AGS cells. Even the mutants P12Δ*cagI*(320) and P12Δ*cagI*(320/326), which produced a smaller amount of CagL in respect to the P12 wild-type strain were defective in CagA translocation and IL-8 secretion. The wild-type phenotype was significantly restored by complementation of these mutants with plasmid pWS322 containing full-length *cagI* which had been integrated into the *recA* locus and expressed under the control of the *cagA* promoter. The results indicate that not the different levels of CagL are responsible for the defect of the Cag-T4SS, but rather that CagI itself is required for a proper functionality of the Cag-T4SS.

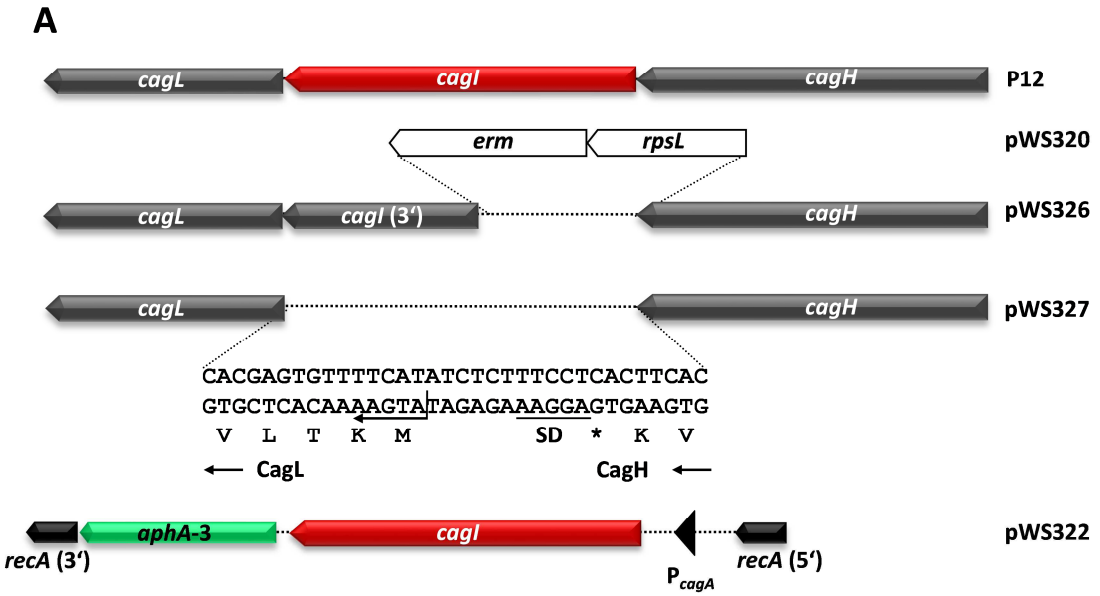

Figure 3.4. Schematic representation of constructs used for generating deletion mutants of *cagI* and complemented strains

The P12Δ*cagI* mutants generated using plasmids pWS320 and pWS326 have retained the 3' part of *cagI* containing the *cagL* transcriptional start site, whereas the mutant generated using pWS327 contains no trace of *cagI*. Instead, the Shine-Dalgarno sequence of *cagH* is used as a ribosome binding site for *cagL* allowing the transcription directly from *cagH* to *cagL*. The complementation of these mutants was performed *in trans* using a chromosomal integration vector containing *cagI* (pWS322). The *cagI* gene was integrated into the *recA* locus and expressed under the control of the *cagA* promoter.

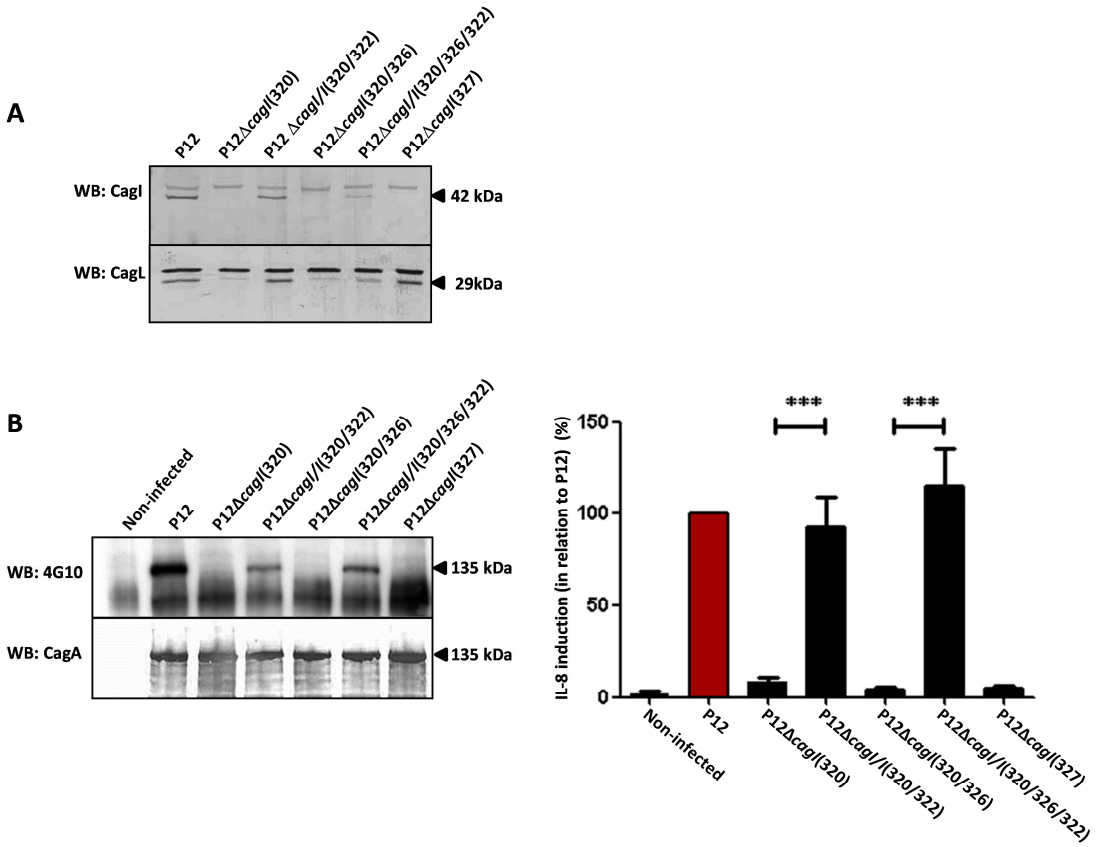

Figure 3.5. Analysis of CagI and CagL production in different *cagI* mutants

(A) CagI and CagL immunoblot analysis from whole cell lysates of strain P12 and the indicated mutants or complemented mutants. (B) Functionality of the Cag-T4SS from strain P12 and the indicated mutants was tested by performing infection assays of AGS cells to determine CagA tyrosine phosphorylation. The IL-8 values induced by the P12 wild-type were set to 100% and other values were normalized to these values (%). The data collected from at least 3 independent experiments were statistically analyzed by One-way ANOVA (***P < 0.001).

3.1.2.3 CagL has a stabilizing effect on CagI

Since the complementation of a complete *cagI* deletion mutant (strain P12Δ*cagI*(327)) (section 3.1.2.2) was not successful (data not shown), another approach was applied to generate a mutant which lacks the complete *cagI* gene. A double mutant (strain P12Δ*cagIL*) lacking both *cagI* and *cagL* was constructed from the P12 wild-type strain by replacing both *cagI* and *cagL* with a chloramphenicol resistance gene cassette using plasmid pPT2 (Figure 3.6). The loss of CagI, and CagL production in this mutant was tested by immmunoblotting as shown in Figure 3.7A. As expected, the P12Δ*cagIL* double mutant was defective in production of CagI and CagL. Subsequently, this mutant

was complemented using chromosomal *recA* integration vectors containing either *cagI* (pWS322) alone, *cagL* alone (pWS255), or both genes together (pPT3). These plasmids were constructed as described in section 2.1.5. The complementation of the double mutant with *cagI* alone (strain P12Δ*cagIL/I*) restored production of the CagI protein, but at lower levels than the P12 wild-type strain, whereas complementation with *cagL* alone (strain P12Δ*cagIL/L*) resulted in production of CagL at wild-type levels (Figure 3.7A). Wild-type phenotypes were rescued when both genes were complemented (strain P12Δ*cagIL/IL*). Thus, in the same mutant background, the complementation of both genes (*cagI* and *cagL*) recovered production of CagI at the level of the P12 wild-type strain, whereas the complementation of *cagI* only did not. Notably, as mentioned before, the effect of CagL on CagI was observed in the *cagL* knock-out mutant as well (Figure 3.3A). Taken together, these data provide evidence for a stabilizing effect of CagL on CagI. In contrast, CagL production showed unchanged levels in the presence or the absence of CagI, providing the first hint that CagI is not absolutely required for CagL production and/or stability.

The functionality of these mutants was assessed by infection experiments of AGS cells. The results obtained from IL-8 induction and CagA phosphorylation showed that deletion of *cagI* and *cagL* resulted in a deficiency of the double mutant (strain P12Δ*cagIL*) for both phenotypes. Neither the *cagI* nor *cagL*-complemented double mutant has an ability to translocate CagA and induce IL-8. In contrast, complementation of this mutant with *cagI* and *cagL* together (strain P12Δ*cagIL/IL*) fully rescued the P12 wild-type phenotype (Figure 3.7B). These data confirmed that CagI and CagL are independently required for Cag-T4SS functionality.

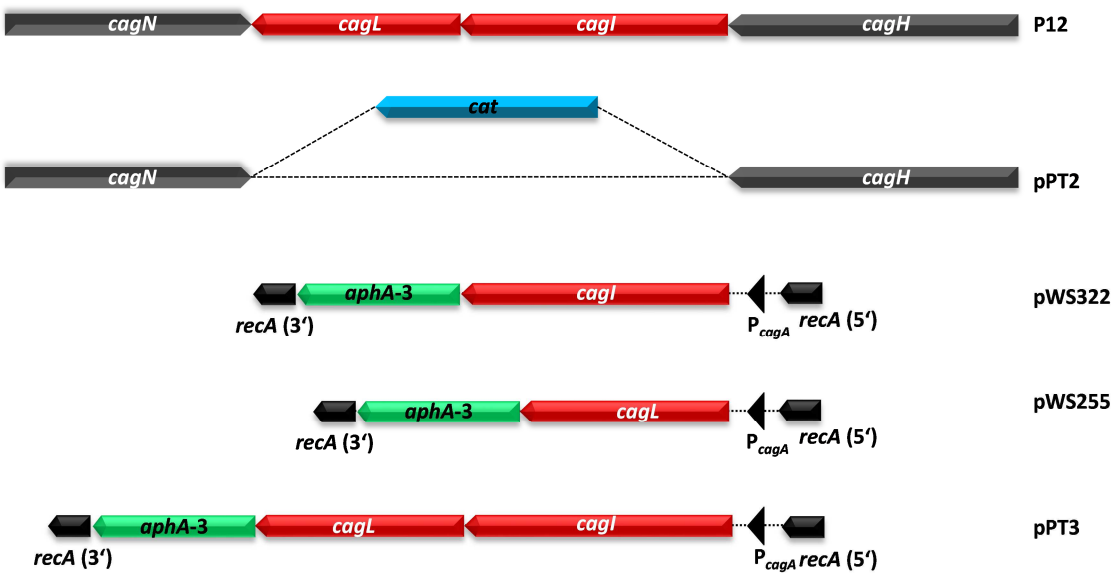

Figure 3.6. Schematic representation of constructs used for generation of the P12Δ*cagIL* double mutant and for complementation of this mutant

The P12Δ*cagIL* double mutant was constructed by transforming plasmid pPT2 containing a terminatorless chloramphenicol resistance cassette into strain P12. The resulting strain subsequently, the P12Δ*cagIL* double mutant was complemented with plasmids contaning *cagI* or *cagL*, or both genes (pWS322, pWS255 and pPT3, respectively). The genes were integrated into the *recA* locus and expressed under the control of the *cagA* promoter.

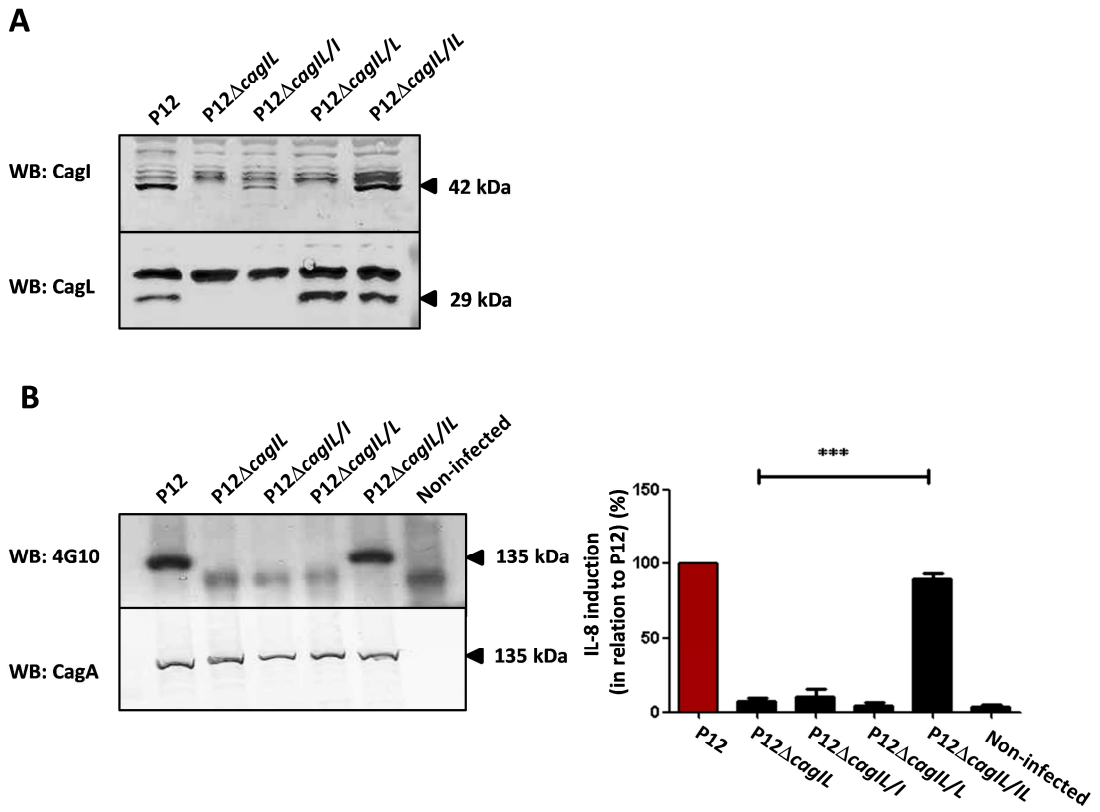

Figure 3.7. Functional analysis of the P12Δ*cagIL* double mutant

(A) Whole cell lysates from strain P12 and the indicated mutant strains were immunoblotted using CagI and CagL antibodies, respectively. The production of CagI and CagL was defective in strain P12Δ*cagIL,* and restored by genetic complementation. (B) Functionality of the Cag-T4SS from the P12Δ*cagIL* double mutant and complemented strains was tested by performing infection assays of AGS cells to determine CagA tyrosine phosphorylation. The IL-8 values induced by the P12 wild-type strain were set to 100% and other values were normalized to these values (%). The data collected from at least 3 independent experiments were statistically analyzed by One-way ANOVA (***P < 0.001).

3.1.2.4 *cagI* deletion does not influence *cagL* transcription

To corroborate the conclusion drawn above that *cagI* deletion results in the CagL protein destabilization, rather than a loss of the *cagL* transcription, a quantification of *cagL* transcript levels in the different *cagI* mutants which produced varying levels of CagL was performed. For this purpose, total RNA from liquid cultures of the P12 wild-type strain and the different *cagI* mutants was prepared and used for cDNA synthesis via a reverse transcription using a random primer. Subsequently, conventional PCR and real-time PCR were carried out using specific primer pairs for *cagL* gene and primers for 16S RNA. The specific primers for *cagL* and 16S RNA were designed for

amplifying a fragment with the size of 91 bp and 79 bp, respectively. The control PCR showed amplified PCR bands for *cagL* using specific primers WS379 and WS304, and 16S RNA using primers UB044 and UB045 from cDNAs but not from mRNA samples (Figure 3.8A), showing that the preparation of cDNA was not contaminated by genomic DNA. The quantification of *cagL* mRNA by qPCR showed no significant difference between the P12 wild-type strain and most of the different *cagI* mutants (Figure 3.8B). Interestingly, however, in the mutant P12Δ*cagI*(327), in which the entire *cagI* gene had been deleted, the *cagL* mRNA transcript level was 6,04 ± 4,67 fold increased in respect to the P12 wild-type strain. As mentioned above, this mutant produced normal amounts of CagL in comparison to the wild-type strain, nevertheless was defective in CagA translocation and IL-8 induction. This suggests that the decreased CagL stability was overturned by the higher *cagL* transcription rate in this mutant. Taken together, these data demonstrated that the transcription of *cagL* is not generally influenced by deletion of *cagI.*

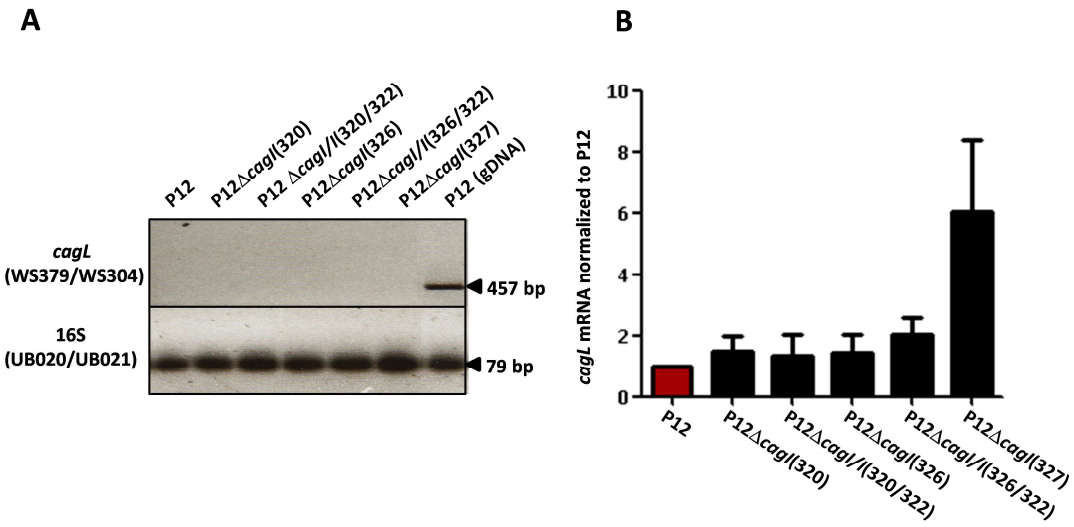

Figure 3.8. *cagL* transcription analysis

The P12 wild-type strain and the indicated *cagI* mutants were cultured in liquid media to mid exponential phase before being harvested for RNA extraction and cDNA synthesis. (A) The control PCR was done from cDNA templates using primers pair WS379 and WS304 for *cagL*, and UB020 and UB021 for 16S RNA. (B) Quantitative real-time PCR using primers UB044 and UB045 was carried out to analyze the transcript levels of *cagL* in each cDNA samples. The analysis of 16S RNA transcript levels was performed in parallel for normalization. The values obtained from P12 wild-type were set to one and other values from at least 3 independent experiments were given in relation to P12 with standard errors of the mean and statistically analyzed by One-way ANOVA.

3.1.3 Localization of CagI and CagL

To characterize the CagH, CagI and CagL proteins, we sought to localize these unique Cag protein components in *H. pylori*. Except for CagL, there were no experimental data available about the localization of these proteins in *H. pylori*. The CagL protein has been described as a cytoplasmic or periplasmic protein [Kutter *et al.*, 2008], a pilus-covering protein [Kwok *et al.*, 2007] or a membrane-associated protein [Tegtmeyer *et al.*, 2010]. In the current study, different approaches were used for localization of these proteins.

For subcellular localization of CagI and CagL, *H. pylori* cells were fractionated into a soluble and an insoluble fraction containing membrane-associated components. The insoluble components were then extracted by the non-ionic detergent Triton X-100, which preferably solubilizs cytoplasmic membrane proteins [Pattis *et al.*, 2007]. The presence of CagI and CagL proteins was tested by Western blotting using CagI and CagL antibodies. As shown in Figure 3.9A, CagI was found both in the membrane fraction and the soluble fraction containing cytoplasmic and periplasmic proteins. CagI was not extracted completely by Triton X-100, suggesting that it might be inner membrane-associated. Unlike CagI, CagL was mostly found in the soluble fraction and only a minor part in the total membrane fraction which was not solubilized by Triton X-100. The fractionation of the P12 wild-type strain and the P12Δ*cagI* was performed in parallel and the results indicated that there is no significant difference between the P12 wild-type strain and the *cagI* deletion mutant. Control immunoblots showed that the outer membrane-associated proteins CagX and AlpB were present only in the membrane fraction and were not extracted by Triton X-100, whereas the inner membrane-associated protein RecA was considerably extracted with this detergent.

To gain more evidence for the localization of CagI and CagL, the total membrane vesicles which had been suspended in Triethanolamine buffer were also subjected to sucrose density gradient centrifugation. Each fraction from sucrose gradients was examined for the presence of CagI, CagL, and as a control, of the outer membrane-associated proteins CagX and AlpB and the inner membrane-associated protein RecA by immunoblotting. The results showed that CagI and CagL occur both in outer and inner membrane associated pools, whereas the control proteins CagX and AlpB were

present only in high density fractions and RecA was found in several fractions (Figure 3.9B).

Since CagI and CagL were found both in the outer and inner membrane-associated protein fractions, it still remained unclear whether these two proteins might be partially surface- exposed. To investigate a possible surface localization, CagI and CagL, as well as control proteins were analyzed for susceptibility to proteinase K digestion. Equal amounts of treated and untreated cells were immunoblotted using specific antibodies. As shown in Figure 3.9C, CagI and CagL were substantially digested by proteinase K treatment. The AlpB protein, which is known to be surface exposed, was digested completely, whereas the inner membrane protein RecA was not affected by proteinase K digestion. CagI was strongly degraded by proteinase K treatment, whereas CagL was only slightly reduced.

Taken together, these observations suggest that CagI and CagL exist in a non-surface localization to a considerable degree, and are partly localized at the surface of bacteria as well.

Immunofluoresence staninings were performed in order to localize CagI in *H. pylori*. However, the results were not conclusive because of unspecific background stainning (data not shown). Likewise, in this study, attempts to generate a tagged-CagI for this purpose have not been successful (data not shown). Therefore, surface localization of CagI could not be confirmed by this method.

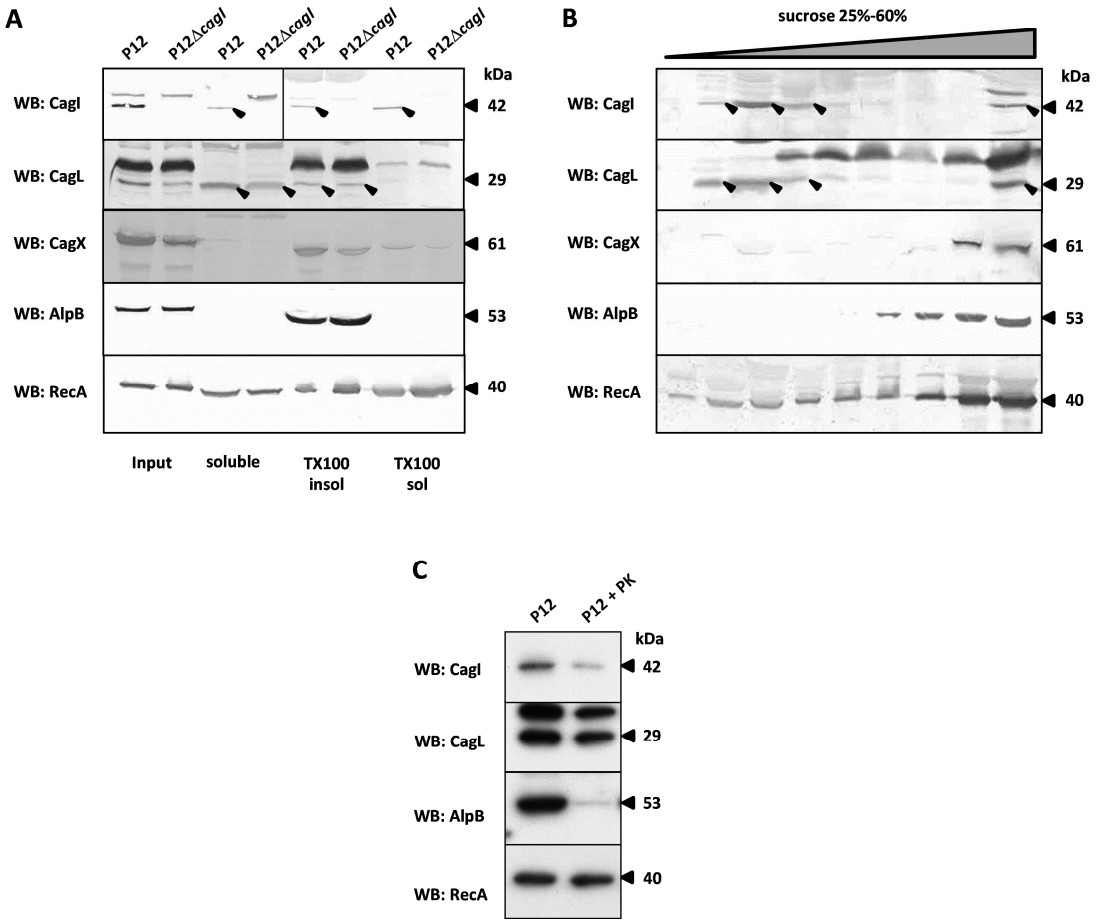

Figure 3.9. Localization of CagI and CagL in baterial cell fractions

(A) Cell pellets from 24 h liquid cultures of the P12 wild-type and the P12Δ*cagI* strain were ultrasonicated and fractionated into soluble and insoluble proteins by ultracentrifugation. The supernatants contain soluble proteins, whereas the membrane associated and other insoluble proteins are located in the pellets which were subsequently extracted with 1% Triton X-100 for separating outer membrane-associated (TX100 insol) from inner membrane-associated proteins (TX100 sol). Anti-CagI and anti-CagL western blot analysis was done to compare the amounts of CagI and CagL in different fractions. Western blots against the outer membrane-associated proteins CagX, AlpB and the partly soluble and partly inner membrane-associated protein RecA were performed in parallel as controls. (B) The ultrasonication pellets were resuspended in preparation buffer and subjected to preparative sucrose density gradient centrifugation on 25-60% sucrose gradients. Collected fractions were analyzed for the presence of CagI, CagL and control proteins by immunoblotting with the indicated antisera. (C) Whole bacterial cells were subjected to limited proteolytic digestion with proteinase K. Equal amounts of treated (P12 PK) and untreated bacteria (P12) were immunoblotted with the indicated antisera[3].

[3] was performed by Luisa Jimenez Soto

3.1.4 Influence of *cag* genes on the interaction between *H. pylori* and α5β1 integrin

CagL was previously found as a pilus component [Kwok *et al.*, 2007]. It has also been shown that *H. pylori,* via the Cag apparatus, can bind to integrin α5β1 expressed on the host cell surface. By Yeast Two Hybrid assays and protein pull-down assay, several proteins of the Cag apparatus such as CagY and CagL, and the CagA effector protein, were found to interact with β1 integrin [Jimenez-Soto *et al.*, 2009]. Recently, Shaffer *et al*. [Shaffer *et al.*, 2011] reported that CagH, CagI and CagL have important roles in the formation of the type IV secretion-associated pili. Based on these observations, we sought to set up an easy assay for investigating the production of pili and the role of CagH, CagI and CagL proteins, by detecting the binding of integrin α5β1 to *H. pylori.*

We investigated the binding of the closed and open forms of the integrin α5β1, which were used as purified recombinant proteins, with *H. pylori* (described in section 2.2.3.16). The soluble integrin α5β1 was initially in an in inactive form (Figure 3.10, upper panel). To create an active form of integrin α5β1, a TEV protease cleavage was carried out[4]. With this step, a His-tag which had been used for purification of integrin α5β1, and a BASE peptide responsible for the interaction, were cleaved off and the open form (active) of integrin was released (Figure 3.10, lower panel). For detection purposes, these forms of integrin α5β1 were coupled to Alexa 647 dye. After purification and quantification, they were used at the same amounts for binding assays.

Based on the hypothesis that pilus formation is stimulated by cell contact, we performed experiments under two conditions. On the one hand, bacteria were collected and subjected to binding assays. On the other hand, a short infection experiment with AGS cells was performed before unbound bacteria were harvested for binding experiments. Bacteria were incubated with purified and soluble Alexa 647 fluorescently labeled integrin α5β1 protein complex (closed and open). Several *cag* gene deletion mutants such as *cagI* and *cagL* deletion mutants were used in parallel with the P12 wild-type

[4] was performed by Lea Holsten

strain and the *cag*-PAI mutant, which served as a positive control and a negative control, respectively.

The binding of active and inactive α5β1integrins shown by the level of fluorescence was determined on BD Biosicence CantoII flow cytometry. Data were analyzed using the Flowjo software. Unexpectedly, there was no stronger binding of bacteria to the integrin α5β1 active and the inactive forms after being exposed to cells (data not shown). As seen in Figure 3.11A and B, bacteria show a higher specificity and a higher affinity to the inactive α5β1 integrin than to the active one. There was a significant decrease in binding affinity of the active and the inactive forms to the *cag*-PAI or *cagI* deletion mutants compared to the P12 wild-type strain. However, we observed no significant difference between the P12 wild-type and the *cagL* mutant. These data suggest that *H. pylori* were able to bind to both forms of integrin α5β1 with a higher affinity to the inactive form of integrin α5β1 than to the active form. These findings provide another experimential evidence for the role of CagI and CagL in mediating the binding of the Cag-T4SS to integrin. However, further studies are required to clarify this point.

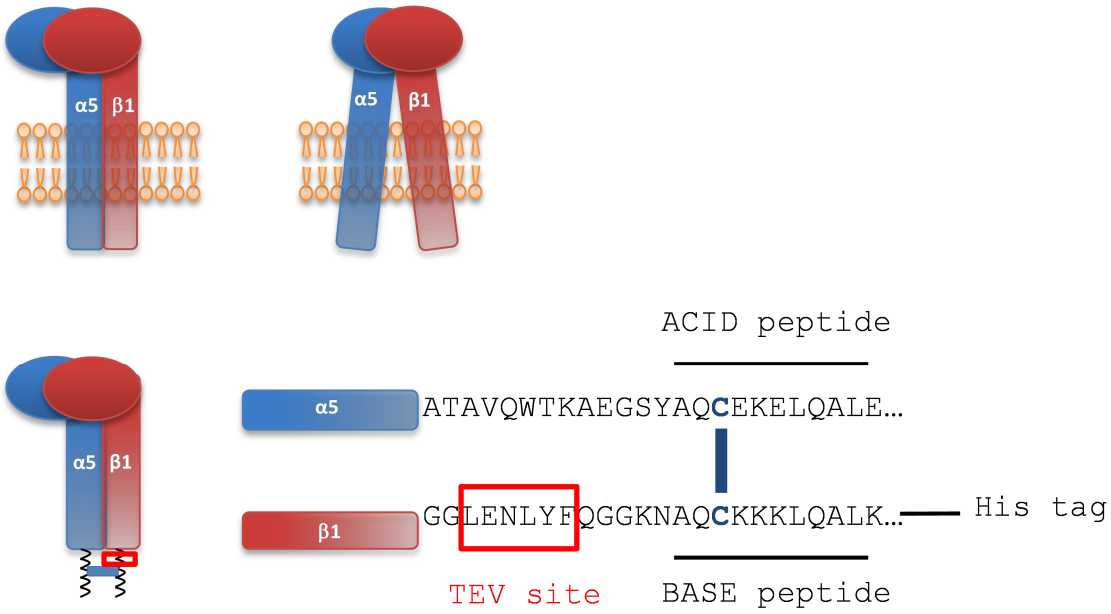

Figure 3.10. Scheme for release of the C-terminal claspe of the recombinant integrin α5β1by TEV cleavage

The inactive (left) and active (right) forms of the soluble integrin α5β1 forms of the soluble integrin α5β1. To generate the active form of integrin α5β1, a TEV protease cleavage was carried out. With this step, a His-tag and base peptide which had been used for purification of integrin α5β1, were cleaved off and the open form of integrin was released. These forms of integrin α5β1 were coupled to an Alexa 647 dye.

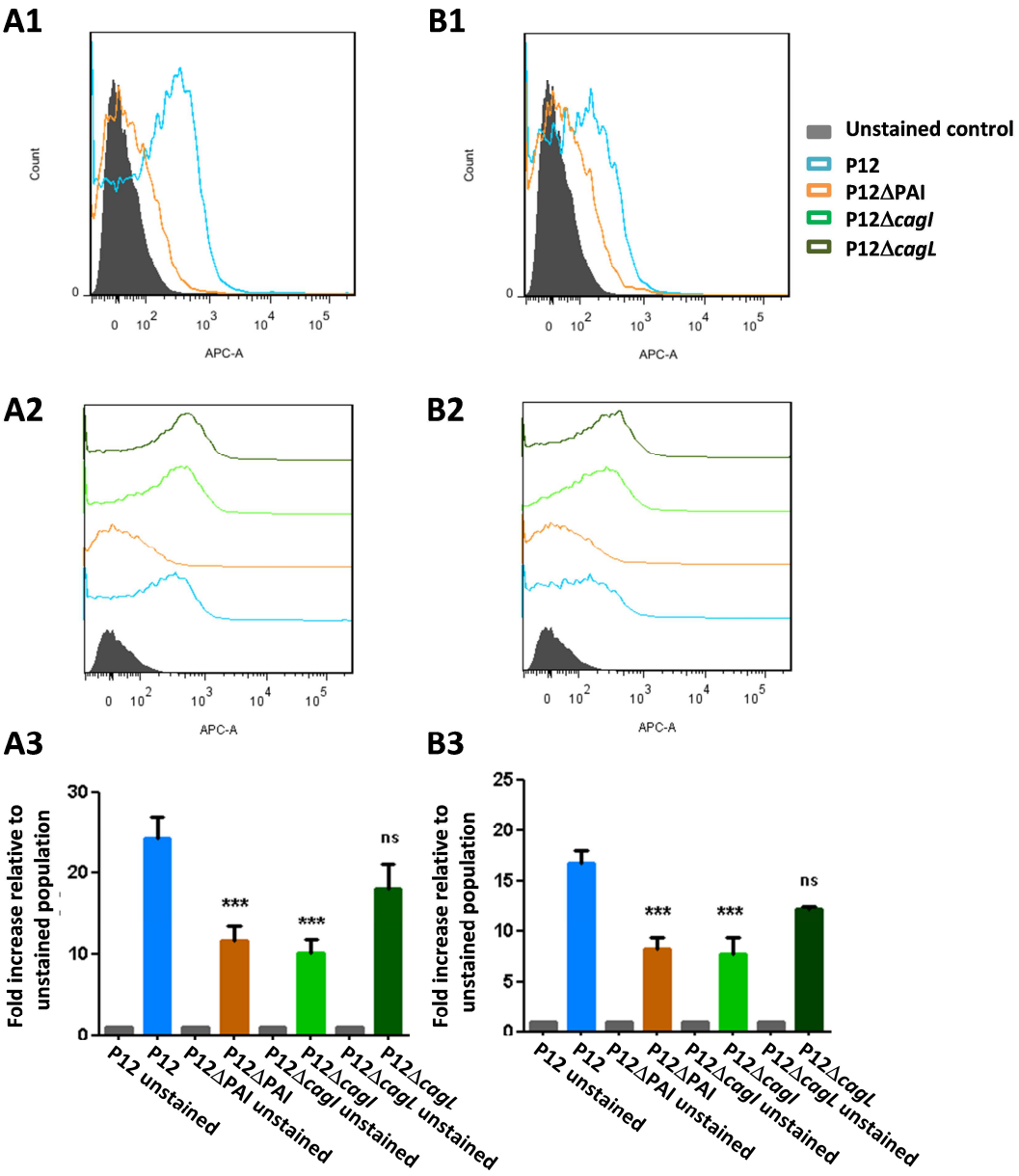

Figure 3.11. Invwhenestigation of α5β1 integrin binding

(A-B) Bacterial suspensions off the P12 wild-type strain and the indicated mutants were incubated with purified integrin α5β1 labelled with Alexa fluor 647. The cell binding measured using flow cytometry analysis (FACS BD CantoII) is shown in the histograms. Filled histogram corresponds to unstained P12 wild-type control. The blue, orange, green, dark green and red curves correspond to P12, P12ΔPAI, P12Δ*cagI*, P12Δ*cagL*, respectively. The representative histograms were from 5 independent experiments with duplicated samples. (A) Bacteria stained with the active α5β1 labelled Alexa fluor 647. (B) Bacteria stained with the inactive α5β1 labelled Alexa fluor 647. (A3), (B3) The fluorescence intensity was analyzed by FACS. Bar graphs show the mean values, and error bars indicate s.e.m. The fluorescence intensity from stained bacteria of the indicated strains was given in relation to unstained controls which were set to 1. The differences from unstained control values were analyzed by One-way ANOVA (***P < 0.001).

3.2 Interaction between CagH, CagI and CagL

Multiple protein-protein interactions have been observed among components of well-known type IV secretion systems from other bacterial species, as well as among Cag proteins of the Cag-T4SS in *H. pylori*. Based on the observations about expression levels of *cagI* or *cagL*, in the different isogenic deletion mutants generated in strain P12, we hypothesize that the stability of these proteins might depend on the presence of the other components. Such interactions might be crucial for functionality of the Cag-T4SS.

3.2.1 Determination of CagI- and CagL- interacting proteins by immunoprecipitation

To determine whether CagH, CagI and CagL proteins interact with each other in strain P12, immunoprecipitation (IP) experiments were conducted from whole cell extracts using the CagI antiserum. Immunoblot analysis of CagI, CagL and CagH of the immunoprecipitated fractions was performed using the corresponding antibodies. The mutants lacking either *cagI* or *cagL* were extracted in parallel and served as negative controls. Immunoblot analysis of CagI and CagL after IP using the polyclonal CagI antibody showed that CagL was successfully precipitated with CagI from a cell extract of the P12 wild-type strain but not from the *cagI* mutant. The same results were obtained in the reverse IP using the CagL antibody, demonstrating the specificity of the IP, and that CagI indeed interacts with CagL. Likewise, CagH was observed to be precipitated together with CagI or CagL from P12 extracts, but not in extracts of either the *cagI* or the *cagL* mutant (Figure 3.12). It might be that in these mutants, CagH was not highly expressed or unstable because of stabilizing effects between these three proteins, therefore it was below the detection limit of our blots. These observations provided evidence for the interaction of CagH, CagI and CagL proteins. They might form a complex in *H. pylori* cells.

In order to obtain further evidence for the interaction of CagI and CagL, we performed IP experiments using the CagL antibody from the soluble fraction of the bacterial subcellular fractionation (section 3.1.3), which is supposed to contain cytoplasmic and periplasmic proteins. The precipitated proteins from the soluble fraction of the P12 wild-type strain and the *cag*-PAI deletion mutant were examined for the presence of CagI and CagL proteins by Western blotting using the corresponding antibodies (Figure

3.12B). The results show that CagI was precipitated with CagL in the soluble fraction, suggesting this interaction might take place in the bacterial periplasm after being exported from the bacterial cytoplasm.

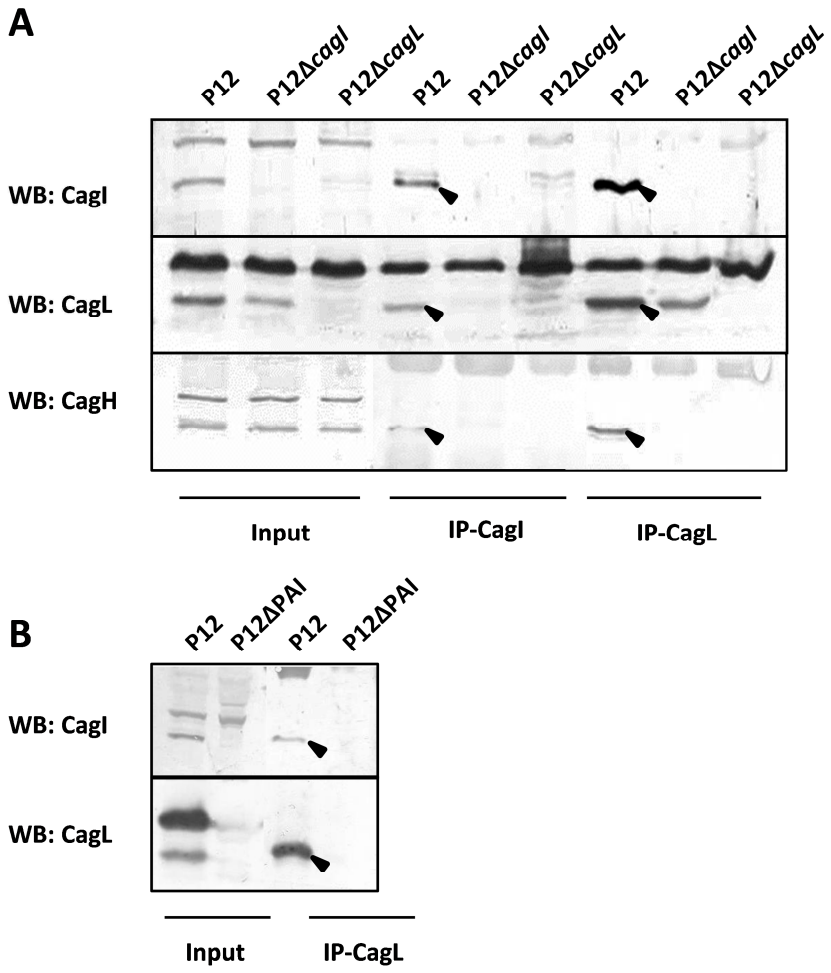

Figure 3.12. CagH, CagI and CagL interact with each other

(A) Whole cell lysates of the P12 wild-type strain, or its isogenic *cagI* or *cagL* mutants were tested for the presence of CagH, CagI and CagL proteins with the corresponding antibodies. Cell extracts from strain P12 and indicated mutants were subjected to immunoprecipitaton using CagI and CagL antisera. The immunoprecipitated proteins were checked for the presence of CagH, CagI and CagL by Western blotting using corresponding antisera. (B) Cell pellets from 24 h liquid cultures of the P12 wild-type and the P12ΔPAI strains were ultrasonicated and fractionated into soluble and insoluble proteins by ultracentrifugation. Supernatants containing soluble proteins were used for immunoprecipitaton using the CagL antiserum. The immunoprecipitated proteins were checked for the presence of CagI and CagL by Western blotting.

3.2.2 Generation of a Myc tagged-CagI variant for IP using the monoclonal Myc antibody

Since CagI was very unstable and produced at low levels, working with this protein turned out to be very difficult. Based on the complementation established earlier (section 3.1.2.3) we generated a construct for introducing a tag into CagI. A Myc tag was chosen since it had proven to work properly in *H. pylori* [Jurik *et al.*, 2010]. A Myc tag was first introduced at the C-terminus part of CagI. Although the resulting strains are able to express Myc tagged-CagI, they were not able to translocate CagA and to induce IL-8 (data not shown). This might be explained by interference of the Myc tag with the C-terminal motif of CagI, which seems to play a role in interaction of CagI with other Cag proteins [Shaffer *et al.*, 2011]. The Myc coding sequence was cloned behind the DNA sequence coding for the N-terminal signal peptide and into a predicted exposed loop (residue 51) to ensure the proper translocation, resulting in plasmid pPT4 (contructed as described in 2.1.5). The tagged-*cagI* construct was introduced into the *recA* locus of the double mutant P12Δ*cagIL* and expressed under the control of the *cagA* promoter (Figure 3.13A).

The expression of CagI-Myc and CagL was checked by immunoblotting using the CagI, CagL and Myc antibodies (Figure 3.13B). The results showed that the CagI-Myc fusion protein was expressed in the complemented mutant with a reduced amount compared to the level of the wild-type protein. Another tag, the M45 tag, was used to replace the Myc tag (plasmid pPT6), but this construct was not successful (data not shown). Nevertheless, infection experiments were performed to check for Cag-T4SS functionality of the strain producing Myc-taaged CagI. The results showed that the IL-8 induction capability was rescued, but CagA translocation efficiency was extremely reduced in comparision to the P12 wild-type strain (Figure 3.13C). It might be that the introduced tag interfered with expression and activity of CagI. Therefore, one possible explanation for the reduction of CagA translocation efficiency observed in the *Myc-cagI* complemented strain might be due to the reduced amount of CagI.

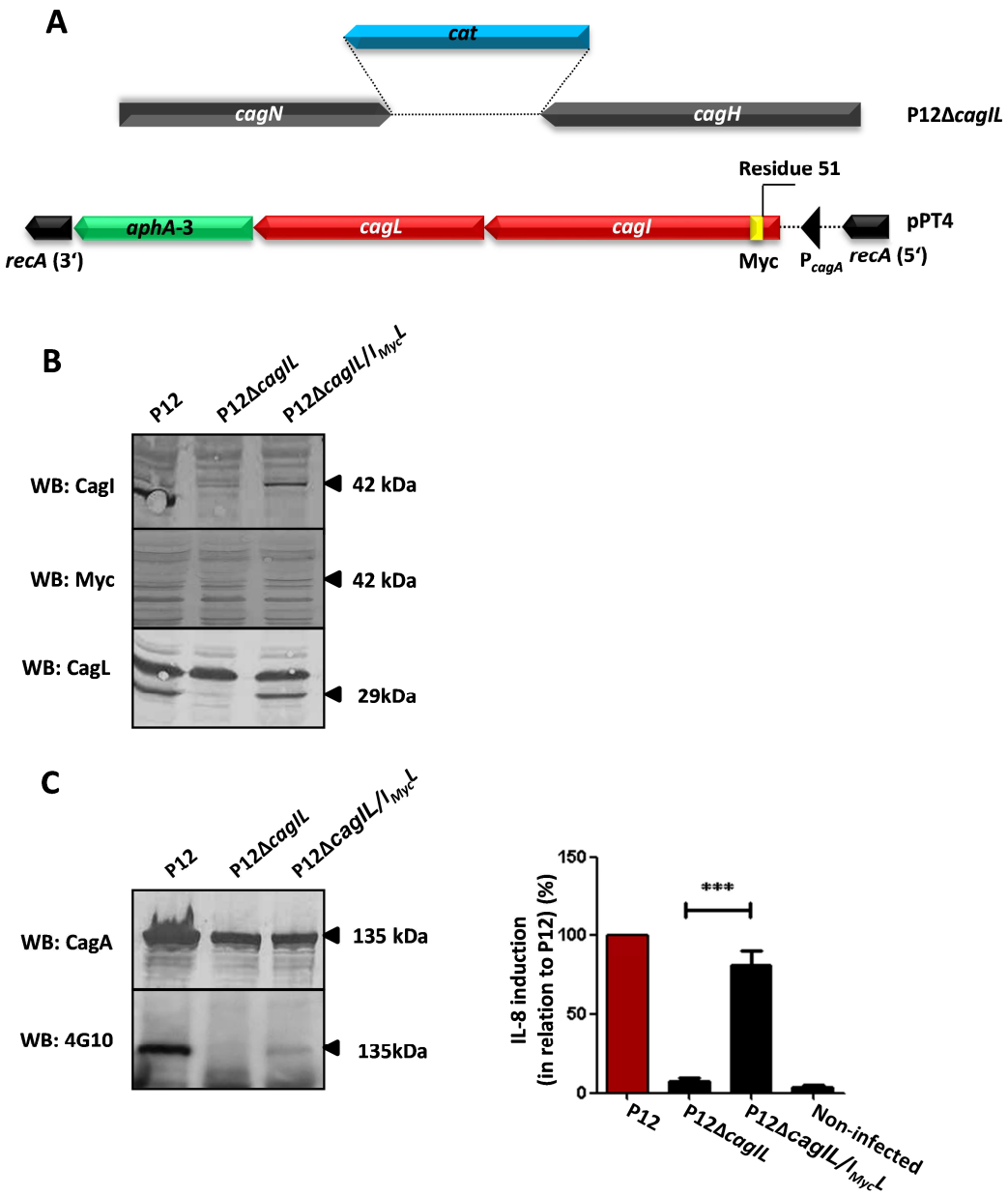

Figure 3.13. Generation of Myc tagged-CagI

Schematic representation of constructs used for generation of epitope-tagged CagI. The P12Δ*cagIL* mutant was transformed with plasmid pPT4 containing *cagI-Myc* and *cagL* with a kanamycin resistance gene cassette. The *Myc* gene was cloned into the N-terminal part at residue 51 of *cagI*. The epitope-tagged *cagI* together with *cagL* were introduced into the *recA* gene of the P12Δ*cagIL* double mutant and expressed under the control of the *cagA* promoter. (B) Whole bacterial lysates of strain P12 and of the indicated mutants were immunoblotted using antisera against CagI, CagL and Myc proteins. (C) Functionality of the Cag-T4SS of the *Myc-cagP*-complemented mutant was tested by performing infection assays of AGS cells to determine CagA tyrosine phosphorylation. The IL-8 values induced by the P12 wild-type were set to 100% and other values were normalized to these values (%). The data collected from at least 3 independent experiments were statistically analyzed by One-way ANOVA (***P < 0.001).

Since CagI is still functional with respect to IL-8 induction after adding a Myc epitope tag into the N-terminal part of this protein, we performed immunoprecipitation experiments of the P12Δ*cagIL/I*$_{Myc}$*L* strain using a monoclonal Myc antibody. The P12 wild-type strain and the *cagI* (P12Δ*cagIL/L*) and *cagL* (P12Δ*cagIL/I*) mutants, which served as negative controls, were performed in parallel in order to show the specificity of this method. Immunoblots of the immunoprecipitated proteins and the starting materials were done using the CagI, CagL and Myc antibodies. The results showed the presence of the Myc and the CagI proteins in the cell preparation derived from the Myc-tagged-CagI-complemented strain only. The CagL protein was detected to be immunoprecipitated with the Myc protein in cell extracts of the complemented strain, however it showed up with a comparative strength in the P12 wild-type strain as well (indicated with red arrowheads), suggesting an unspecific interaction of the monoclonal Myc antibody with CagL (Figure 3.14). Attempts to get rid of unspecific binding of contaminating proteins by a pre-incubation of cell lysates with G-agarose beads, removing intact cells by ultracentrifugation or using a buffer with a higher salt concentration were not successful. Therefore, the interaction between CagI and CagL could not be conclusively shown by this assay.

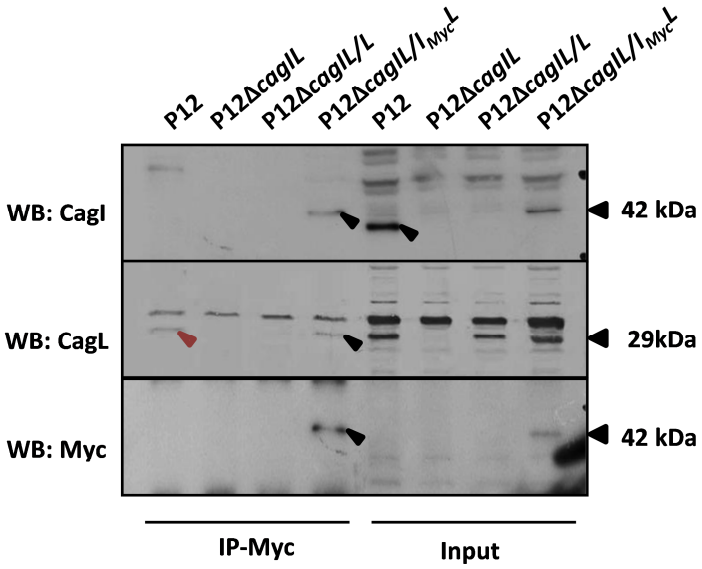

Figure 3.14. Investigation of an interaction between CagI and CagL by Myc immunoprecipitation

Whole cell lysates of strain P12, or the indicated mutants were tested for the presence of CagI, CagL and Myc-CagI with the corresponding antibodies. As controls, the mutants which had been complemented with either *cagI* or *cagL* (strains P12Δ*cagIL/I* and P12Δ*cagIL/L*) were used. Cell extracts from strain P12 and the indicated mutants were subjected to immunoprecipitaton using the Myc monoclonal antibody. The immunoprecipitated proteins were checked for the presence of CagI, CagL and Myc-CagI by Western blotting using corresponding antisera.

3.2.3 Pull-down experiments

3.2.3.1 GST pull-down experiments

To further investigate potential interactions of CagI and CagL, a direct interaction assay using GST fusion proteins was performed. On the one hand, for confirmation of the IP results, full-length versions of either CagI or CagL coupled to Glutathione Sepharose 4B beads were used for capturing interacting proteins from *H. pylori* lysates. A GST protein which is 220 amino acids (26 kDa) in size, was added to the N-terminus of CagI and CagL proteins lacking their signal sequences (the first 23 and 20 amino acids, respectively). On the other hand, to find out a potential binding domain between CagI and CagL, different truncated versions of either GST-CagI or -CagL fusion proteins were generated in parallel and used in the same GST pull-down experiments.

All constructs which were used for expressing fusion proteins are shown in Figure 3.15. *E. coli* BL21 (DE3) containing pWS258 and pPT8 were used for expressing full-length

CagI and CagL, respectively. Furthermore, as described above, CagH, CagI and CagL contain a conserved C-terminal motif with 6 amino acids (Figure 3.1C). Besides, a closer inspection of CagH, CagI and CagL amino acid sequences using the JPred software predicted coiled-coil structures, close to the C-terminal ends of CagI and CagL, but not of CagH (http://www.compbio.dundee.ac.uk/www-jpred/). Therefore, to investigate whether the C-terminal motifs and/or the coiled-coil structures are involved in interactions of CagI and CagL, we generated different truncation variants of CagI and CagL fusion proteins (Figure 3.15). CagI and CagL were truncated from the C-terminus by removing the C-terminal motif coding sequences (7 and 8 amino acid, respectively) or the DNA regions coding the coiled-coil structures (57 and 44 amino acids, respectively). The *cagI* gene was furthermore truncated in such a way that the predicted transcriptional start site of *cagL* located in *cagI* was excluded. The plasmids were constructed as described in section 2.1.5.

As shown in Figure 3.16A1 and B1, full-length proteins and variants of CagI and CagL were expressed in *E. coli* (indicated by black arrowheads). The samples were immunoblotted using the GST monoclonal antibody and either CagI (Figure 3.16A2) or CagL (Figure 3.16B2) antibody. As expected, the GST protein was detected in all samples. Taken together with these data obtained from SDS-PAGE analysis, the results showed a successful production of CagI and CagL from all constructs in *E. coli* BL21 (DE3). However, CagI could not be detected in *E. coli* lysates containing either pPT15 or pPT16 by immunoblotting, because the CagI-specific antiserum had been generated using a synthetic peptide against the coiled-coil region of CagI, which is missing in these two truncated CagI versions.

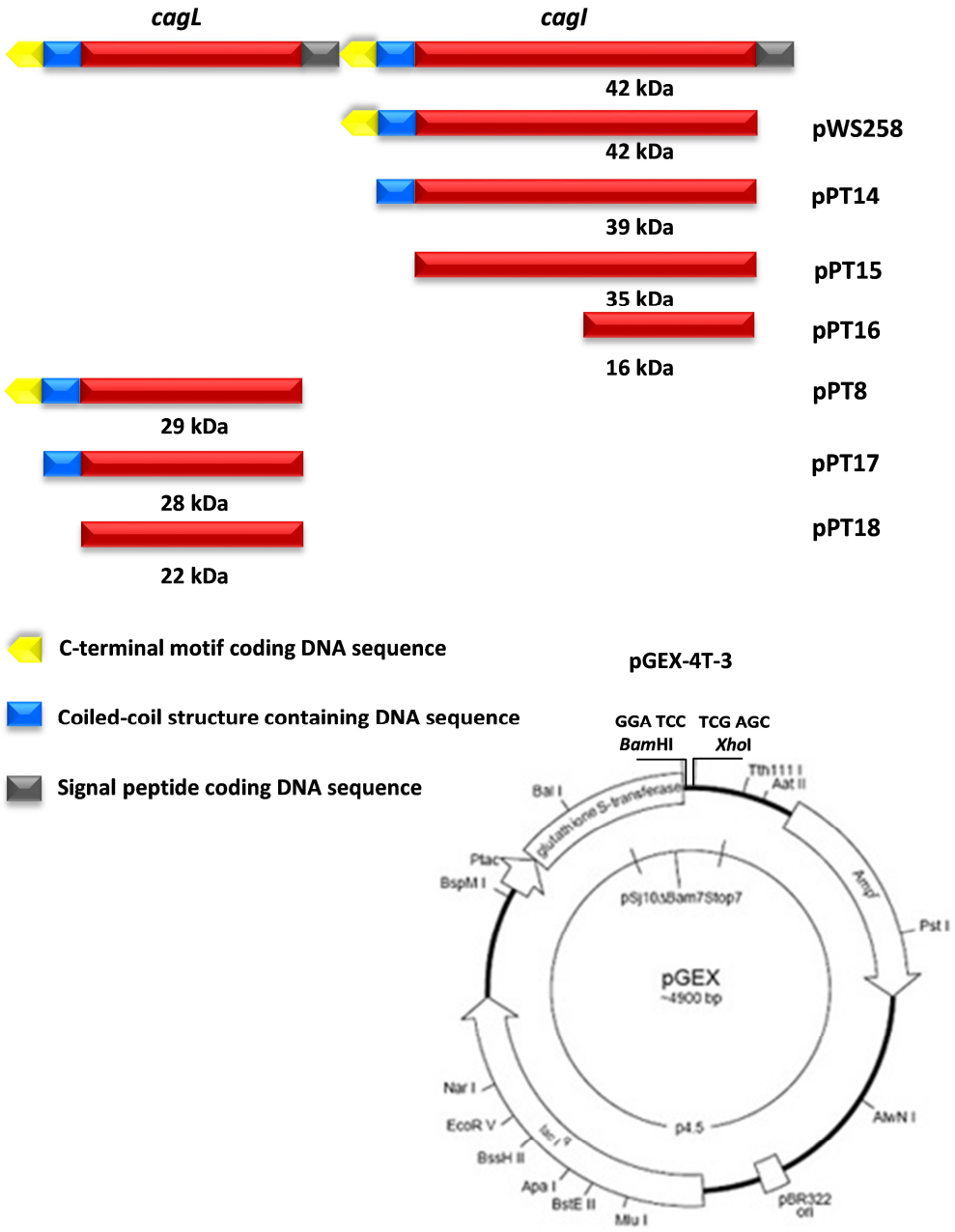

Figure 3.15. Schematic representation of plasmid contructs used to generate GST-CagI-, and GST-CagL-fusion proteins

Full-length versions without the N-terminal signal sequences of either *cagI* (pWS258) or *cagL* (pPT8), and other constructs were cloned in pGEX-4T-3. The DNA sequences coding for the C-terminal motif of CagI (7 amino acids) and CagL (8 amino aicds) were deleted in plasmids pPT14 and pPT17, respectively. CagI and CagL were truncated further by removing the sequences (57 amino acids and 44 amino acids, respectively) coding for the coiled-coil structures (pPT15 and pPT18, respectively). In the case of CagI, pPT16 was constructed in such a way that the transcriptional start site of *cagL* from *cagI* was deleted together with DNA sequences coding for the C-terminal motif and the coiled coil structure. The signal sequences, the C-terminal motifs and the coiled-coil structures are indicated in grey, yellow and blue block arrows, respectively

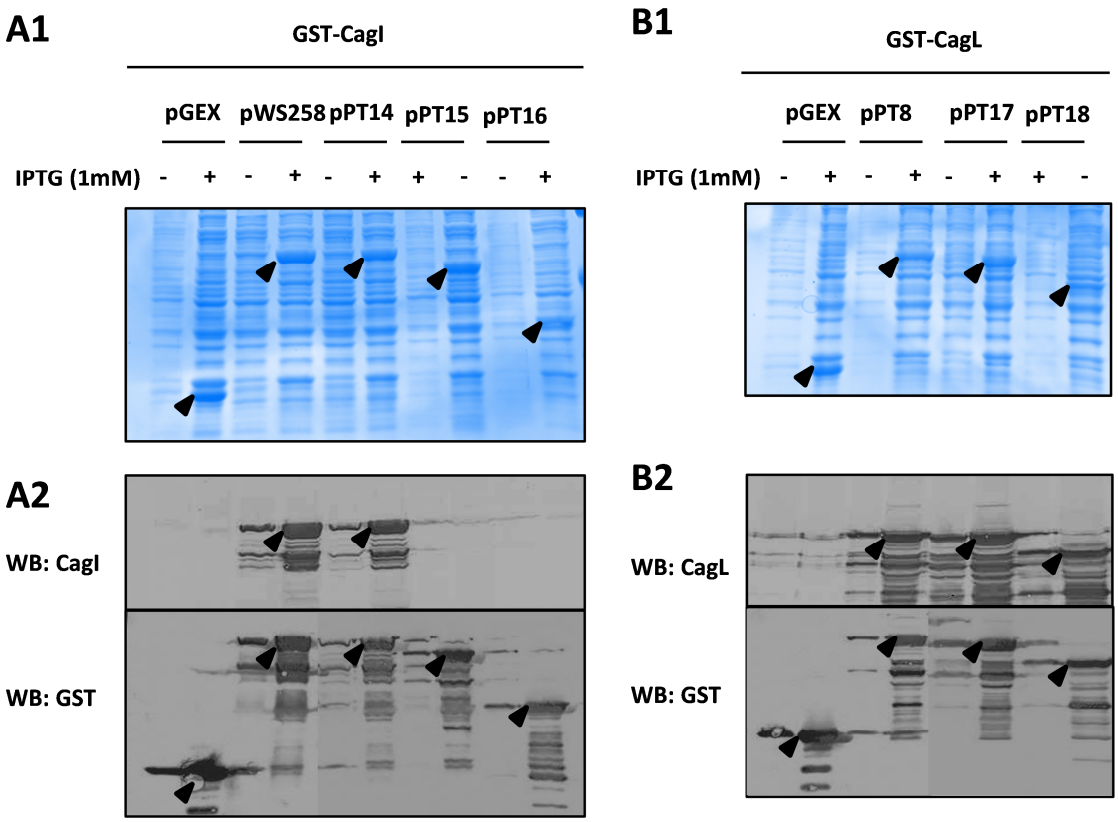

Figure 3.16. Expression of GST-CagI fusion proteins

(A1 and B1) Coomassie Brilliant Blue staining showed the expression of different truncation versions of either GST-CagI or GST-CagL. The truncated CagI versions were detected at predicted molecular weights of 68, 65, 61 and 42 kDa, respectively. The CagL truncations were detected at predicted molecular weights of 55, 54, 48, respectively. The GST protein was found at 26 kDa. (A2 and B2) Detection of GST-CagI and and GST-CagL via immunoblots.

For coupling, cell extracts of *E. coli* expressing the GST-fusion proteins, or the GST protein alone were incubated with Glutathione sepharose 4B beads (GE Healthcare). These coupled beads were then used for pull-down experiments, in which cell extracts of the P12 wild-type strain and, *cagI* and *cagL* deletion mutants as negative controls, were added as described in section 2.2.3.12. To avoid unspecific bindings of *H. pylori* proteins to glutathione sepharose 4B beads, *H. pylori* extracts were pre-incubated with GST-coupled beads.

As shown in Figure 3.17, the native CagI and CagL proteins were precipitated with the GST-CagL and GST-CagI beads, respectively (indicated by black arrowheads). However, the native CagI and CagL proteins were pulled down with the GST beads as

well (indicated by red arrowheads), suggesting unspecific interactions. Our attempts to to remove non-specific proteins prior to eluting the proteins of interest were unsuccessful. Because of these results, the truncated versions were not used further.

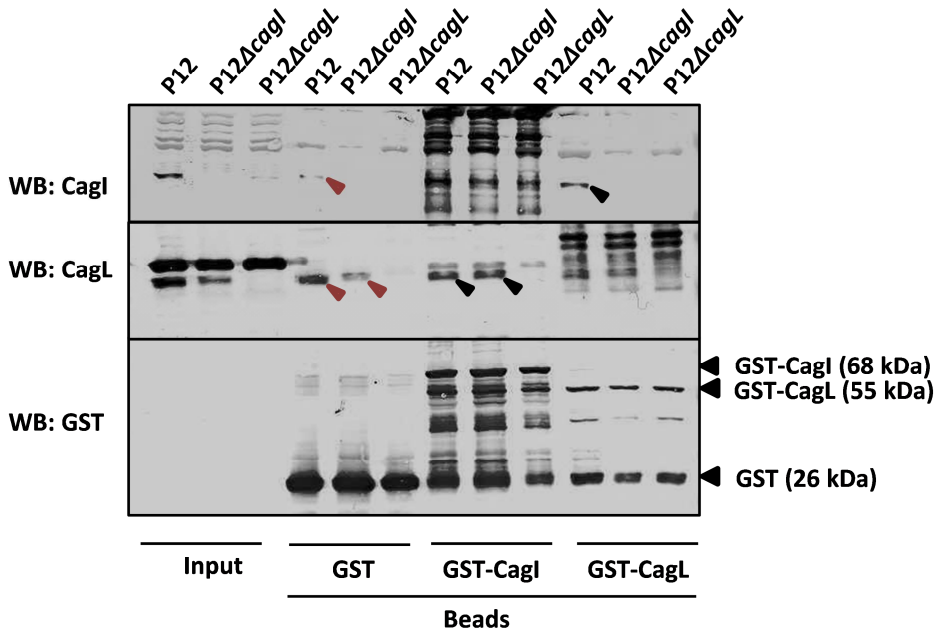

Figure 3.17. Pull-down experiments to show interactions between CagI and CagL

Whole cell lysates of the P12 wild-type strain and the indicated mutants were tested for the presence of CagI, CagL and GST proteins using the corresponding antibodies. As controls, lysates of P12Δ*cagI* and P12Δ*cagL* mutants were used. Cell extracts of strain P12 and the indicated mutants were subjected to pull-down eperiments using GST, CagI-GST and CagL-GST beads. The precipitated proteins were checked by CagI, CagL and GST immunoblots.

3.2.3.2 MBP pull-down experiments

Since the pull-down experiments using GST-fusion protein coupled beads had not been successful, another strategy was used to verify the interaction between CagI, CagL and CagH. In these pull-down assays, CagH was used as a bait protein for investigating possible direct interactions with the putative prey proteins CagI and CagL. The *cagH* gene which lacks the DNA sequence coding for a transmembrane region was cloned into pMal(g) vector and expressed in *E.coli* BL21 (DE3) as an MBP fusion protein (data not shown). A cell lysate of an induced culture of the strain producing MBP-CagH was incubated with the amylose resin. These MBP-CagH-coupled beads were then used for a pull-down assay in which either the purified target protein CagI or the CagL protein was added. The affinity purified protein samples were analyzed by Western blotting

using the CagI, CagL and MBP antibodies. As a negative control, an *E. coli* lysate containing the empty vector pMal(g) was processed in the same way, and the resulting MBP-coupled beads were used to show the specificity of this method.

The MBP and MBP-CagH-fusion proteins expressed in *E. coli* were successfully coupled to the amylose resin as shown by Comassie Brilliant Blue staining (Figure 3.18A). After adding either purified CagI or CagL protein into MBP-coupled beads and MBP-CagH coupled beads, precipitated proteins were immunoblotted using either the CagI or CagL, and MBP antibodies (Figure 3.18B). As expected, CagI was isolated with MBP-CagH-coupled beads but did not interact with MBP-coupled beads alone, suggesting the specificity of this assay. Unfortunately, in the case of CagL, CagL was precipitated with MBP-CagH but it was pulled down with MBP-coupled beads as well (indicated by a red arrowhead), suggesting an unspecific interaction of CagL and MBP beads Therefore, the interaction between CagL and CagH could not be confirmed using these assays.

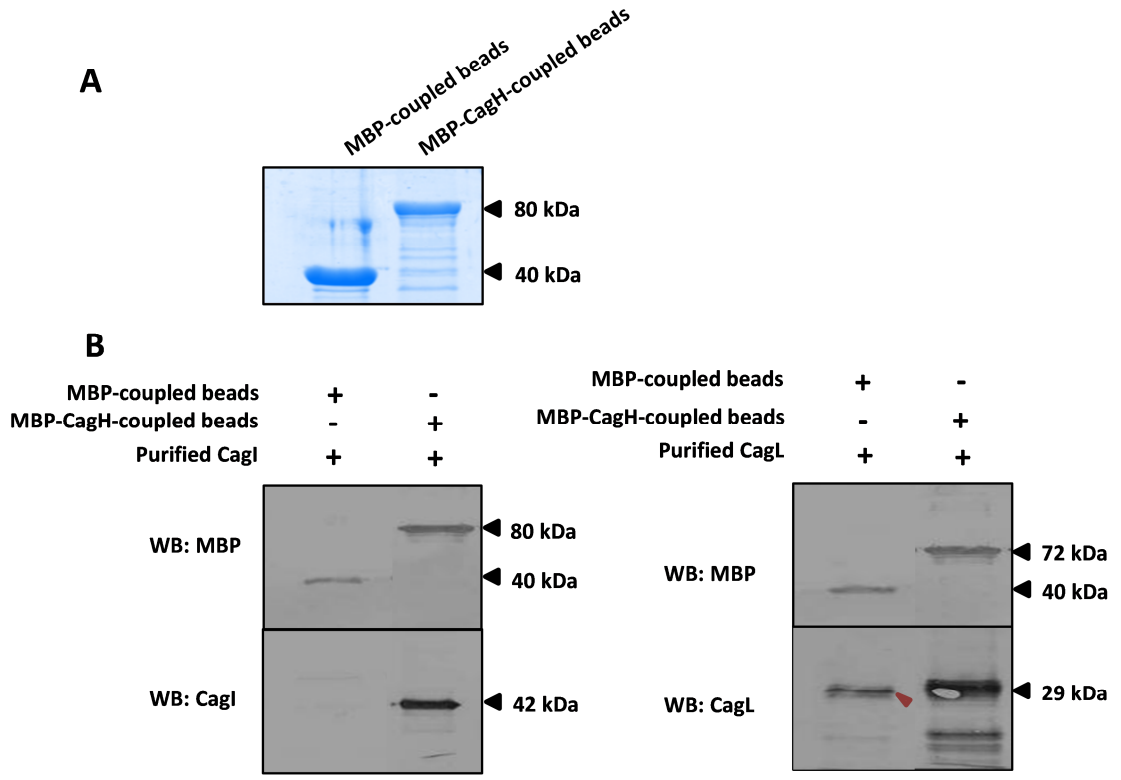

Figure 3.18. Detection of a direct interaction between CagH and CagI

(A) The MBP- and the MBP-CagH-fusion proteins were expressed in *E. coli* and coupled to the amylose resins. The proteins coupled to the beads were detected on SDS-PAGE by Comassie Brilliant Blue staining at approximately 40 and 80 kDa, respectively. (B) The purified CagI and CagL proteins were added to the MBP-CagH coupled beads and the MBP-coupled beads which were served as a negative control. The complex was eluted from beads by boiling in SDS sample buffer and analyzed by the anti-MBP and anti-CagI or anti-CagL Western blotting.

Another attempt to find out the interaction between CagL and CagH were done, in which MBP-CagH-coupled beads were incubated with the GST-CagL-fusion protein. The MBP-CagH- and GST-CagL-fusion proteins were expressed, prepared and coupled to the amylose resin and the glutathione sepharose 4B beads, respectively, as described above (section 2.2.3.12). The MBP-CagH was retained on the amylose beads, whereas GST-CagL was eluted from the glutathione sepharose 4B beads by adding reduced Glutathione. As controls, MBP-coupled beads and GST alone were used. The starting materials are shown in Figure 3.19A. MBP-coupled beads or MBP-CagH-coupled beads were mixed with GST alone or GST-CagL at the same amounts. To detect an interaction between MBP-CagH and GST-CagL, the affinity-purified protein samples were immunoblotted using MBP, GST and CagL antibodies. Unfortunately, GST-CagL

interacted with MBP-CagH-coupled beads as well as with MBP-coupled beads (indicated by red arrowheads), as shown by the CagL immunoblot. Additionally, the GST control blot showed an interaction with MBP control beads and MBP-CagH-coupled beads, suggesting an unspecific binding of GST protein to MBP-coupled beads (indicated by red arrowheads). Interestingly, MBP-CagH-coupled beads did not show an unspecific interaction with GST alone and GST-CagL (Figure 3.19B).

Together with the IP data (section 3.2), these results not only supported the conclusion that CagH is a part of the complex containing CagI and CagL, but also provided evidence for a direct interaction between CagI and CagH.

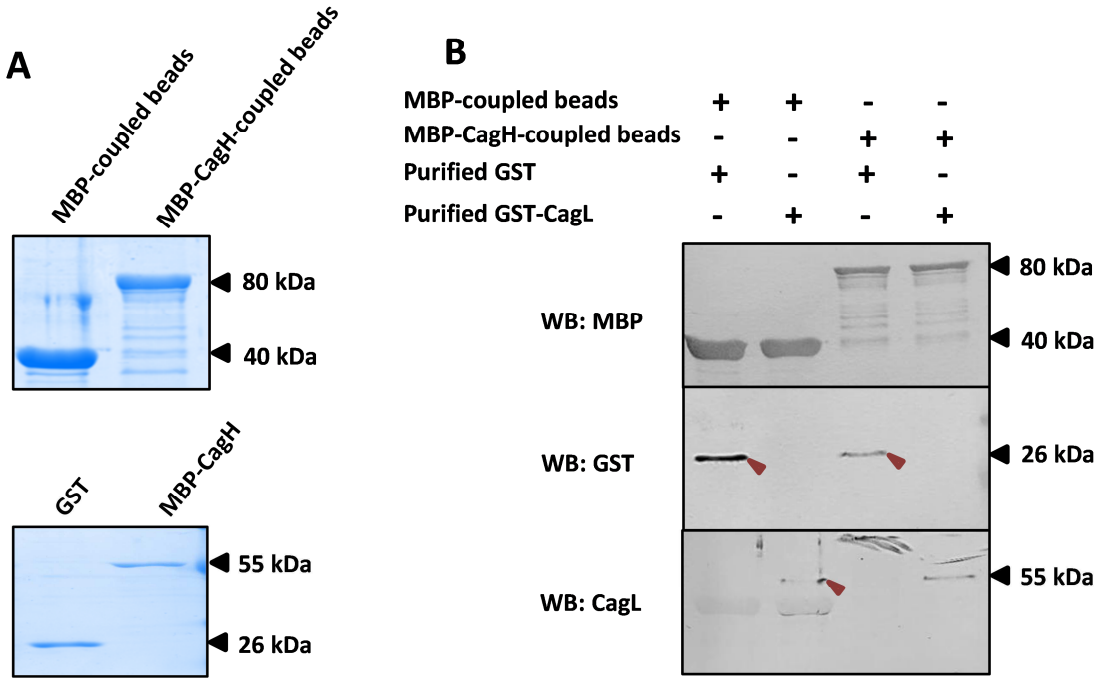

Figure 3.19. Pull-down experiments to show an interaction of CagH and CagL

(A) The MBP and MBP-CagH proteins from protein coupled beads detected on SDS-PAGE were used for pull-down experiments (as shown in Figure 3.10). The GST and GST-CagL fusion proteins were expressed in *E. coli* and coupled to the glutathione sepharose 4B beads and detected on SDS-PAGE by Comassie Brilliant Blue staining at approximately 26 and 55 kDa, respectively. (B) The purified GST or CagL protein was mixed to MBP-CagH-coupled beads and MBP-coupled beads which served as a negative control. The complex was eluted from beads by boiling in SDS sample buffer and analyzed by anti-MBP, anti-GST and anti-CagL Western blotting.

3.3 Characterization of CagH, CagI and CagL functional domains

3.3.1 Role of CagH, CagI and CagL domains in functionality of the Cag apparatus

3.3.1.1 Truncation of CagH, CagI and CagL

Since the *in vitro* pull-down assays using GST-fusion protein were unsuccessful, we sought to find an *in vivo* assay to determine the interactions between CagH, CagL and CagI. Based on the complementation system described above (section 3.1.2.3), in which the plasmid pPT3 containing *cagI* and *cagL* was used to complement the *cagIL* double mutant (strain P12Δ*cagIL*), either CagI or CagL was truncated from the C-terminus in order to remove their C-terminal motifs or their coiled-coil structures as well. In the case of CagI, this protein was truncated further in order to exclude the transcription of *cagL* from a transcriptional start site within *cagI*, which was proposed by Sharma and coworkers [Sharma *et al.*, 2010]. The plasmids pPT9 and pPT10 containing *cagL* variants, and pPT11, pPT12 and pPT13 contaning *cagI* variants were constructed as described above (section 2.1.5). Since the *cagI* locus overlaps at its 3' end with the start codon of *cagL* (Figure 3.1A), *cagI* in all of the *cagI* truncation constructs was designed in such a way that the start codon, and the Shine-Dalgarno sequence of *cagL* were retained. Then, by complementation of the P12Δ*cagIL* mutant, chromosomal integration vectors containing the cloned genes enable integration of *cagI* and *cagL* together into the *recA* locus and expression of the these genes under the control of the *cagA* promoter (Figure 3.20). The production of CagI and CagL was analyzed by immunoblotting.

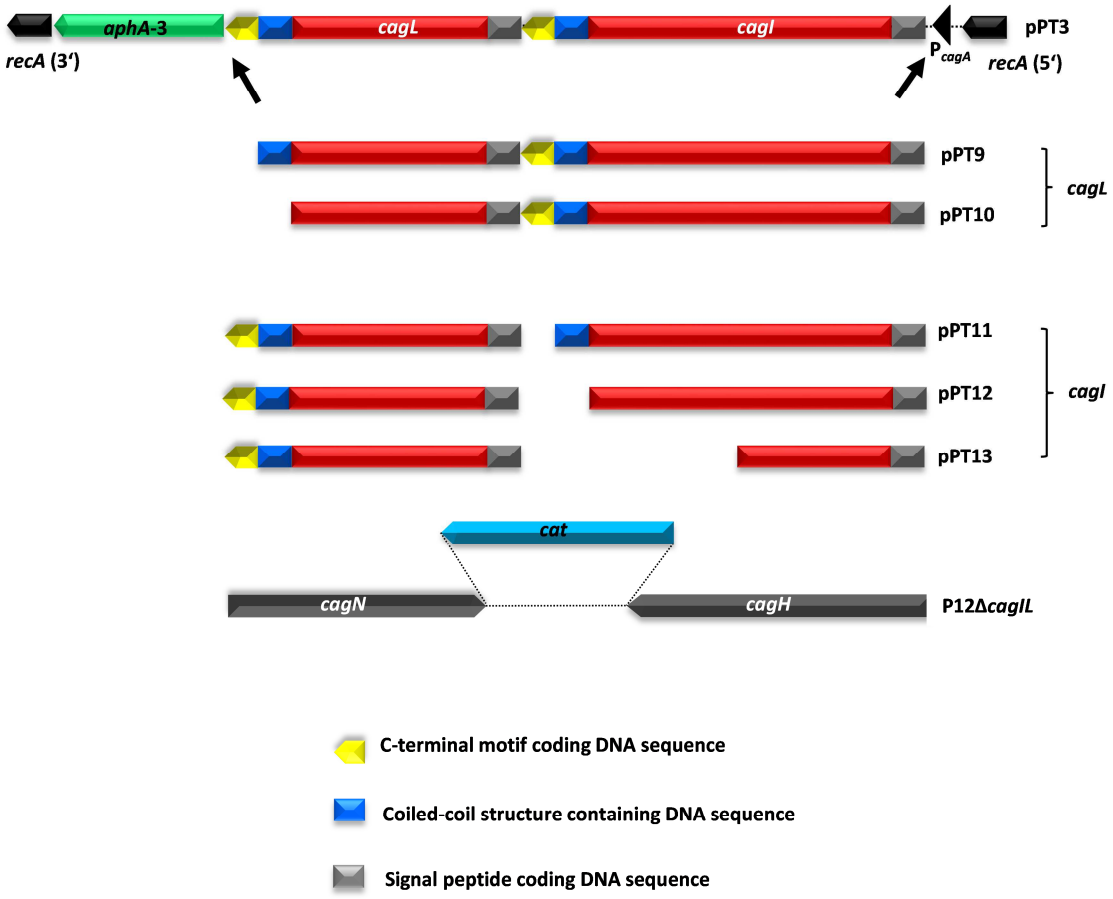

Figure 3.20. Schematic representation of constructs used for generation of either *cagI* or *cagL* truncation mutants

The C-terminal motifs of each protein were removed by transforming the P12Δ*cagIL* double mutant with pPT9 and pPT11. The C-terminal motif and the coiled-coil structure together were removed from either CagI or CagL by transforming the P12Δ*cagIL* double mutant with either pPT10 or pPT12. The cagL transcriptional start site was removed from cagI by transforming the P12Δ*cagIL* double mutant with pPT13. *cagI* and *cagL* together were introduced into the *recA* locus and expressed under the control of the *cagA* promoter in the P12Δ*cagIL* double mutant. The signal sequences, the C-terminal motifs and the coiled-coil structures are indicated in grey, yellow and blue block arrows, respectively.

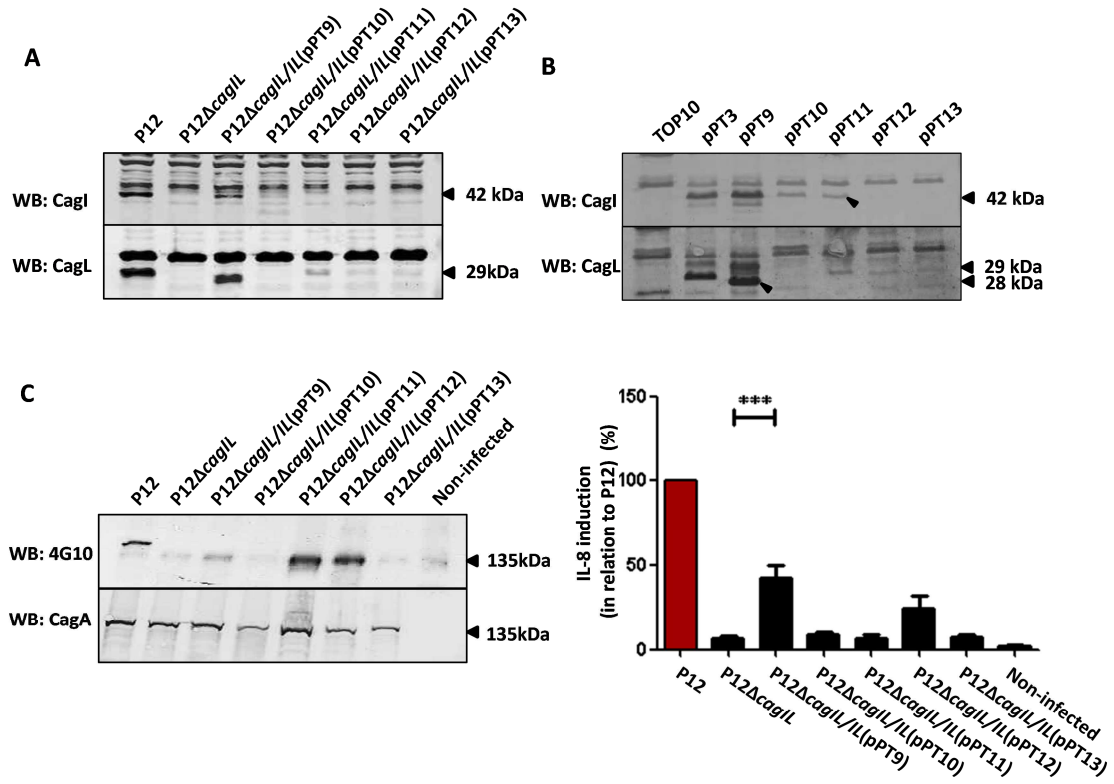

Figure 3.21. Functional analysis the variants of CagI and CagL

(A) Whole cell lysates from P12 and the indicated mutant strains were probed with CagI and CagL antibodies. Numbers in brackets indicate plasmid constructs used for complementation. (B) These plasmid constructs were checked for CagI and CagL expression in *E. coli* TOP10 by Western blotting using the corresponding antibodies. (C) Functionality of the Cag-T4SS of the complemented strains was tested by performing infection assays to determine CagA tyrosine phosphorylation and IL-8 induction. The IL-8 values induced by P12 wild-type were set to 100% and others values were normalized to these values (%). The data collected from at least 3 independent experiments were statistically analyzed by One-way ANOVA (***P < 0.001).

The expression of CagI and CagL in all strains was examined by Western blotting (Figure 3.21A). As mentioned in section 3.1.2.3, the P12Δ*cagIL* double mutant was successfully complemented with plasmid pPT3, containing the full-length *cagI* and *cagL* genes. However, when this mutant was complemented with plasmids containing different truncations of *cagI* or *cagL*, only CagI and CagL proteins from the pPT9 construct were successfully complemented (strain P12Δ*cagIL/IL*(pPT9)). CagL was restored to wild-type levels, but at a smaller size due to the lack of its C-terminal motif while CagI was expressed at a reduced amount compared to the P12 wild-type strain. The reduction of CagI in the absence of the C-terminal motif of CagL suggests a role of

this motif in stabilizing CagI. Unexpectedly, by truncating CagL further to remove the coiled-coil structure this protein, the resulting strain P12Δ*cagIL/IL*(pPT10) was not able to produce a detectable amount of CagL, whereas it produced an extremely low level of CagI, as shown by a very faint band obtained in the CagI immunoblot. In the case of CagI truncation, CagL expression was observed in all of the mutants at considerably reduced amounts with respect to the P12 wild-type strain. None of the *cagI* complementation strains was able to produce CagL at wild-type levels. As mentioned above, the CagI antiserum recognizes part of the coiled-coil structure containing 19 amino acids (350-368) of the protein; therefore it was obviously unable to detect mutated CagI in strain P12Δ*cagIL/IL*(pPT12) and strain P12Δ*cagIL/IL*(pPT13). However, the loss of CagI expression in the mutant lacking C-terminal motif (strain P12Δ*cagIL/IL*(pPT11)) could not be explained (Figure 3.21A).

Since the *cagA* promoter is known to be functional in *E. coli*, we sought to investigate the expression of these truncated proteins in *E. coli.* As shown in Figure 3.21B, in comparison to *E. coli* expressing full-length CagI and CagL together (pPT3), we found expression of CagL in all constructs but not in *E. coli* containing pPT10, which lacks the DNA sequence coding for the C-terminal motif and the coiled-coil structure of CagL. These results suggest that without these 2 parts, CagL might be misfolded and degraded, or could not be recognized by the CagL antibody. Therefore, CagL might not be detectable in strain P12Δ*cagIL/IL*(pPT10) as well. We could not find CagI with the size of the corresponding protein from the P12 wild-type strain. However, a protein band with a size of 30 kDa was obtained in *E. coli* containing pPT3, pPT9, pPT10 and pPT11 but did not appear in the lysate of TOP10. These findings suggest that the polyclonal CagI antibody recognized a breakdown product of CagI from these lysates. Since the CagI protein is recognized by the CagI antiserum in its C-terminal part, it is likely that this processed CagI contains the C-terminal part of this protein. The degraded CagI was detected in *E. coli,* suggesting that the constructs pPT10 and pPT11 should have been expressed in *H. pylori* as well. However, it might be that the CagI protein produced by these mutants was under the detection limit of our immunoblots. The lower levels of CagI in the absence of CagL confirm the previous observation that CagL plays an important role in stabilization of CagI in *H. pylori.*

These complemented strains were then examined for Cag-T4SS functionality by infection experiments. Translocation and phosphorylation of CagA were checked by Western blotting using the CagA and 4G10 antibodies, respectively, and the ability to induce IL-8 were detected by ELISA. The results showed a deficiency of these strains in CagA translocation. The mutant lacking the C-terminal motif of CagL can produce CagI and CagL at comparable amounts; nevertheless it was defective in CagA translocation and remarkably reduced in IL-8 induction to 50% compared with the P12 wild-type strain. These data support the conclusion that CagL needs its C-terminal motif to be fully functional. However, a residual functionality is present in the absence the C-terminal motif (Figure 3.21C).

3.3.1.2 Generation of CagH lacking its C-terminal motif

The existence of a conserved C-terminal motif among CagH, CagI and CagL raised the question whether this motif is involved in the function and the interaction between these three proteins. Therefore, we sought to evaluate the role of this motif on CagH stability and function as well. A deletion of the DNA coding for the C-terminal motif (TKIIVK) was introduced into the gene bank plasmid HP2kb05G17 as described above (section 2.1.5). The stop codon of *cagH*, which overlaps the Shine-Dalgarno sequence of *cagI*, was retained. The resulting plasmid was used for complementation of the *cagH* mutant (strain P12Δ*cagH*), by which the *cagH* gene was inserted into the chromosome by homologous recombination with *cagG* and *cagI* flanking regions and replaced the *erm-rpsl* cassette (Figure 3.22). As seen in Figure 3.23A, the *cagH* mutant (strain P12Δ*cagH*) was defective in production of CagI and CagL proteins, whereas the *cagH* complemented strain using the gene bank plasmid HP2kb05G17 (strain P12Δ*cagH*/*H*) recovered both the wild-type phenotypes, suggesting an important role of this protein for CagI and CagL stability and/or production. Unlike strain P12Δ*cagH*/*H*, the *cagH* mutant lacking the C-terminal motif (strain P12Δ*cagH*/$H_{\Delta C}$) showed considerably reduced levels of CagI and CagL compared to strain P12 (Figure 3.23A), indicating that this motif of CagH caused an effect on CagI and CagL stability or production. Functionality of the Cag-T4SS was assessed by performing infection experiments of AGS cells with the P12 wild-type strain, the *cagH* mutant and the *cagH* C-terminal

motif deletion mutant. The results showed that deletion of the C-terminal motif significantly blocked the translocation of CagA as well as IL-8 secretion, suggesting that this C-terminal motif is critical for the function of CagH (Figure 3.23B).

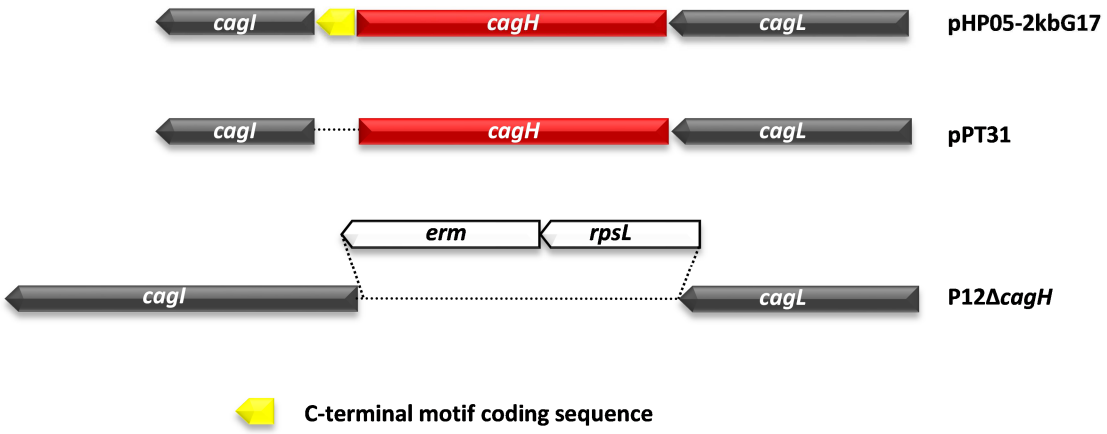

Figure 3.22. Schematic representation of constructs for generation of the *cagH* C-terminal motif deletion mutant

The DNA sequence coding for 6 amino acids of the C-terminal motif was removed from the gene bank plasmid pHP2kb-05G17 by a site directed mutagenesis PCR to generate plasmid pPT31. By transforming the P12Δ*cagH* mutant containing an *rpsL-erm cassette* with plasmid pPT31, *cagH* was reintroduced into the *cagH* locus. The C-terminal motif of *cagH* is indicated as a yellow block.

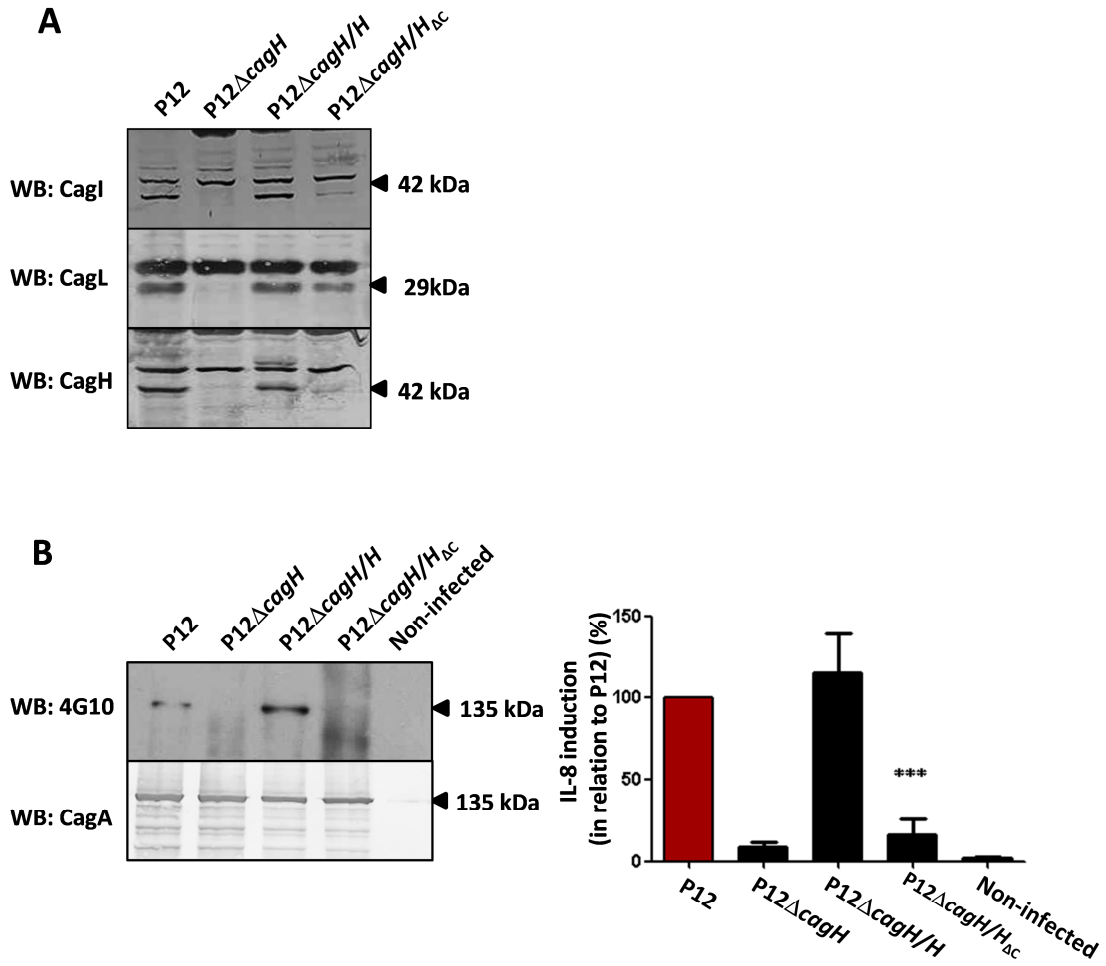

Figure 3.23. Functional role of the C-terminal motif of CagH

(A) Whole cell lysates from strain P12 and the indicated mutant strains were probed with CagI and CagL antibodies. (B) Functionality of the Cag-T4SS of the complemented strains was tested by performing infection assays to determine CagA tyrosine phosphorylation and IL-8 induction. The IL-8 values induced by strain P12 were set to 100% and other values were normalized to these values (%). The data collected from at least 3 independent experiments were statistically analyzed by One-way ANOVA (***P < 0.001).

3.3.1.3 Mutagenesis of a CagH and CagL conserved internal motif

The crystal structure of CagL revealed a disulfide linkage between Cys128 from the α4 helix and Cys139 from the α5 helix. This covalent bond links α4 to a three-helix bundle formed by the upper half of α2, α5, and α6 together with α3 [Barden *et al.*, 2013] (Figure 3.24A). Careful analysis of CagH, CagI, and CagL amino acid sequences showed that a conserved amino acid sequence between the two cysteine residues (C128-C139) of CagL is similarly present in CagH (C261-C272) (with a similarity of 92%)

(Figure 3.24B). Furthermore, the protein containing C128-C139 is close to the C-terminus of CagL.

To investigate the role of this disulfide bond in the function of CagH and CagL, we constructed site-specific mutants in which either the codons for cysteine or aspartic acid was substituted with serine or alanine, respectively, or the 5 residues from cysteine to aspartate was deleted as described in section 2.1.5.

For introducing mutations into CagH, and CagL, the pHP2kb05G17 plasmid (containing *cagH*), or the pPT3 plasmid (containing *cagI* and *cagL*) were used for directed mutagenesis, respectively. The plasmids containing mutations of *cagH* were transformed into the P12Δ*cagH* mutant, whereas those containing the *cagL* mutations were introduced into the P12Δ*cagIL* double mutant as described before (section 3.1.2.3).

Bacterial cell lysates of all mutants were checked for production of CagI and CagL by Western blotting. Infection experiments were carried out in order to assess the capability of these mutants to translocate CagA and induce IL-8, and to elucidate the effect of amino acid substitution or deletion on functionality of the Cag-T4SS. As observed in Figure 3.25A, the complementation of the deletion mutants with full-length *cagH* or *cagL*, restored both CagI and CagL production. Meanwhile, the single amino acid mutations resulted in a reduction of CagI and CagL,but this did not impair the ability of these strains to translocate and obtain phosphorylated CagA or to induce IL-8. A marked reduction of CagI and CagL was observed in both the *cagH* and *cagL* mutants in the absence of the CPIGD/CGISD motifs. Interestingly, the smaller amounts of CagI and CagL produced by strain P12Δ*cagL/L*$_{\Delta CGISD}$ were still sufficient for CagA translocation to occur at a low efficiency, and for IL-8 induction at almost wild-type levels. In contrast, the P12Δ*cagH/H*$_{\Delta CPIGD}$ strain showed no functional CagA translocation and a strong reduced IL-8 induction in compared to strain P12 (Figure 3.25B). The low amounts of CagI and CagL furthermore suggest that the deficiency of the P12Δ*cagH/H*$_{\Delta CPIGD}$ strain in CagA translocation and IL-8 induction is attributable to CagH production. Thus, these provide evidence that CagH itself is independently required for Cag-T4SS functionality.

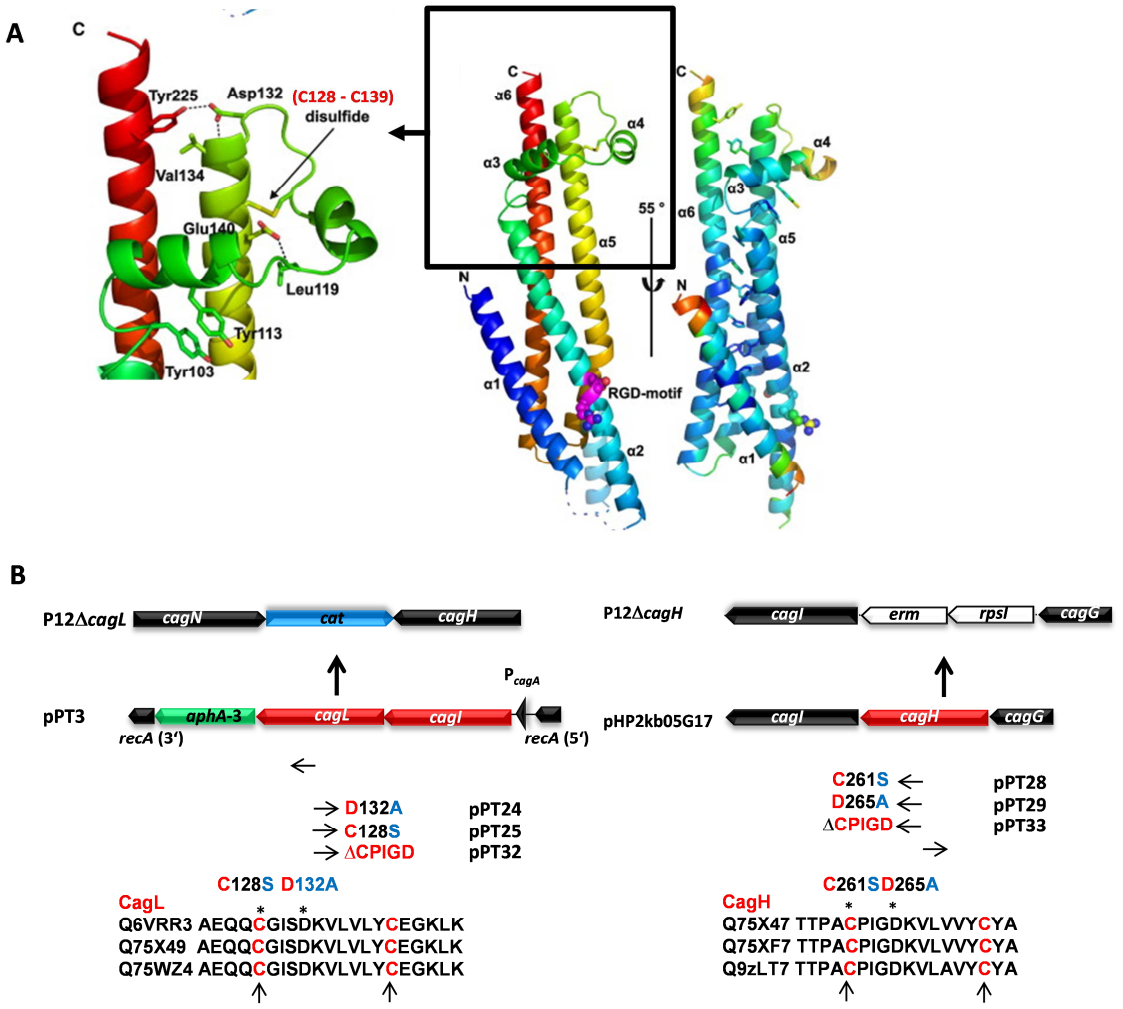

Figure 3.24. Schematic representation of constructs used for *cagH* and *cagL* mutagenesis

(A) (Left) The disulfide links Cys128 to Cys139, (Right) Structure of CagL [Barden *et al.*, 2013]. (B) Amino acid sequence analysis of several CagH and CagL proteins revealed a conserved amino acid sequence between two cysteine residues of CagL (C128-C139) and of CagH (C261-C272). To disrupt these disulfide bonds, cysteine 128 of CagL and cysteine 261 of CagH, respectively, were substituted with serine, whereas aspartic acid 132 of CagL and aspartic acid 265 of CagH, respectively were replaced by alanine. Furthermore, amino acids 128-132 of CagL and 261-265 of CagH were removed, respectively. Plasmids pPT25, pPT24, pPT32 carrying the C128S, D132A and ΔCPIGD mutations in *cagL*, respectively, were used for complementation of the P12Δ*cagIL* double mutant, resulting in integration into the *recA* gene and expression under the control of the *cagA* promoter. Likewise, plasmids pPT28, pPT29, pPT33 carrying C261S, D265A and ΔCPIGD muations in *cagH*, respectively, were used for complementation of P12Δ*cagH*. These plasmids were constructed from gene bank plasmid HP2kb05G17 by a site directed mutagenesis PCR.

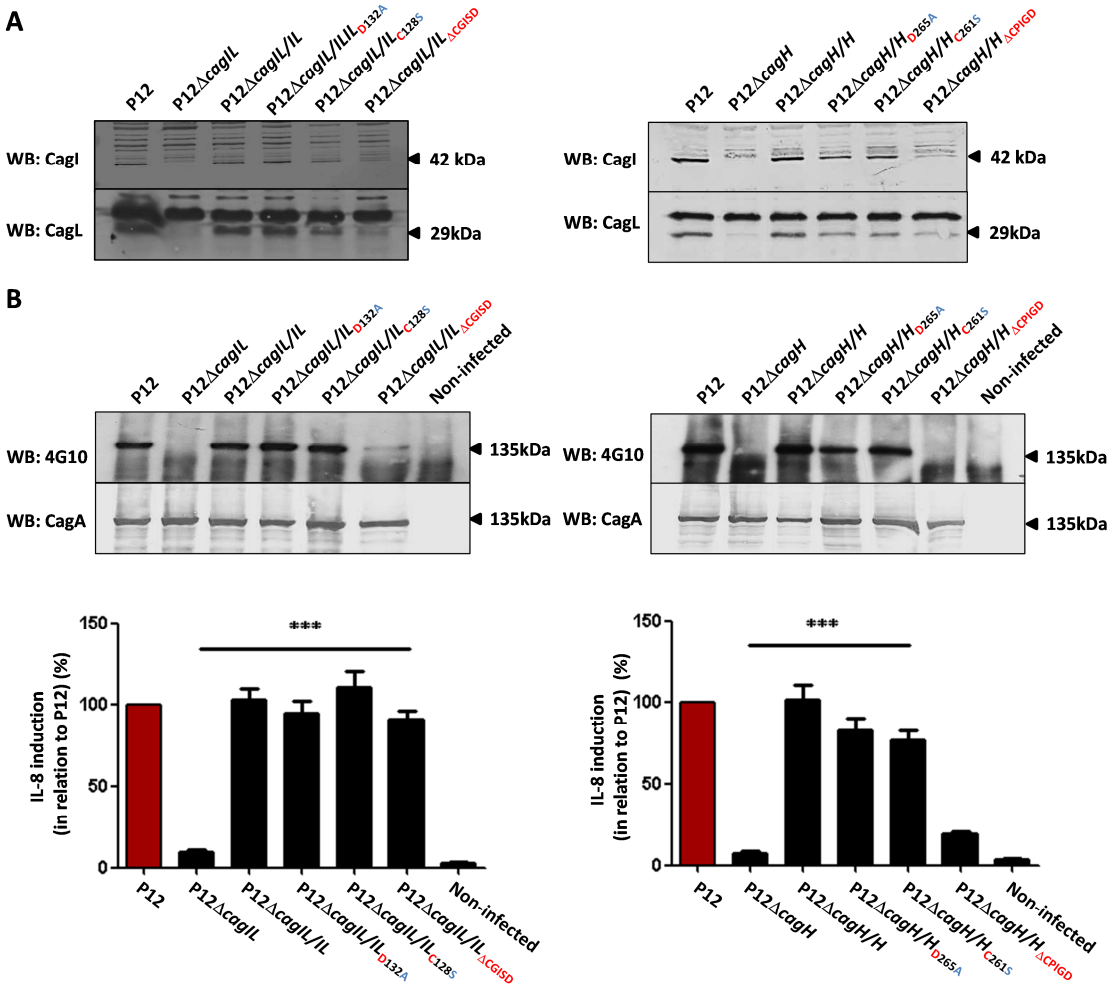

Figure 3.25. Functional analysis of the CagH and CagL disulfide bonds and internal motifs

(A) Whole cell lysates of the P12 wild-type strain and the indicated mutants were immunoblotted with CagI and CagL antisera. (B) Functionality of the Cag-T4SS from strain P12 and the indicated mutants were tested by performing infection assays to determine CagA tyrosine phosphorylation and IL-8 induction. The IL-8 values induced by the P12 wild-type strain were set to 100% and other values were normalized to these values (%). The data collected from at least 3 independent experiments were statistically analyzed by One-way ANOVA (*P < 0.05, ***P < 0.001).

3.3.2 Examination of domains involved in binding between CagH, CagI and CagL

3.3.2.1 Role of the conserved C-terminal motif

As mentioned in section 3.1.1, the presence of a conserved C-terminal motif containing 6 amino acids in CagH, CagI and CagL (Figure 3.1C) raises the possibility that these motifs are recognized by a common interaction partner of these 3 proteins. To investigate the role of this C-terminal motif in interaction of these 3 proteins, the

P12Δ*cagH/H*$_{\Delta C}$ and P12Δ*cagIL/IL*$_{\Delta C}$ strains expressing shorter forms of CagH and CagL, respectively, were subjected to co-immunoprecipitation experiments using the CagL antibody. The P12 wild-type strain and the P12Δ*cagL* mutant were used in parallel and served as positive and negative controls, respectively. The presence of CagH, CagI and CagL in the precipitated fractions was examined by immunoblotting. Immunoblots revealed that CagI and CagH were co-immunoprecipitated with CagL from the P12 wild-type strain and the P12Δ*cagIL/IL*$_{\Delta C}$ mutant but not from the P12Δ*cagH/H*$_{\Delta C}$ mutant (Figure 3.26), which suggests that the C-terminal motif of CagL is not absolutely important for interaction between CagI and CagL, and that there might be another interacting domain between these 2 proteins instead. In contrast, the C-terminal motif of CagH seems to have a role in the interaction among these proteins. CagH and CagI were observed to interact with each other directly by MBP pull-down assays (section 3.2.3.2), the absence of CagH in precipitated fractions provides evidence for a direct interaction of these two proteins via the C-terminal motif of CagH. Since bacterial lysates contain a cross-reacting protein at almost the same size as CagH, it cannot be excluded that CagH was not produced in the mutants at the same level in the P12 wild-type, possibly because it is unstable due to a stabilizing effect of CagL on CagH, which might require the presence of the C-terminal motif. Unfortunately, the mutant expressing CagI lacking the C-terminal motif (strain P12Δ*cagIL/IL* (pPT11)) did not produce a stable protein, therefore we could not examine the role of the C-terminal motif of CagI in these interactions.

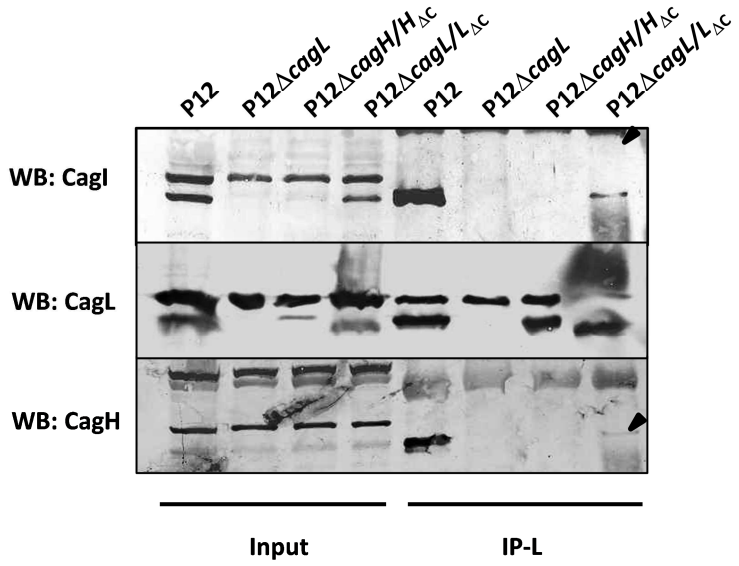

Figure 3.26. Role of the C-terminal motifs in interactions between CagH, CagI and CagL

Whole cell lysates of P12 wild-type strain and the indicated mutants were tested for the presence of CagI, CagL and CagH with the corresponding antibodies. Cell extracts of these strains were subjected to immunoprecipitaton using CagL antiserum (IP-L). As a control the P12Δ*cagL* muant was used. The immunoprecipitated proteins were checked for the presence of CagI, CagL and CagH by Western blotting.

3.3.2.2 Role of a disulfide bond in functionality of CagH and CagL

The defect of strain P12Δ*cagH/H*$_{\Delta CPIGD}$ in CagA translocation and IL8- induction raised the possibility that these 5 amino acids take part in the interactions between CagH, CagI and CagL. To investigate the role of these 5 amino acids for these interactions, co-immunoprecipitation experiments using the CagL antibody were performed. The presence of CagH, CagI and CagL was detected using Western blotting with the corresponding antibodies. As seen in Figure 3.27, CagI and CagH were pulled down with the CagL antibody in the wild-type strain but not in the *cagH* mutant lacking the CPIGD motif. However, the lack of CagI in the precipitated fraction might also be due to the lower expression of CagI in this mutant. Again, we cannot exclude that the CagH levels produced by this mutant were low.

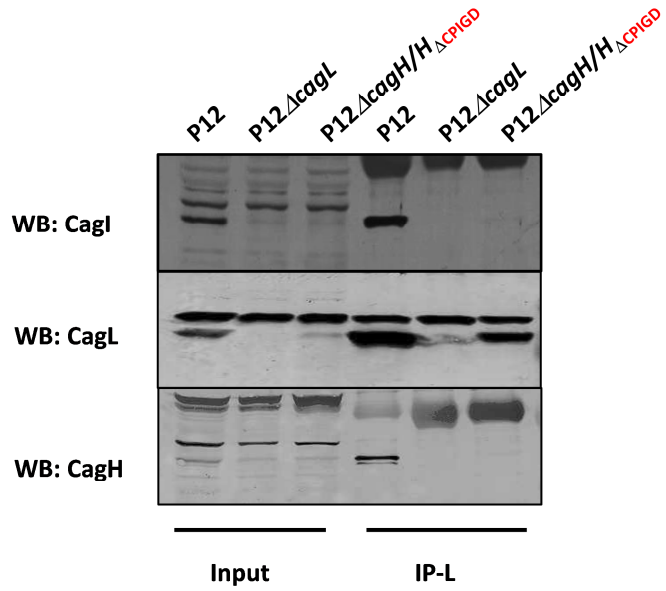

Figure 3.27. Investigation of the role of the CPIGD motif in interactions between CagH, CagI and CagL

Whole cell lysates of P12 wild-type and the indicated mutants were tested for the presence of CagI, CagL and CagH with the corresponding antibodies. Cell extracts of these strains were subjected to immunoprecipitaton using CagL antiserum (IP-L). As a control, the *cagL* deletion mutant, P12Δ*cagL* was used. The immunoprecipitated proteins were checked for the presence of CagI, CagL and CagH by Western blotting.

3.4 Role of CagP protein or sRNA-*cagP* on production of CagI and CagL

With the aim of investigating the effects of different Cag components on expression of CagI and CagL in strain P12, isogenic mutants of all *cag* genes coding for proteins involved in the function of the Cag-T4SS were generated and examined for CagI and CagL protein levels by immunoblotting. As shown in Figure 3.28, CagI and CagL production was influenced by the absence of several *cag* genes. Notably, the *cagX*, *cagY*, *cagH* and *cagG* mutants produced virtually no CagI and several further mutants (Δ*cagδ*, Δ*cagW*, Δ*cagV*, Δ*cagU*, Δ*cagM*, Δ*cagL* and Δ*cagE*) produced significantly reduced amounts of CagI. Interestingly, CagL levels were reduced with different levels in these mutants as well. In contrast, the *cagF* mutant produced unchanged levels of CagI and CagL compared to the wild-type proteins. Additionally, *cagQ* and *cagS* deletion mutants of strain P12 were tested, since these deletion mutants had been shown before to cause strain-specific effects (data not shown). Investigation of the *cagP* gene

deletion showed that deletion of *cagP* indeed resulted in reduced levels of CagI and CagL compared to strain P12 (Figure 3.31A).

The *cagP* gene is probably a monocistronic gene [Ta *et al.*, 2012]and the gene product comprises of 114 amino acids. However, there have been no studies confirming the production of CagP *in vitro*. Recently, Sharma *et al*. described transcription of a small non-coding RNA, named HPnc2630, upstream of *cagP* (Figure 3.29A) [Sharma *et al.*, 2010]. Using the Target RNA 2 software (http://cs.wellesley.edu/~btjaden/TargetRNA2/), the 5' untranslated regions of the *cagG* and *cagF* genes were predicted as possible binding/target sites (Figure 3.29B). As mentioned before (section 3.1.1), the putative promoters upstream of *cagG* and *cagF* have been reported to be involved in the transcription of t*cagI* and *cagL* genes [Sharma *et al.*, 2010; Ta *et al.*, 2012]. Taken together, we hypothesized that the sRNA HPnc2630 might act as a regulator targeting the *cagG* or *cagF* promoter to control the expression of *cagI* and *cagL.*

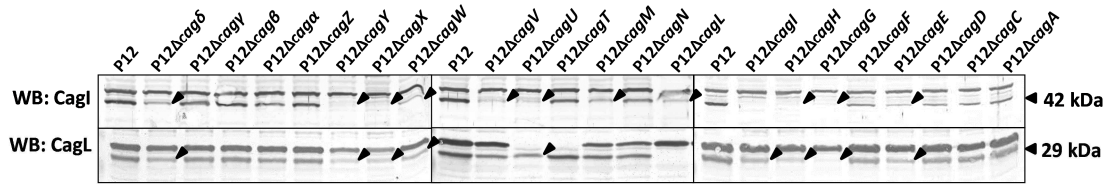

Figure 3.28. Influence of the *cag* gene deletion on production of CagI and CagL[5]

Whole cell lysates of equal amounts of the wild-type strain P12 and of isogenic mutants in single *cag* genes were separated by SDS-PAGE and examined by immunoblotting with the anti-CagI and anti-CagL antisera, respectively. Representative immunoblots are shown. Note that the *cagI* mutant shown here was generated with plasmid pWS327. Arrowheads indicate the positions of CagI and CagL protein bands, respectively.

[5] was performed by Evelyn Weiss

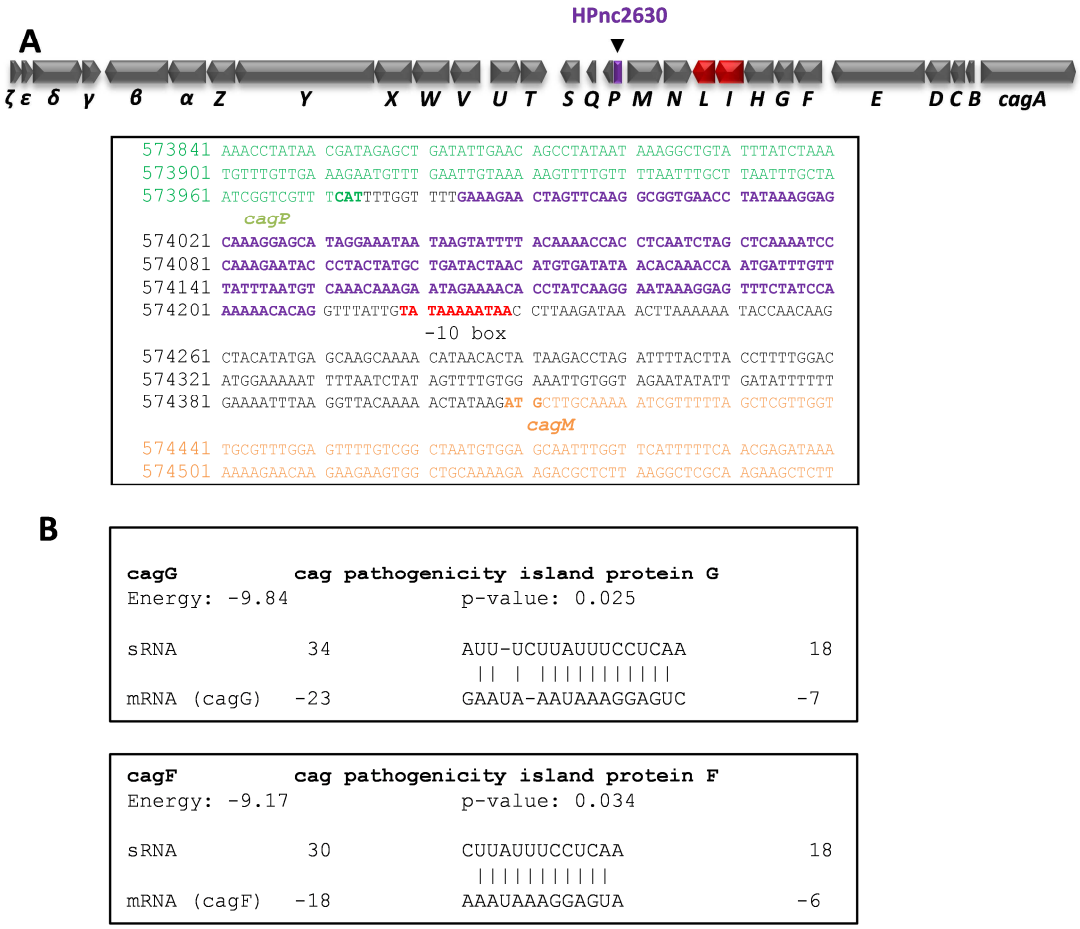

Figure 3.29. Analysis of the sRNA

(A) The sRNA which is shown in purple is located upstream of the *cagP* gene. The *cagP* and *cagM* gene nucleotides are coloured green and orange, respectively. (B) The sRNA target prediction using the Target RNA 2 software (http://cs.wellesley.edu/~btjaden/TargetRNA2/) identified possible binding sites to 5' UTR of *cagG* and *cagF* which are labeled in red and blue, respectively.

3.4.1 Deletion of *cagP* leads to abolishment of Cag-T4SS functionality

To further investigate the influence of either *cagP* or HPnc2630 or both, on production of Cag proteins. The different *cagP* and/or sRNA deletion and complementation strains were generated from strain P12 using plasmids as described in Figure 3.30 and in section 2.1.5. Bacterial lysates of these strains were subjected to Western blotting analysis using different Cag antisera. Of all antisera tested, the *cagP* and/or sRNA deletion mutants showed a reduced expression of CagI and CagL compared to P12 wild-type (Figure 3.31A). Because of the lack of a CagP antibody, we could not check for the

production of the CagP protein in these strains. The ability to phosphorylate CagA and to induce IL-8 was analyzed after AGS cell infection of these strains. As seen in Figure 3.31A, the mutants lacking *cagP* or HPnc2630 produced less CagI and CagL in comparison to the P12 wild-type and were deficient for CagA phosphorylation and IL-8 expression. Unlike these strains, the sRNA deletion mutant was able to produce CagI and CagL at wild-type levels and had a functional T4SS (Figure 3.31B). These results indicated that CagP plays a role in stabilization and/or production of CagI and CagL. Interestingly, the complementation of P12Δ*cagP* mutant using plasmid pWS338 containing the sRNA upstream of *cagP* restored the wild-type phenotype, whereas complementation of this strain using plasmid pWS337 (containing only *cagP*) did not (data not shown). Therefore, it remained unclear whether the sRNA has a direct role in regulating the expression of CagI and CagL.

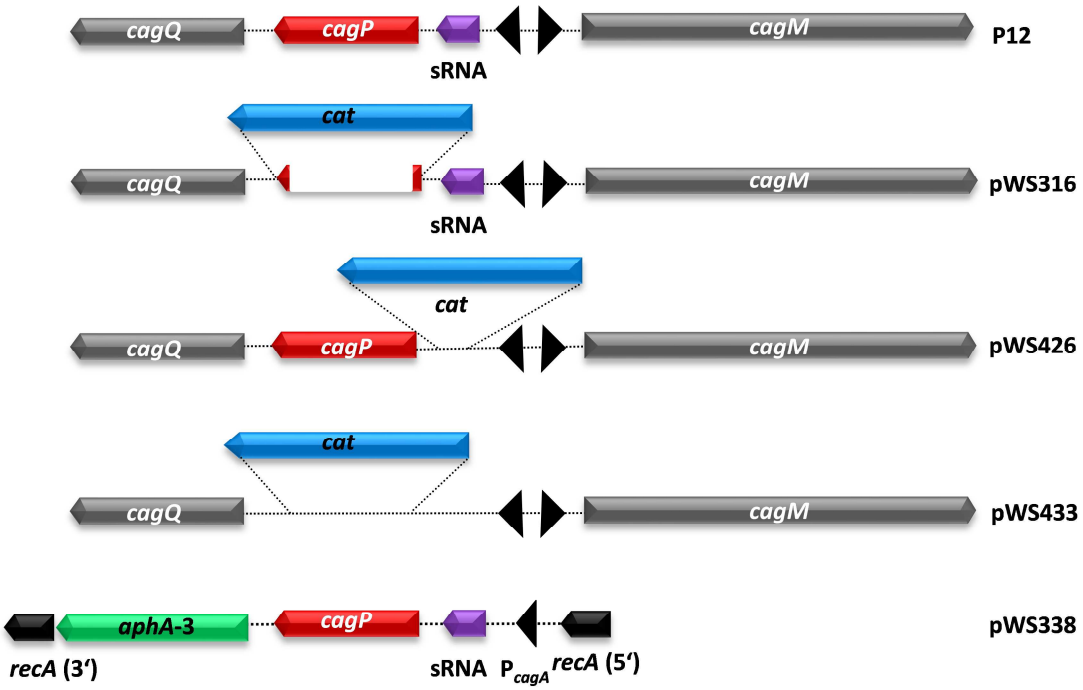

Figure 3.30. Schematic representation of constructs used for generation of *cagP* or sRNA deletion mutants and complemented strains

Either *cagP* or the sRNA, or both, were deleted from strain P12 by insertion of a chloramphenicol resistance gene cassette, using plasmids pWS316, pWS426 and pWS433, respectively. The *cagP* deletion mutant was complemented using a chromosomal integration vector containing *cagP* together with the sRNA (pWS338). *cagP* and the sRNA were introduced into the *recA* locus and expressed under the control of the *cagA* promoter[6].

[6] was performed by Evelyn Weiss

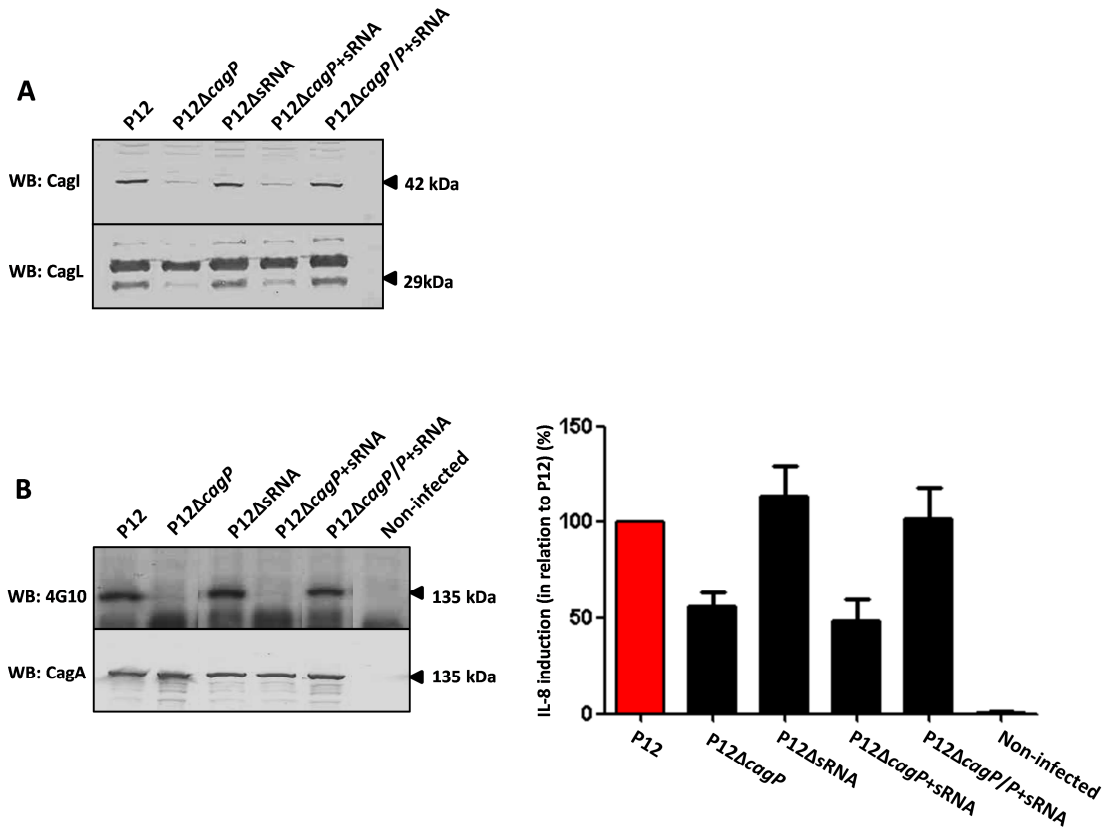

Figure 3.31. Functional analysis of *cagP* and the sRNA

(A) Whole cell lysates of strain P12 and the indicated *cagP* and/or sRNA mutants were subjected to CagI and CagL immunoblots. (B) Functionality of the Cag-T4SS of the mutated or complemented strains was tested by performing infection assays to determine CagA tyrosine phosphorylation and IL-8 induction. The IL-8 values induced by P12 wild-type were set to 100% and other values were normalized to these values (%). The data collected from at least 3 independent experiments were statistically analyzed by One-way ANOVA.

3.4.2 Deletion of *cagP* or HPnc2630 does not exert a negative transcriptional effect on *cagI*

To analyze whether the reduction of the CagI protein in the different *cagP* and/or sRNA deletion mutants is attributable to reduced transcription of the *cagI* gene, *cagI* transcripts were quantified by real-time PCR using specific primers for the *cagI* gene, and primers for 16S RNA as a reference. The control PCR showed PCR amplification products for the *cagL* and 16S RNA genes from cDNAs, but not from mRNA samples, suggesting that the preparation of cDNA was not contaminated with genomic DNA. As seen in Figure 3.32, quantification of the *cagI* mRNA by qPCR showed no significant

difference between the P12 wild-type and the various *cagP* and/or sRNA mutants and complemented strains. These results indicate that there is no transcription effect caused by the absence of *cagP* or the sRNA.

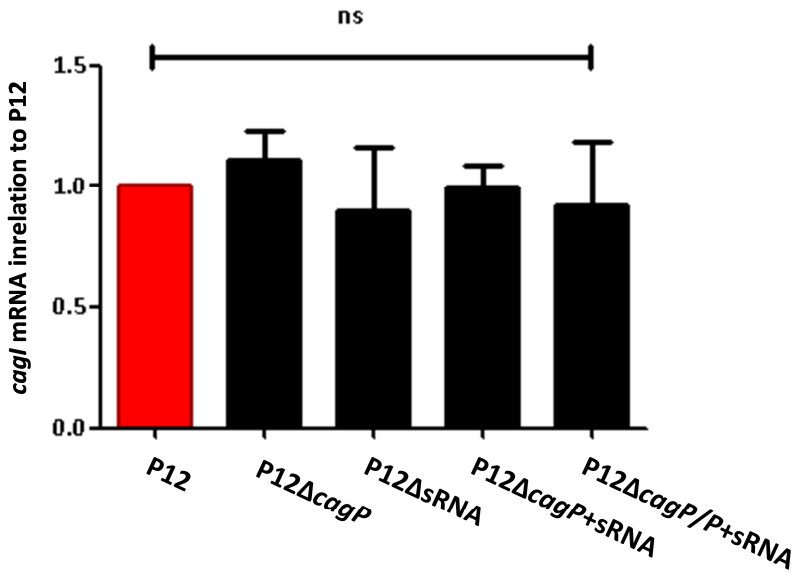

Figure 3.32. *cagI* transcription analysis

H. pylori strain P12 and the indicated *cagP* mutants were cultivated in liquid media to mid-exponential phase before being harvested for RNA extraction and cDNA synthesis. Quantitative real-time PCR was carried out to analyze the transcript levels of *cagI* in each cDNA sample. An analysis of 16S RNA transcript levels was performed in parallel for normalization. The values obtained from strain P12 were set to one and other values compared to strain P12 by One-way ANOVA. Bar graphs represent the means from at least 3 independent experiments with standard errors of the mean.

3.4.3 Generation of a tagged CagP variant

Since the deletion of *cagP* and/or the sRNA did not cause any transcriptional effects, there might be a stabilizing effect of the CagP protein on CagI and CagL instead. For facilitating a characterization of the CagP protein, we intended to construct *H. pylori* strains producing tagged-CagP versions (Figure 3.33). DNA sequences coding for the M45 epitope tag [Hohlfeld *et al.*, 2006] were introduced at the 3' end of *cagP*. First, $cagP_{M45}$ together with the sRNA sequence was introduced into the *cagP*-sRNA locus in strain P12, using plasmid pPT7. The production of CagI and CagL in the resulting strain (P12$cagP_{M45}$) was examined by Western blotting, showing a reduction of CagI and

CagL compared to the P12 wild-type strain, but no expression of the M45 tag was observed (Figure 3.34A).

Another attempt to introduce a tag into the CagP protein was carried out. Based on the complementation of the *cagP* deletion mutant using plasmid pWS338 containing *cagP* and HPnc2630, which had restored the wild-type phenotypes, another construct was designed to introduce $cagP_{M45}$ into the *recA* locus using a chromosomal integration vector (pPT20). The resulting strain (strain P12Δ$cagP/P_{M45}$) was, however, not able to restore CagI and CagL production to wild-type levels and not fully recovered ability to transclocate CagA. Again, we could not detect production of the M45 tag (Figure 3.34A).

It has been known that the mRNA levels of *cagP* were low *in vitro* compared to other *cag* genes [Ta *et al.*, 2012]. On the other hand, another study on expression of the *cagP* promoter *in vitro* provided evidence about an increased expression of *cagP* in the presence of host cells [Joyce *et al.*, 2001]. Therefore, to investigate the expression of M45 tagged-CagP, infection experiments were performed. However, the P12Δ$cagP/P_{M45}$ strain lost the ability to translocate CagA (Figure 3.34B) and produced no M45-tagged-CagP protein, which could not be detected on the blot (data not shown). Another epitope tag, the Myc tag, was introduced into the CagP protein; however the results were the same as observed from the M45-tagged CagP (data not shown).

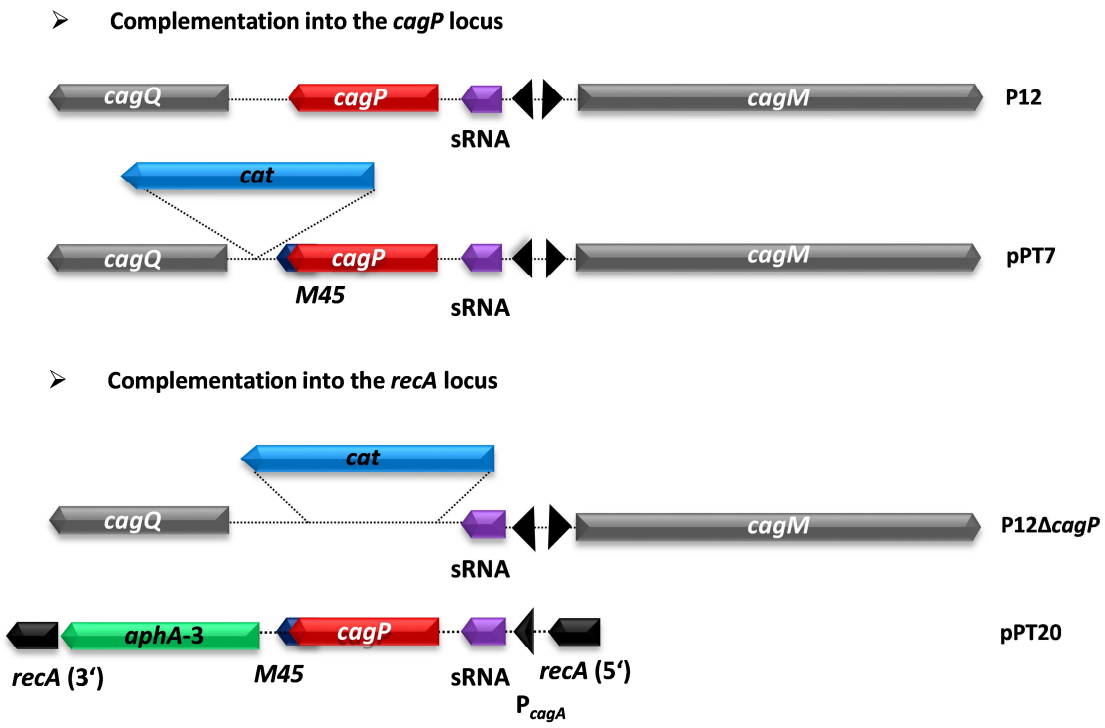

Figure 3.33. Schematic representation of constructs used for generating a tagged-CagP variant

As a first strategy, *cagP*$_{M45}$ together with the sRNA was integrated into chromosome to replace the wild-type *cagP-sRNA* by transforming strain P12 with plasmid pPT7. In the second approach, *cagP* and the sRNA were introduced into the *recA* locus of the P12Δ*cagP* mutant by transforming with plasmid pPT20, and were expressed under the control of the *cagA* promoter. In both cases, the M45 tag was introduced in to the C-terminal end of CagP.

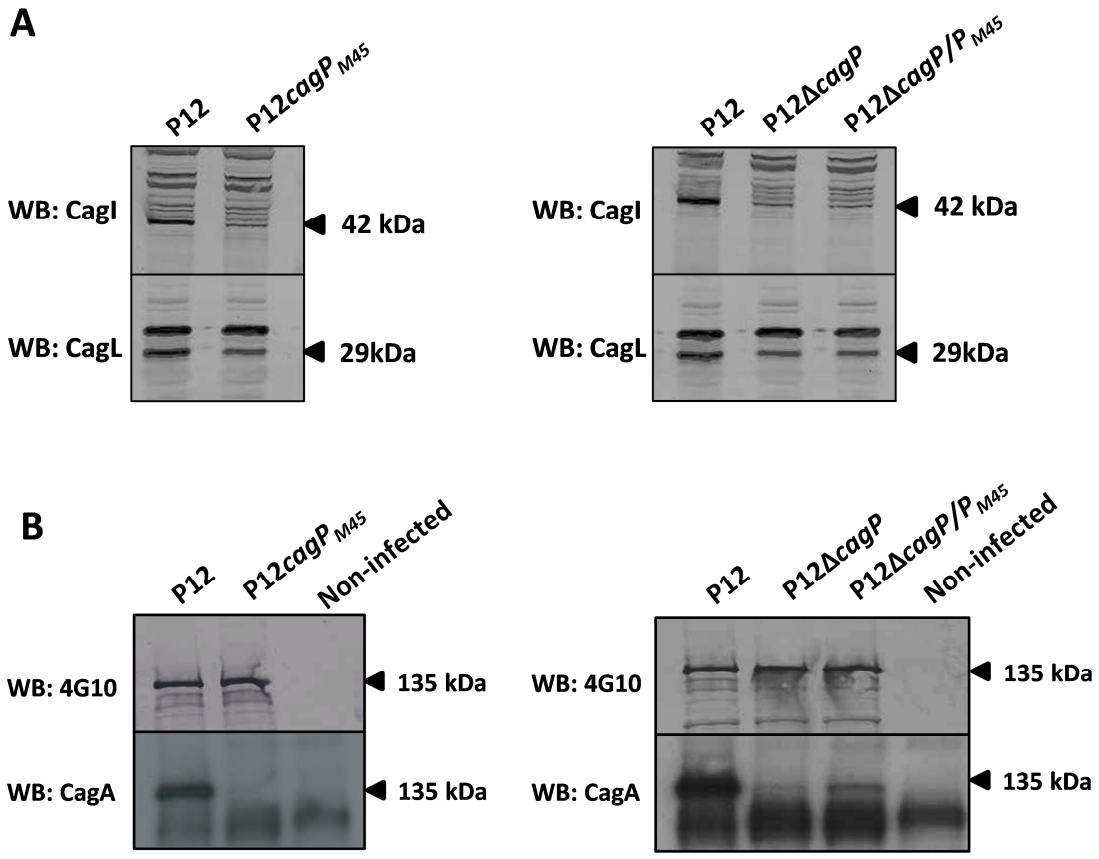

Figure 3.34. Functional analysis of the tagged-CagP

(A) Whole cell lysates of the P12 wild-type strain and the indicated mutants were subjected to CagI, CagL imunnoblotting using the corresponding antibodies. (B) Functionality of the Cag-T4SS from strain P12 and the indicated mutants was tested by performing infection assays of AGS cells to determine CagA tyrosine phosphorylation. The IL-8 values induced by the P12 wild-type strain were set to 100% and other values were normalized to these values (%). The data collected from at least 3 independent experiments were statistically analyzed by One-way ANOVA (***$P < 0.001$).

4 DISCUSSION

The action of the bacterial oncoprotein CagA contributes significantly to pathogenesis of *H. pylori* infection. Translocation of CagA is facilitated by a transmembrane protein complex containing at least 15 proteins, the Cag-Type IV secretion apparatus. The Cag apparatus comprises not only conserved essential components but also several additional proteins which are unique to this system. The activities of several essential components in CagA translocation have been investigated before, but complementation studies are often lacking. In this work, we have provided new insights into the functional role of three components of the Cag-T4SS that lack homologs in other T4SSs – CagH, CagI, and CagL.

4.1 CagP exerts a stabilizing effect on CagI and CagL

The data from mutagenesis studies of *cag* genes revealed a contribution of *cagP* and/or the sRNA associated with *cagP*, HPnc2630, on functionality of the Cag-T4SS in strain P12 (Figure 3.28, Figure 3.31B). Additionally, the results obtained from an RNA target prediction using Target RNA 2 software showed that HPnc2630 may bind to the 5' untranslated region of the *cagG* and/or *cagF* genes, which are located upstream of *cagI* and *cagL* (Figure 3.29). Therefore, we hypothesized that either the *cagP* gene product might have a functional role and exert an influence on expression of *cagI* and *cagL*, or that the sRNA HPnc2630 may act as a regulator targeting the *cagG* or *cagF* promoter to control the expression of the putative operon containing *cagI* and *cagL*.

Using gene deletion and complementation studies of *cagP* and/or the sRNA, we found that the absence of *cagP* or *cagP* together with HPnc2630 exerted an effect on production of CagI and CagL (Figure 3.31A), which led to a deficiency of these mutants in CagA translocation and IL-8 induction, suggesting that CagP might play a role in stability and/or production of CagI and CagL. Interestingly, the sRNA deletion mutant was still able to produce both CagI and CagL at wild-type levels, and was not defective in CagA translocation as well as IL-8 induction by AGS cells (Figure 3.31B). Similarly, a recent study characterized a small non coding RNA (termed *cnc*R1) in strain G27 [Vannini, 2013], which corresponds to the 5' untranslated region (termed HPnc2630) uptream of *cagP* in strain 26695 [Sharma *et al.*, 2010]. Interestingly, they found that the *cnc*R1 might reduce the mRNA stability or the transcription rate of the *cagP* promoter

under normal growth conditions by showing that in the absence of the *cnc*R1, transcript levels of the *cagP* promoter were even higher than transcript levels from the *cagA* promoter [Vannini, 2013]. In addition, a terminator containing 29 bp, which was identified in the 3' region of *cnc*R1, might strongly reduce the downstream transcription of the putative *cagP* coding sequence. Thus, it is possible that in our sRNA deletion mutant (strain P12ΔsRNA), the high efficiency of the *cagP* promoter and the absence of the terminator resulted in an abundance of the *cagP* transcript and the CagP protein, which promoted CagI stability, and thus did not abolish the function of the Cag-T4SS. These results suggest that the sRNA is not absolutely necessary for the type IV-associated function of CagP. Surprisingly, complementation of the P12Δ*cagP* mutant with plasmid pWS338 containing *cagP* and the sRNA HPnc2630 restored the wild-type phenotype (Figure 3.31B), whereas complementation of this strain with pWS337 containing only *cagP*, did not (data not shown), implying that the sRNA has a certain role *in cis* on *cagP* expression, which is not consistent with the previous conclusion. The plasmid pWS337 was constructed in a the way that the putative terminator located in the 3' region of this sRNA was retained, while plasmid pWS338 contains the whole sequence spanning the *cagP* promoter, the sRNA and the putative *cagP* gene. Therefore, it is possible that the transcription from the *cagA* promoter (pWS337) could not read over the terminator, whereas transcription from the *cagP* promoter (pWS338) could. Importantly, we show that there is no transcriptional effect exerted by deletion of *cagP* and/or the sRNA on transcription of the *cagI* gene (Figure 3.32). These results are in line with the data provided in a recent study where the sRNA was observed to have no effect on the *cag* genes under normal growth conditions using the microarray transcriptional analyses and primer extension assay. In contrast, the sRNA exerts down-regulation effects on the regulation of motility functions [Vannini, 2013]. Unfortunately, our attempts to construct an epitope-tagged CagP version were unsuccessful, possibly due to the low transcriptional level of *cagP* as observed in different studies [Boonjakuakul *et al.*, 2005; Ta *et al.*, 2012] and in the presence of the terminator located in the 3' region of the sRNA [Vannini, 2013]. Taken together, at present, it is apparent that the CagP protein, but not HPnc2630, is required for the full function of the Cag-T4SS. Further experiments should be done to characterize the function of CagP and the sRNA.

4.2 Functional dependence of the Cag-T4SS on CagH, CagI and CagL components

The requirement of several Cag proteins for CagA translocation as well as IL-8 induction has been demonstrated in several mutagenesis studies [Censini *et al.*, 1996; Fischer *et al.*, 2001b; Selbach *et al.*, 2002; Shaffer *et al.*, 2011]. Among the essential components of the type IV secretion apparatus, CagH, CagI and CagL are not homologous to any components of other bacterial T4SSs. In the current study, using careful mutation and complementation studies, we show that CagH, CagI and CagL are essential components of the Cag type IV secretion apparatus in *H. pylori* strain P12. These results are generally consistent with previous studies, which showed that the individual deletion of *cagH* [Fischer *et al.*, 2001b; Shaffer *et al.*, 2011], *cagI* [Censini *et al.*, 1996; Selbach *et al.*, 2002; Shaffer *et al.*, 2011] and *cagL* [Fischer *et al.*, 2001b; Jimenez-Soto *et al.*, 2009; Kwok *et al.*, 2007; Shaffer *et al.*, 2011] resulted in a deficiency of CagA translocation and IL-8 induction. However, in previous works, complementation has only been performed for *cagL* [Jimenez-Soto *et al.*, 2009; Kwok *et al.*, 2007], showing that both phenotypes were fully restored by complementation of this gene. Complementation of *cagH* and *cagI* deletions has only recently been shown while this work was conducted [Shaffer *et al.*, 2011]. In the case of CagI, the conflicting results regarding the role of CagI in CagA translocation [Wang *et al.*, 2012] and IL-8 induction [Fischer *et al.*, 2001b] from gastric epithelial cells might be explained either by different strain-specific requirement of these components, by differences in gene expressions between the *cagI* mutants, or by differences in construction of the *cagI* deletion mutants.

The study published during the work on this thesis [Shaffer *et al.*, 2011], used the marker-free *cagH* and *cagI* deletion mutants and included complementation studies for functional characterization of these proteins, but determined only CagL production in the absence of either *cagH* or *cagI*. Other previous and recent studies used isogenic mutants containing resistance gene cassettes, which were not complemented [Censini *et al.*, 1996; Fischer *et al.*, 2001b; Kumar *et al.*, 2013; Kwok *et al.*, 2007; Selbach *et al.*, 2002; Wang *et al.*, 2012]. Therefore, it could not be concluded whether the deficiency of either CagA translocation or IL-8 induction, or both, resulted from the absence of the

corresponding proteins, or from reduced levels of other proteins caused by a polar effect caused by insertion of a resistance gene cassette. In this work, we show that not only CagL whose essential requirement has clearly been shown before [Jimenez-Soto *et al.*, 2009; Kwok *et al.*, 2007], but also CagH and CagI are required individually for CagA translocation and IL-8 induction. Deletion of *cagI* and its replacement by a resistance gene cassette, or deletion without a resistance marker, showed no severe transcriptional effects on *cagL* (Figure 3.8). It is worth noting that deletion of *cagI* led to a reduction of CagL to varying levels. Nevertheless, these differing CagL levels were not responsible for a defect of the Cag-T4SS, since the complete *cagI* marker-free deletion mutant producing wild-type levels of CagL has no functional Cag-T4SS (Figure 3.5). These results were substantiated by data obtained by complementation of the *cagI* and *cagL* double mutant with *cagL* only, which showed that despite producing unchanged levels of CagL in respect to the P12 wild-type (Figure 3.7A), the *cagL* complemented strain was not able to translocate CagA and induce IL-8 secretion, demonstrating that the effect has to be ascribed to the lack of CagI (Figure 3.7B). These findings suggest that CagI itself is required for a proper functionality of the *H. pylori* Cag-T4SS.

Regarding the functional role of CagH, although we failed to construct a marker-free *cagH* mutant to exclude a possible polar effect caused by insertion of an antibiotic resistance cassette, the complementation of a *cagH* deletion mutant not only *in cis* but also *in trans* (Figure 3.3) recovered the defect of Cag-T4SS functionality observed in the *cagH* mutant. Taken together, we can conclude that CagH is independently responsible for the defect of CagA translocation and IL-8 induction, and exclude that these phenotypes are indirectly caused by low levels of CagI and CagL. A recent study in which HA-tagged *cagH* was complemented in the *ureB* locus of a *cagH* marker-free mutant reached the same conclusion [Shaffer *et al.*, 2011].

4.3 CagH, CagI and CagL have stabilizing effects on each other

The chromosomal region containing the *cagI* gene was reported to be organized in an operon containing at least five genes (*cagF*, *cagG*, *cagH*, *cagI* and *cagL*), or even eight genes (*cagC, cagD, cagE, cagF*, *cagG*, *cagH*, *cagI* and *cagL)* [Sharma *et al.*, 2010], in which the later three genes, *cagH*, *cagI* and *cagL,* or the ribosome binding sites, overlap each other (Figure 3.1), suggesting a physical or a functional relationship between these

3 gene products. As mentioned above, deletion of *cagI* resulted in a variable reduction of CagL protein levels, and deletion of *cagH* resulted in reduction of both CagI and CagL levels, originally suggesting that transcriptional effects occur. However, complementation of these genes in different loci successfully rescued both phenotypes, suggesting that the proteins are responsible for these effects. Additionally, the quantification of the *cagL* mRNA by qPCR showed no significant difference between the P12 wild-type and the various *cagI* mutants (Figure 3.8), indicating that the transcription of *cagL* is not generally influenced by deletion of *cagI.* Therefore, we concluded that the reduction of CagL was not due to a transcriptional effect caused by deletion of *cagI,* but due to a stabilizing effect of CagI on CagL.

We provide further experimental evidence for a stabilizing effect of CagL on CagI by showing that the reduction of CagI levels was associated with the absence of CagL. As shown in Figure 3.7A, using the same mutant background (strain P12Δ*cagIL*) for complementation of either *cagI* alone or *cagI* and *cagL* together, the *cagI* complemented strain showed a reduced level of CagI, whereas the complementation of both genes (*cagI* and *cagL*) recovered production of CagI at the level of the P12 wild-type. In contrast, CagL production showed unchanged levels in the presence or absence of CagI for at leat one *cagI* mutant (Figure 3.7A). It is likely that in the wild-type strain or in those *cagI* mutants in which the 3' *cagI* region containing the *cagL* transcriptional start site was retained, CagL is at least expressed under the control of the *cagL* promoter. Since the *cagL* transcript level was increased in the mutant lacking complete *cagI* (strain P12Δ*cagI*(327) (Figure 3.5), it can be assumed that the precise deletion of *cagI* resulted in an efficiency increase of *cagL* transcription (Figure 3.8), possibly via the putative *cagF* or *cagG* promoter or another promoter located within the *cagFGHIL* operon [Ta *et al.*, 2012] suggesting that *cagL* transcription is deregulated in this mutant. Collectively, these data demonstrate that CagI is not absolutely required for CagL production. However, it is possible that the presence of the CagI protein and its interaction with CagL accounts at least partly for maintenance of CagL wild-type levels.

In the case of CagH, the stabilizing effect of CagH on CagI and CagL was obvious by the marked reduction of CagI and CagL levels produced by the *cagH* mutant (Figure 3.3A), given that these effects were restored by complementation of this mutant *in cis* and *in trans* (Figure 3.3A). Reduction of CagI levels in a *cagH* deletion mutant have

also been reported by Kumar *et al*. [Kumar *et al.*, 2013] and Shaffer *et al.* [Shaffer *et al.*, 2011], but only the complementation studies done here demonstrate that this is due to stabilization on the protein level, and can be explained by a direct interaction of these two proteins as observed in Co-IP and MBP pull-down experiments (Figure 3.19).

4.4 Cellular localization and interaction of the CagH, CagI and CagL proteins

Based on the combined data from the gene locus analysis, transcriptional arrangement of genes, sequence features of the corresponding gene products, and stabilizing effects among CagH, CagI and CagL, it was reasonable to hypothesize that CagH, CagI and CagL form a complex or a subcomplex with other components of the Cag-T4SS, and that these interactions might play crucial roles in CagA translocation mechanism. Previous studies using yeast two-hybrid assays [Busler *et al.*, 2006; Jurik *et al.*, 2010] demonstrated interactions between CagI and several other Cag proteins, including CagG, but none of them was confirmed, except for an interaction between recombinant CagI and CagZ fusion proteins *in vitro* [Busler *et al.*, 2006]. In the current work, we conducted immunoprecipitation studies that clearly demonstrate interactions between the native CagH, CagI and CagL proteins. The reduced CagI levels in mutants lacking components of the putative type IV secretion apparatus core complex (Δ*cagV*, Δ*cagW*, Δ*cagX*, Δ*cagY*, and possibly Δ*cagE*), or in mutants lacking components of the putative outer membrane-associated subcomplex (Δ*cagδ*, Δ*cagM*, Δ*cagX*) (Figure 3.28), indicated that corresponding protein-protein interactions might exist. However, we were unable to detect any interaction of CagI (or CagL) with CagX or CagY (data not shown). The identified interactions between CagH, CagI and CagL are generally in line with the findings of two studies published while this work was conducted, in which CagH, CagI and CagL interactions were shown by immunoprecipitation of either CagH or CagI [Kumar *et al.*, 2013], or by immunoaffinity purification of CagL from *H. pylori* lysates [Shaffer *et al.*, 2011]. Interestingly, we found the interaction of CagI and CagL in the soluble fraction of cellular fractionation (Figure 3.12B), suggesting that this interaction might take place in the bacterial periplasm, given that both proteins possess N-terminal signal sequences. Furthermore, consistent with recent data gained from *in vitro* studies of Kumar *et al.* [Kumar *et al.*, 2013], we show here an evidence for a direct

interaction between the recombinant CagH and CagI proteins by MBP pull-down experiments (Figure 3.19). However, our attempts to verify a direct interaction between CagH and CagL were unsuccessful because of unspecific interactions. We tried to prove whether the interaction between CagI and CagL is direct or mediated by a common interacting partner by using an *E. coli* strain expressing *cagH*, *cagI*, *cagL* under the control of the *cagA* promoter. However, we observed severe difficulties in expressing *cagH* without mutation in *E. coli*, suggesting that *E. coli* cells are intolerant to *cagH* gene expression. Therefore, we have not been able to produce the CagH protein in *E. coli.*

Other than for CagL, there is little known about the localization of CagH and CagI. As mentioned previously, topology prediction of these proteins shows that because of the predicted signal sequences, CagI and CagL might be secreted proteins (Figure 3.1). Evidence for binding of CagI and CagL to β1 integrin, a receptor for the Cag type IV secretion apparatus on host cells [Jimenez-Soto *et al.*, 2009; Kwok *et al.*, 2007], as well as a direct evidence for localization of CagL on the type IV secretion pili (Kwok *et al*., 2007), have been shown. By using scanning electron microscopy, Shaffer *et al*. showed that when bacteria were co-cultured with gastric epithelial cells, pili were found at the bacterial-host cell interface. However, the pili were not detectable in the bacteria lacking CagI and CagL or in the absence of cell contact. Unlike the *cagI* or *cagL* deletion mutants, the *cagH* deletion mutant was able to produce pili in the co-infection experiments with AGS cells, and it was speculated that CagH might be a regulator of pili dimensions. However, they could not detect CagH, CagI and CagL on the pili when *H. pylori* was co-cultured with AGS cells [Shaffer *et al.*, 2011]. Another study on localization of CagI showed that CagI was detected on pili under non-infection condition using transmission electron microscopy [Kumar *et al.*, 2013]. Furthermore, our preliminary data showed that deletion of *cagI* or *cagL* led to a reduction of integrin binding efficiency as observed in the *cag*-PAI deletion mutant (Figure 3.11), suggesting that CagI and CagL take part in the interaction between *H. pylori* and the host cell α5β1 integrin receptor. Taken together, these data on CagI and CagL indicate that both proteins are (partly) surface exposed. Using fractionation studies and proteinase K digestion, we have shown that CagI and CagL are present in different subcellular pools, and that both proteins are partly surface-exposed. It is intriguing that these two proteins

do not have a similar localization pattern in bacterial cell fractions (Figure 3.9A). CagI is mostly associated with the membrane fractions and not readily extracted by triton X-100, suggesting that CagI might localizes to the outer membrane. Meanwhile, in agreement with previous reports [Kutter *et al.*, 2008; Rohde *et al.*, 2003; Shaffer *et al.*, 2011], the majority of CagL was found in a soluble fraction, and only a smaller amount in the membrane fraction (Figure 3.9A). In addition, CagI and CagL seem to be equally distributed in membrane-associated fractions obtained by sucrose gradient centrifugation (Figure 3.9B). That might be explained by the limitation of this method in separating cytoplasmic and outer membrane proteins of *H. pylori,* as described previously [Kutter *et al.*, 2008; Pattis *et al.*, 2007]. However, the protease digestion experiments showed a higher susceptibility for CagI than for CagL (Figure 3.9C), and CagL was only slightly degraded by proteinase K digestion, suggesting that the majority of CagL is either located inside the bacteria, or that surface-associated CagL is not accessible for the proteinase. This finding is consistent with previous studies proposing that CagL was localized mainly in the periplasm [Kutter *et al.*, 2008; Shaffer *et al.*, 2011]. Since pili have been found on the surface of bacteria in the absence of host cells [Kumar *et al.*, 2013; Rohde *et al.*, 2003], it remains unclear whether the surface-exposed CagI and CagL as observed by proteinase K digestion, is pilus-associated or just at the outer membrane. The multiple pools of CagH and CagL with different localizations might be due to the different stages of Cag-T4SS assembly.

Unfortunately, our efforts to extract and purify pili for determination of their composition were unsuccessful. Therefore, we could not prove whether CagI and CagL are localized and interact on pili. We have so far been unable to localize CagI at the bacterial surface by immunofluorescence, since the CagI antiserum does not seem to recognize the native protein. Several attempts to generate an epitope-tagged variant of CagI which could be used for immunofluoresence staining and other purposes have not been successful either. Thus, it remains to be elucidated whether CagI is really associated with the pilus-like type IV surface appendages.

4.5 Conserved C-terminal motifs and internal motifs contribute to the function of CagH, CagI and CagL

Starting from the interesting observation that there is a high similarity of the C-terminal

6 amino acids of CagH, CagI and CagL (Figure 3.1C), we reasoned that these motifs play functional roles for example as a common binding motif for interaction between these three proteins. In agreement with a recently published study [Shaffer *et al.*, 2011], we found that the C-terminal motifs of CagH and CagL are important for CagA translocation and IL-8 induction (Figure 3.21C and 3.23B). However, in contrast to that study, deletion of the C-terminal motif from CagL did not result in the abolishment of IL-8 induction in our hands, but accounted only for an approximately 50% reduction of of IL-8 levels compared to wild-type P12 (Figure 3.21C), suggesting that CagL can induce IL-8 independently of its function in mediating T4SS substrate translocation. Interestingly, a recent study showed that recombinant CagL lacking the C-terminal motif retained its full adherence capability to human adenocarcinoma (MKN-45) cells [Barden *et al.*, 2013]. Since CagL was proposed as a ligand for integrin binding, our finding indicates that in the absence of the C-terminal motif, CagL is still able to mediate binding of the Cag-T4SS to host cells. Assuming that IL-8 secretion is induced by physical interaction of the secretion apparatus with host cells, rather than by active type IV secretion, it seems reasonable that in the absence of the C-terminal motif, CagL still triggers IL-8 secretion. Which part of CagL, which might be involved in IL-8 induction, is currently not clear. Although it has been reported that CagL induces IL-8 secretion through the interaction of its RGD motif with integrin receptors [Gorrell *et al.*, 2012], other data [Jimenez-Soto *et al.*, 2009] suggest that the RGD motif is not necessary for IL-8 induction. In any case, the complete deficiency of the mutant lacking C-terminal motif for CagA translocation indicates that different regions of CagL are required for IL-8 induction, and for CagA translocation, respectively.

Unexpectedly, we failed to construct a CagI C-terminal motif deletion mutant producing a detectable CagI protein using the same strategy which had been used for generating the CagL mutant lacking the C-terminal motif. The $CagI_{\Delta C}$ mutant (strain P12Δ*cagIL/IL* (pPT11)) still produced CagL, but no detectable traces of CagI (Figure 3.21A). When the plasmid (pPT11) was checked in *E. coli*, CagI was detected with a smaller size, indicating that it is unstable in *E. coli* cells (Figure 3.21B), whereas *cagL* is still expressed. This interesting finding also suggests that CagI lacking the C-terminal motif might have been degraded in *H. pylori* to a level that was under the detection limit of the Western blot. This instability of CagI might be explained by a direct interaction of

CagH and CagI (Figure 3.18), possibly via the C-terminal motifs of each protein.

Although these motifs play important roles in functionality of the Cag-T4SS [Shaffer *et al.*, 2011], there has been no study concerning the contribution of these motifs on interactions of CagI, CagL and CagH. In the current study, we show that the C-terminal motif of CagH affects the interactions between CagI and CagL, but the C-terminal motif of CagL does not. This result might be explained by a direct interaction of CagH and CagI, as suggested by MBP pull-down experiments (Figure 3.18). However, as shown in Figure 3.26, the amounts of CagI and CagH precipitated with CagL were reduced compared to the wild-type P12, suggesting that the absence of the C-terminal motif of CagL reduces the affinity of binding between these three proteins. Based on these findings, it is likely that all interactions are needed for a full functionality of the Cag apparatus and for a maximal induction of IL-8.

The presence of these conserved C-terminal motifs as a common binding motif for interaction between these three proteins was mentioned above. On the other hand, the CagL structure revealed that the CGISD motif is close to the C-terminal motif of CagL; separated by two alpha helices [Barden *et al.*, 2013]. These helices and these motifs are possibly conserved in CagI and CagH [Barden *et al.*, 2014]; this may imply that these regions bind to a common interaction partner; or that region from one component replaces the same region from the next component. This is reminiscent of "donor-strand complementation'' in type I pilus biogenesis (reviewed in [Lillington *et al.*, 2014]). In this process, two proteins are involved, a periplasmic chaperone and an outer membrane usher. The chaperone is essential for stabilization/folding of subunits, for avoiding premature subunit polymerization in the periplasm, and for targeting chaperone-subunit complexes to the usher protein which forms the outer membrane pilus assembly site. All pilus subunits exhibit an incomplete Ig-like fold and an exposed hydrophobic groove resulting from the lack of the seventh β-strand. In addition, each subunit has a flexible N-terminal extension peptide of 10-20 residues. Once pilus subunits are secreted and folded in the periplasm, the chaperone interacts with each subunit reconstituting the incomplete Ig-like fold by inserting its G1 β-strand into the subunit's hydrophobic groove. This interaction is called donor-strand complementation. The subunit is next transferred to the periplasmic N-terminal domain of the usher and incorporated into the pilus. During incorporation into the pilus, the chaperone G1 β-strand is replaced by the

N-terminal extension domain of the incoming subunit. This process is termed donor-strand exchange. In the *H. pylori* Cag-T4SS, a similar assembly mechanism might explain the conserved regions between CagH, CagI and CagL, but in the absence of a crystal structure of CagH-CagI-CagL complex, this remains speculative.

As observed in the crystal structure of CagL, the protein region containing the C-terminus and the alpha helicies α3, α4, α5, α6 contains a disulfide bond between Cys128 located in the α4 helix and Cys139 in the α5 helix (Figure 3.24) [Barden *et al.*, 2013]. Amino acid sequence analysis revealed that the sequence between these two cysteine residues (C128-C139) of CagL is similar to a region in CagH (C261-C272), which also contains two equally spaced cysteine residues (92% similarity). Particularly, Tyr225 of CagL was shown to form a hydrogen bond with Asp132, which is conserved between CagH and CagL (Figure 3.24). Therefore, we assumed that a point mutation leading to the loss of the disulfide bond, or deletion of some amino acids might lead to a defect of protein function. Using site-directed mutagenesis, this amino acid sequence was analyzed for its role in functionality of the Cag-T4SS and in the interactions among CagH, CagI and CagL. We found that neither a cysteine nor an aspartic acid substitution resulted in a defect of CagA translocation and IL-8 induction. However, deletion of 5 amino acids between the two cysteine residues resulted in a marked reduction of CagI and CagL levels, and consequently in a deficiency in the functionality of $CagH_{\Delta CPIGD}$ for CagA translocation and IL-8 induction. In contrast, although the $CagL_{\Delta CGISD}$ mutant produced markedly reduced levels of CagI and CagL, this strain was still able to translocate CagA into host cells, but with a lower efficiency compared to wild-type. Interestingly, this strain induced IL-8 induction as the wild-type (Figure 3.25), supporting the finding that CagL induces IL-8 secretion independently of promoting CagA translocation. Besides, these data provide evidence that these five amino acids play an important role to stabilize the part of the CagL protein structure, which affects the CagA translocation process.

4.6 The Cag-T4SS displays numerous specific features

The Cag-T4SS consists of several conserved components, which have been identified first by comparison with the *A. tumefaciens* VirB/VirD4 system, a prototypical T4SS (section 1.3.2). In general, the essential components of the T4SSs are important for pilus

assembly and/or substrate transfer. Interestingly, many essential components of the Cag-T4SS are unique for the Cag apparatus, having no functional counterparts in other systems [Fischer, 2011]. The components analysed in the current study CagH, CagI and CagL show no sequence similarities to components of other T4SSs. Functional analysis demonstrated that CagH, CagI and CagL are critically important for translocation of the effector CagA protein and IL-8 induction by AGS cells.

The existence of pilus components which might act as adhesins in establishing a tight bacterial contact with target cells is a distinguished feature of the contact-dependent T4SS systems. Both CagI [Jimenez-Soto *et al.*, 2009] and CagL [Kwok *et al.*, 2007] were observed to interact with β1 integrin *in vitro*, which is supported by our integrin binding experiments. Moreover, CagI and CagL were shown to contribute to the formation of pili, whereas CagH might have a regulatory role in pili dimension [Shaffer *et al.*, 2011]. Taken together, it is reasonable to conclude that CagI, CagL and CagH might belong to the group of pilus or pilus-associated components, or that the presence of these proteins is at least critically important for pilus biogenesis. CagL has been considered before as a functional homolog of *A. tumefaciens* VirB5, or the VirB5 homolog TraC of the *E. coli* F-type conjugation system. VirB5 is considered as the most divergent protein in the T4SSs [Backert and Selbach, 2008], and it is even absent in some systems such as the Ptl system of *Bordetella pertussis* [Zechner *et al.*, 2012]. Since CagI and CagL were shown to function as integrin ligands and form a complex or a subcomplex, which seems to be important for Cag-T4SS functionality, we may assume that the CagI-L complex fulfils the function similar to the VirB5 protein. However, it has to be noted that CagL structure is very different from the VirB5 structure [Barden *et al.*, 2013].

Localization studies of pilus-associated components such as VirB5 and TraC have shown that these proteins are first located in the cytoplasm, or associated with the inner membrane, and become later extracellularly secreted and incorporated to the pilus as their final localization. According to sequence predictions, CagH, CagI, and CagL are all acidic proteins with predicted isoelectric points between 4 and 6, and CagI and CagL are exported to the periplasm, from where they might reach the bacterial surface for integrin binding (Figure 3.1). Our localization studies showed that CagI and CagL exist in a non-surface localization at a considerable amount and partially on the bacterial

surface (Figure 3.9). Although we could not provide direct evidence for the presence of these proteins on the pili, our data support the hypothesis that they are secreted to reach the final localization on the pili, and then come into contact with the host cell receptor for facilitating the CagA translocation into host cells. The presence of CagI and CagL in different pools in *H. pylori* might be indicative of different stages of CagI and CagL production and incorporation into the pilus.

Based on the model for assembly of the Cag-T4SS proposed by Fischer [Fischer, 2011], in which the core complex is composed of CagT, CagV, CagX and CagY, we present here an updated model of the Cag-T4SS (Figure 4.1). In the *A. tumefaciens* T4SS, VirB5 has been shown to interact with the core complex components VirB8, and the inner membrane-bound NTPase VirB4. Apart from these structural components, VirB5 forms a complex with the major pilus subunit VirB2 [Yuan *et al.*, 2005], which is critically important for the incorporation of the VirB2 proteins into T-pili. In contrast, no interaction between CagI (or CagL) and CagT (VirB7), CagX (VirB9), CagY (VirB10), or CagC (VirB2) by immunoprecipitation (data not shown) could be detected. Since the interaction of CagI and CagL was observed in the soluble fraction (Figure 3.12B), we assume that this interaction might take place in the bacterial periplasm, where both proteins might bind to the periplasmic part of CagH. Interestingly, although CagH is predicted to be an integral cytoplasmic membrane protein [Kutter *et al.*, 2008], at least the N-terminus of CagH was shown to be exposed to the surface to play a role as a regulator of pilus dimensions [Shaffer *et al.*, 2011]. Taken together, we speculate that the interaction of CagH, I and L in the bacterial periplasm may lead to the export of all three proteins by an unknown mechanism to the bacterial surface where they assemble, possibly together with further unknown components of the Cag-T4SS, to form the extracellular pili. Although CagC (VirB2 homolog) was proposed as a major pilus component due to its features [Andrzejewska *et al.*, 2006; Kalkum *et al.*, 2002; Kutter *et al.*, 2008], there is so far no direct evidence for localization of CagC on the pilus. One recent study showed that despite being important for Cag-T4SS functionality, CagC was not required for the pilus formation [Johnson *et al.*, 2014]. Therefore, it raises the question whether this protein is present on the pilus at all. Thus it is well possible that the T4SS pili of the Cag system are formed exclusively by CagH, CagI and CagL (Figure 4.1). In addition, the pilus surface was proposed to be covered locally by the

CagY protein. This hypothesis is supported by an interaction of the surface-exposed C-terminus of CagY with the β1 integrin [Jimenez-Soto *et al.*, 2009].

Taken together, the available data suggest that the Cag-T4SS has an atypical pilus component. Further studies are required to elucidate the mechanism involved in pilus assembly.

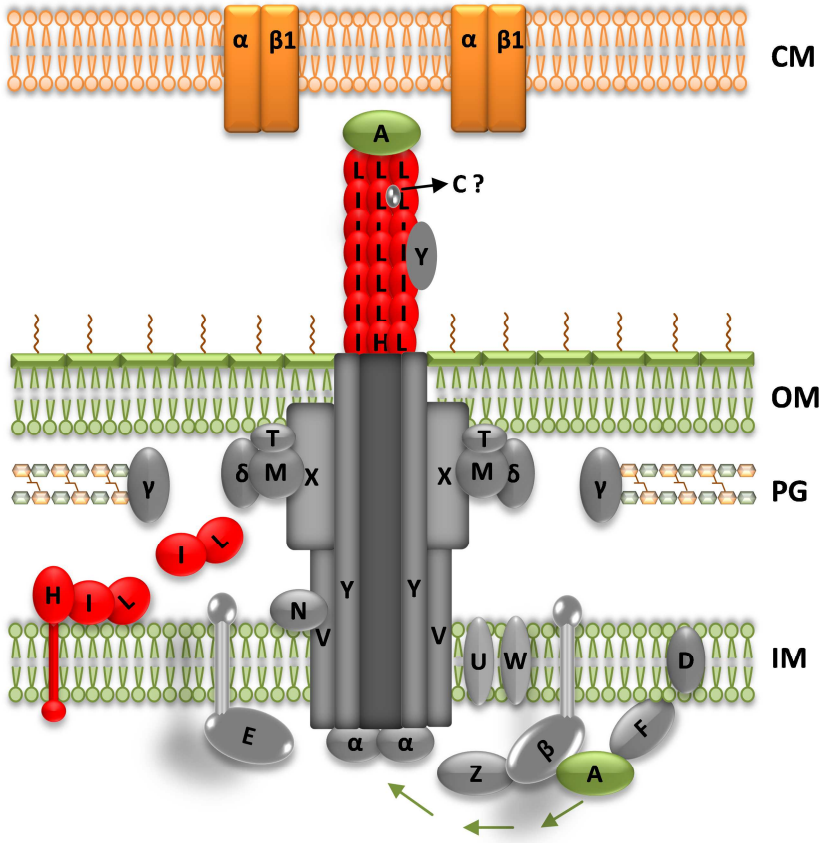

Figure 4.1. Assembly model of the Cag type IV secretion apparatus

According to this model, the pilus is a mix of CagH, CagI, and CagL, (and possibly CagC) and covered by CagY. The tip of the pilus is decorated with CagL. CagH may be a pilus component and located at the base of the pilus, where it forms an initial complex with CagI and CagL. IM: inner (bacterial) membrane; PG: peptidoglycan layer; OM: outer (bacterial) membrane; CM: cytoplasmic membrane of an eukaryotic target cell.

5 CONCLUSIONS AND OUTLOOK

The present study explores the role of the *cag*-PAI-encoded proteins, CagH, CagI and CagL, and their interactions in Cag-T4SS functionality in order to gain insights into the mechanism of pilus assembly in the process of CagA translocation. The presence of these proteins plays a central role in formation of the functional Cag apparatus. While investigating the role of the sRNA in regulating *cagI* and *cagL* expression, the role of the CagP protein in stabilizing these gene products was discovered. However, the mechanism by which this protein exerts its effects is not known, which might open up an interesting area for future studies. In addition, functional analysis of CagH, CagI and CagL and their interactions strongly suggests that the assembly of a complete pilus relies on these interactions. Whether the CagH, CagI and CagL proteins are incorporated into pili in the early stage of pilus assembly, or appear as late components of pili, has to be explored further in the future. The presence of the C-terminal motifs of each protein and their functional significance are other important results obtained in this study. Whether these motifs act as common interacting regions or play a role in the process of pilus assembly are also points of interest for further studies.

REFERENCES

Akopyants, N. S., Clifton, S. W., Kersulyte, D., Crabtree, J. E., Youree, B. E., Reece, C. A., Bukanov, N. O., Drazek, E. S., Roe, B. A., and Berg, D. E. (1998). Analyses of the *cag* pathogenicity island of *Helicobacter pylori*. *Mol Microbiol* **28**, 37-53.

Algood, H. M., and Cover, T. L. (2006). *Helicobacter pylori* persistence: an overview of interactions between *H. pylori* and host immune defenses. *Clin Microbiol Rev* **19**, 597-613.

Allison, C. C., Kufer, T. A., Kremmer, E., Kaparakis, M., and Ferrero, R. L. (2009). *Helicobacter pylori* induces MAPK phosphorylation and AP-1 activation via a NOD1-dependent mechanism. *J Immunol* **183**, 8099-8109.

Alvarez-Martinez, C. E., and Christie, P. J. (2009). Biological diversity of prokaryotic type IV secretion systems. *Microbiol Mol Biol Rev* **73**, 775-808.

Andrzejewska, J., Lee, S. K., Olbermann, P., Lotzing, N., Katzowitsch, E., Linz, B., Achtman, M., Kado, C. I., Suerbaum, S., and Josenhans, C. (2006). Characterization of the pilin ortholog of the *Helicobacter pylori* type IV cag pathogenicity apparatus, a surface-associated protein expressed during infection. *J Bacteriol* **188**, 5865-5877.

Aspholm-Hurtig, M., Dailide, G., Lahmann, M., Kalia, A., Ilver, D., Roche, N., Vikstrom, S., Sjostrom, R., Linden, S., Backstrom, A., Lundberg, C., Arnqvist, A., Mahdavi, J., Nilsson, U. J., Velapatino, B., Gilman, R. H., Gerhard, M., Alarcon, T., Lopez-Brea, M., Nakazawa, T., Fox, J. G., Correa, P., Dominguez-Bello, M. G., Perez-Perez, G. I., Blaser, M. J., Normark, S., Carlstedt, I., Oscarson, S., Teneberg, S., Berg, D. E., and Boren, T. (2004). Functional adaptation of BabA, the *H. pylori* ABO blood group antigen binding adhesin. *Science* **305**, 519-522.

Atmakuri, K., Cascales, E., and Christie, P. J. (2004). Energetic components VirD4, VirB11 and VirB4 mediate early DNA transfer reactions required for bacterial type IV secretion. *Mol Microbiol* **54**, 1199-1211.

Backert, S., Clyne, M., and Tegtmeyer, N. (2011). Molecular mechanisms of gastric epithelial cell adhesion and injection of CagA by Helicobacter pylori. *Cell Commun Signal* **9**, 28.

Backert, S., Moese, S., Selbach, M., Brinkmann, V., and Meyer, T. F. (2001). Phosphorylation of tyrosine 972 of the *Helicobacter pylori* CagA protein is essential for induction of a scattering phenotype in gastric epithelial cells. *Mol Microbiol* **42**, 631-644.

Backert, S., and Naumann, M. (2010). What a disorder: proinflammatory signaling pathways induced by *Helicobacter pylori*. *Trends Microbiol* **18**, 479-486.

Backert, S., and Selbach, M. (2008). Role of type IV secretion in *Helicobacter pylori* pathogenesis. *Cell Microbiol* **10**, 1573-1581.

Banno, A., and Ginsberg, M. H. (2008). Integrin activation. *Biochem Soc Trans* **36**, 229-234.

Barczyk, M., Carracedo, S., and Gullberg, D. (2010). Integrins. *Cell Tissue Res* **339**, 269-280.

Barden, S., Lange, S., Tegtmeyer, N., Conradi, J., Sewald, N., Backert, S., and Niemann, H. H. (2013). A helical RGD motif promoting cell adhesion: crystal structures of the *Helicobacter pylori* type IV secretion system pilus protein CagL. *Structure* **21**, 1931-1941.

Barden, S., Schomburg, B., Conradi, J., Backert, S., Sewald, N., and Niemann, H. H. (2014). Structure of a three-dimensional domain-swapped dimer of the Helicobacter pylori type IV secretion system pilus protein CagL. *Acta Crystallogr D Biol Crystallogr* **70**, 1391-1400.

Bayliss, R., Harris, R., Coutte, L., Monier, A., Fronzes, R., Christie, P. J., Driscoll, P. C., and Waksman, G. (2007). NMR structure of a complex between the VirB9/VirB7 interaction domains of the pKM101 type IV secretion system. *Proc Natl Acad Sci U S A* **104**, 1673-1678.

Blaser, M. J., Perez-Perez, G. I., Kleanthous, H., Cover, T. L., Peek, R. M., Chyou, P. H., Stemmermann, G. N., and Nomura, A. (1995). Infection with *Helicobacter pylori* strains possessing *cagA* is associated with an increased risk of developing adenocarcinoma of the stomach. *Cancer Res* **55**, 2111-2115.

Bode, G., Mauch, F., and Malfertheiner, P. (1993). The coccoid forms of *Helicobacter pylori.* Criteria for their viability. *Epidemiol Infect* **111**, 483-490.

Boncristiano, M., Paccani, S. R., Barone, S., Ulivieri, C., Patrussi, L., Ilver, D., Amedei, A., D'Elios, M. M., Telford, J. L., and Baldari, C. T. (2003). The *Helicobacter pylori* vacuolating toxin inhibits T cell activation by two independent mechanisms. *J Exp Med* **198**, 1887-1897.

Boonjakuakul, J. K., Canfield, D. R., and Solnick, J. V. (2005). Comparison of *Helicobacter pylori* virulence gene expression in vitro and in the Rhesus macaque. *Infect Immun* **73**, 4895-4904.

Boren, T., Falk, P., Roth, K. A., Larson, G., and Normark, S. (1993). Attachment of *Helicobacter pylori* to human gastric epithelium mediated by blood group antigens. *Science* **262**, 1892-1895.

Boughan, P. K., Argent, R. H., Body-Malapel, M., Park, J. H., Ewings, K. E., Bowie, A. G., Ong, S. J., Cook, S. J., Sorensen, O. E., Manzo, B. A., Inohara, N., Klein, N. J., Nunez, G., Atherton, J. C., and Bajaj-Elliott, M. (2006). Nucleotide-binding oligomerization domain-1 and epidermal growth factor receptor: critical regulators of beta-defensins during *Helicobacter pylori* infection. *J Biol Chem* **281**, 11637-11648.

Brandt, S., Kwok, T., Hartig, R., Konig, W., and Backert, S. (2005). NF-kappaB activation and potentiation of proinflammatory responses by the *Helicobacter pylori* CagA protein. *Proc Natl Acad Sci U S A* **102**, 9300-9305.

Busler, V. J., Torres, V. J., McClain, M. S., Tirado, O., Friedman, D. B., and Cover, T. L. (2006). Protein-protein interactions among *Helicobacter pylori* Cag proteins. *J Bacteriol* **188**, 4787-4800.

Calderwood, D. A. (2004). Integrin activation. *J Cell Sci* **117**, 657-666.

Camorlinga-Ponce, M., Romo, C., Gonzalez-Valencia, G., Munoz, O., and Torres, J. (2004). Topographical localisation of *cagA* positive and *cagA* negative *Helicobacter pylori* strains in the gastric mucosa; an in situ hybridisation study. *J Clin Pathol* **57**, 822-828.

Campbell, I. D., and Humphries, M. J. (2011). Integrin structure, activation, and interactions. *Cold Spring Harb Perspect Biol* **3**.

Cascales, E., and Christie, P. J. (2003). The versatile bacterial type IV secretion systems. *Nat Rev Microbiol* **1**, 137-149.

Cascales, E., and Christie, P. J. (2004). Definition of a bacterial type IV secretion pathway for a DNA substrate. *Science* **304**, 1170-1173.

Cendron, L., Couturier, M., Angelini, A., Barison, N., Stein, M., and Zanotti, G. (2009). The *Helicobacter pylori* CagD (HP0545, Cag24) protein is essential for CagA translocation and maximal induction of interleukin-8 secretion. *J Mol Biol* **386**, 204-217.

Cendron, L., and Zanotti, G. (2011). Structural and functional aspects of unique type IV secretory components in the *Helicobacter pylori cag*-pathogenicity island. *FEBS J* **278**, 1223-1231.

Censini, S., Lange, C., Xiang, Z., Crabtree, J. E., Ghiara, P., Borodovsky, M., Rappuoli, R., and Covacci, A. (1996). *cag*, a pathogenicity island of Helicobacter pylori, encodes type I-specific and disease-associated virulence factors. *Proc Natl Acad Sci U S A* **93**, 14648-14653.

Chandran, V., Fronzes, R., Duquerroy, S., Cronin, N., Navaza, J., and Waksman, G. (2009). Structure of the outer membrane complex of a type IV secretion system. *Nature* **462**, 1011-1015.

Christie, P. J. (1997). *Agrobacterium tumefaciens* T-complex transport apparatus: a paradigm for a new family of multifunctional transporters in eubacteria. *J Bacteriol* **179**, 3085-3094.

Christie, P. J. (2004). Type IV secretion: the *Agrobacterium* VirB/D4 and related conjugation systems. *Biochim Biophys Acta* **1694**, 219-234.

Conradi, J., Huber, S., Gaus, K., Mertink, F., Royo Gracia, S., Strijowski, U., Backert, S., and Sewald, N. (2012). Cyclic RGD peptides interfere with binding of the *Helicobacter pylori* protein CagL to integrins alphaVbeta3 and alpha5beta1. *Amino Acids* **43**, 219-232.

Cover, T. L., and Blanke, S. R. (2005). *Helicobacter pylori* VacA, a paradigm for toxin multifunctionality. *Nat Rev Microbiol* **3**, 320-332.

Cover, T. L., Glupczynski, Y., Lage, A. P., Burette, A., Tummuru, M. K., Perez-Perez, G. I., and Blaser, M. J. (1995). Serologic detection of infection with cagA+ *Helicobacter pylori* strains. *J Clin Microbiol* **33**, 1496-1500.

Crabtree, J. E. (1996). Gastric mucosal inflammatory responses to *Helicobacter pylori*. *Aliment Pharmacol Ther* **10 Suppl 1**, 29-37.

Crabtree, J. E., and Farmery, S. M. (1995). *Helicobacter pylori* and gastric mucosal cytokines: evidence that CagA-positive strains are more virulent. *Lab Invest* **73**, 742-745.

Dailidiene, D., Dailide, G., Kersulyte, D., and Berg, D. E. (2006). Contraselectable streptomycin susceptibility determinant for genetic manipulation and analysis of *Helicobacter pylori*. *Appl Environ Microbiol* **72**, 5908-5914.

de Bernard, M., Arico, B., Papini, E., Rizzuto, R., Grandi, G., Rappuoli, R., and Montecucco, C. (1997). *Helicobacter pylori* toxin VacA induces vacuole formation by acting in the cell cytosol. *Mol Microbiol* **26**, 665-674.

De Vos, G., and Zambryski, P. (1989). Expression of *Agrobacterium* nopaline-specific VirD1, VirD2, and VirC1 proteins and their requirement for T-strand production in *E. coli*. *Mol Plant Microbe Interact* **2**, 43-52.

Dossumbekova, A., Prinz, C., Mages, J., Lang, R., Kusters, J. G., Van Vliet, A. H., Reindl, W., Backert, S., Saur, D., Schmid, R. M., and Rad, R. (2006). *Helicobacter pylori* HopH (OipA) and bacterial pathogenicity: genetic and functional genomic analysis of *hopH* gene polymorphisms. *J Infect Dis* **194**, 1346-1355.

Dunn, B. E., Cohen, H., and Blaser, M. J. (1997). *Helicobacter pylori*. *Clin Microbiol Rev* **10**, 720-741.

Eaton, K. A., Brooks, C. L., Morgan, D. R., and Krakowka, S. (1991). Essential role of urease in pathogenesis of gastritis induced by *Helicobacter pylori* in gnotobiotic piglets. *Infect Immun* **59**, 2470-2475.

Eaton, K. A., Morgan, D. R., and Krakowka, S. (1992). Motility as a factor in the colonisation of gnotobiotic piglets by *Helicobacter pylori*. *J Med Microbiol* **37**, 123-127.

Egan, B. J., Katicic, M., O'Connor, H. J., and O'Morain, C. A. (2007). Treatment of *Helicobacter pylori*. *Helicobacter* **12 Suppl 1**, 31-37.

Egan, B. J., and O'Morain, C. A. (2007). A historical perspective of *Helicobacter* gastroduodenitis and its complications. *Best Pract Res Clin Gastroenterol* **21**, 335-346.

Eusebi, L. H., Zagari, R. M., and Bazzoli, F. (2014). Epidemiology of *Helicobacter pylori* infection. *Helicobacter* **19 Suppl 1**, 1-5.

Evans, D. J., Jr., and Evans, D. G. (2000). *Helicobacter pylori* adhesins: review and perspectives. *Helicobacter* **5**, 183-195.

Fischer, W. (2011). Assembly and molecular mode of action of the Helicobacter pylori Cag type IV secretion apparatus. *FEBS J* **278**, 1203-1212.

Fischer, W., Buhrdorf, R., Gerland, E., and Haas, R. (2001a). Outer membrane targeting of passenger proteins by the vacuolating cytotoxin autotransporter of *Helicobacter pylori*. *Infect Immun* **69**, 6769-6775.

Fischer, W., and Haas, R. (2004). The RecA protein of *Helicobacter pylori* requires a posttranslational modification for full activity. *J Bacteriol* **186**, 777-784.

Fischer, W., Puls, J., Buhrdorf, R., Gebert, B., Odenbreit, S., and Haas, R. (2001b). Systematic mutagenesis of the *Helicobacter pylori* cag pathogenicity island: essential genes for CagA translocation in host cells and induction of interleukin-8. *Mol Microbiol* **42**, 1337-1348.

Francesco, V. D., Zullo, A., Hassan, C., Giorgio, F., Rosania, R., and Ierardi, E. (2011). Mechanisms of *Helicobacter pylori* antibiotic resistance: An updated appraisal. In World J Gastrointest Pathophysiol, pp. 35-41.

Fronzes, R., Christie, P. J., and Waksman, G. (2009). The structural biology of type IV secretion systems. *Nat Rev Microbiol* **7**, 703-714.

Fujimoto, S., Olaniyi Ojo, O., Arnqvist, A., Wu, J. Y., Odenbreit, S., Haas, R., Graham, D. Y., and Yamaoka, Y. (2007). *Helicobacter pylori* BabA expression, gastric mucosal injury, and clinical outcome. *Clin Gastroenterol Hepatol* **5**, 49-58.

Gebert, B., Fischer, W., Weiss, E., Hoffmann, R., and Haas, R. (2003). *Helicobacter pylori* vacuolating cytotoxin inhibits T lymphocyte activation. *Science* **301**, 1099-1102.

Goodwin, C. S., and Worsley, B. W. (1993). Microbiology of *Helicobacter pylori*. *Gastroenterol Clin North Am* **22**, 5-19.

Gorrell, R. J., Guan, J., Xin, Y., Tafreshi, M. A., Hutton, M. L., McGuckin, M. A., Ferrero, R. L., and Kwok, T. (2012). A novel NOD1- and CagA-independent pathway of interleukin-8 induction mediated by the *Helicobacter pylori* type IV secretion system. *Cell Microbiol.*

Haas, R., Meyer, T. F., and van Putten, J. P. (1993). Aflagellated mutants of *Helicobacter pylori* generated by genetic transformation of naturally competent strains using transposon shuttle mutagenesis. *Mol Microbiol* **8**, 753-760.

Hamilton, H. L., and Dillard, J. P. (2006). Natural transformation of *Neisseria gonorrhoeae:* from DNA donation to homologous recombination. *Mol Microbiol* **59**, 376-385.

Hatakeyama, M. (2004). Oncogenic mechanisms of the *Helicobacter pylori* CagA protein. *Nat Rev Cancer* **4**, 688-694.

Hatakeyama, M., and Higashi, H. (2005). *Helicobacter pylori* CagA: a new paradigm for bacterial carcinogenesis. *Cancer Sci* **96**, 835-843.

Hayashi, T., Senda, M., Morohashi, H., Higashi, H., Horio, M., Kashiba, Y., Nagase, L., Sasaya, D., Shimizu, T., Venugopalan, N., Kumeta, H., Noda, N. N., Inagaki, F., Senda, T., and Hatakeyama, M. (2012). Tertiary structure-function analysis reveals the pathogenic signaling potentiation mechanism of *Helicobacter pylori* oncogenic effector CagA. *Cell Host Microbe* **12**, 20-33.

Higashi, H., Tsutsumi, R., Muto, S., Sugiyama, T., Azuma, T., Asaka, M., and Hatakeyama, M. (2002). SHP-2 tyrosine phosphatase as an intracellular target of *Helicobacter pylori* CagA protein. *Science* **295**, 683-686.

Higashi, H., Yokoyama, K., Fujii, Y., Ren, S., Yuasa, H., Saadat, I., Murata-Kamiya, N., Azuma, T., and Hatakeyama, M. (2005). EPIYA motif is a membrane-targeting signal of *Helicobacter pylori* virulence factor CagA in mammalian cells. *J Biol Chem* **280**, 23130-23137.

Hofreuter, D., Odenbreit, S., and Haas, R. (2001). Natural transformation competence in *Helicobacter pylori* is mediated by the basic components of a type IV secretion system. *Mol Microbiol* **41**, 379-391.

Hohlfeld, S., Pattis, I., Puls, J., Plano, G. V., Haas, R., and Fischer, W. (2006). A C-terminal translocation signal is necessary, but not sufficient for type IV secretion of the *Helicobacter pylori* CagA protein. *Mol Microbiol* **59**, 1624-1637.

Huang, J., O'Toole, P. W., Doig, P., and Trust, T. J. (1995). Stimulation of interleukin-8 production in epithelial cell lines by *Helicobacter pylori*. *Infect Immun* **63**, 1732-1738.

Humphries, M. J. (2000). Integrin structure. *Biochem Soc Trans* **28**, 311-339.

Hynes, R. O. (2002). Integrins: bidirectional, allosteric signaling machines. *Cell* **110**, 673-687.

Ilver, D., Arnqvist, A., Ogren, J., Frick, I. M., Kersulyte, D., Incecik, E. T., Berg, D. E., Covacci, A., Engstrand, L., and Boren, T. (1998). *Helicobacter pylori* adhesin binding fucosylated histo-blood group antigens revealed by retagging. *Science* **279**, 373-377.

Jimenez-Soto, L. F., Kutter, S., Sewald, X., Ertl, C., Weiss, E., Kapp, U., Rohde, M., Pirch, T., Jung, K., Retta, S. F., Terradot, L., Fischer, W., and Haas, R. (2009). *Helicobacter pylori* type IV secretion apparatus exploits beta1 integrin in a novel RGD-independent manner. *PLoS Pathog* **5**, e1000684.

Johnson, E. M., Gaddy, J. A., Voss, B. J., Hennig, E. E., and Cover, T. L. (2014). Genes required for assembly of pili associated with the *Helicobacter pylori* cag type IV secretion system. *Infect Immun* **82**, 3457-3470.

Jones, K. R., Whitmire, J. M., and Merrell, D. S. (2010). A Tale of Two Toxins: *Helicobacter pylori* CagA and VacA Modulate Host Pathways that Impact Disease. *Front Microbiol* **1**, 115.

Joyce, E. A., Gilbert, J. V., Eaton, K. A., Plaut, A., and Wright, A. (2001). Differential gene expression from two transcriptional units in the cag pathogenicity island of *Helicobacter pylori*. *Infect Immun* **69**, 4202-4209.

Juhas, M., Crook, D. W., and Hood, D. W. (2008). Type IV secretion systems: tools of bacterial horizontal gene transfer and virulence. *Cell Microbiol* **10**, 2377-2386.

Jurik, A., Hausser, E., Kutter, S., Pattis, I., Prassl, S., Weiss, E., and Fischer, W. (2010). The coupling protein Cagbeta and its interaction partner CagZ are required for type IV secretion of the *Helicobacter pylori* CagA protein. *Infect Immun* **78**, 5244-5251.

Kalkum, M., Eisenbrandt, R., Lurz, R., and Lanka, E. (2002). Tying rings for sex. *Trends Microbiol* **10**, 382-387.

Kaparakis, M., Turnbull, L., Carneiro, L., Firth, S., Coleman, H. A., Parkington, H. C., Le Bourhis, L., Karrar, A., Viala, J., Mak, J., Hutton, M. L., Davies, J. K., Crack, P. J., Hertzog, P. J., Philpott, D. J., Girardin, S. E., Whitchurch, C. B., and Ferrero, R. L. (2010). Bacterial membrane vesicles deliver peptidoglycan to NOD1 in epithelial cells. *Cell Microbiol* **12**, 372-385.

Kaplan-Turkoz, B., Jimenez-Soto, L. F., Dian, C., Ertl, C., Remaut, H., Louche, A., Tosi, T., Haas, R., and Terradot, L. (2012). Structural insights into *Helicobacter pylori* oncoprotein CagA interaction with beta1 integrin. *Proc Natl Acad Sci U S A* **109**, 14640-14645.

Kim, C., Ye, F., and Ginsberg, M. H. (2011). Regulation of integrin activation. *Annu Rev Cell Dev Biol* **27**, 321-345.

Kim, S. Y., Lee, Y. C., Kim, H. K., and Blaser, M. J. (2006). *Helicobacter pylori* CagA transfection of gastric epithelial cells induces interleukin-8. *Cell Microbiol* **8**, 97-106.

Kumar, N., Shariq, M., Kumari, R., Tyagi, R. K., and Mukhopadhyay, G. (2013). Cag type IV secretion system: CagI independent bacterial surface localization of CagA. *PLoS One* **8**, e74620.

Kusters, J. G., van Vliet, A. H., and Kuipers, E. J. (2006). Pathogenesis of *Helicobacter pylori* infection. *Clin Microbiol Rev* **19**, 449-490.

Kutter, S., Buhrdorf, R., Haas, J., Schneider-Brachert, W., Haas, R., and Fischer, W. (2008). Protein subassemblies of the *Helicobacter pylori* Cag type IV secretion system revealed by localization and interaction studies. *J Bacteriol* **190**, 2161-2171.

Kwok, T., Zabler, D., Urman, S., Rohde, M., Hartig, R., Wessler, S., Misselwitz, R., Berger, J., Sewald, N., Konig, W., and Backert, S. (2007). *Helicobacter* exploits integrin for type IV secretion and kinase activation. *Nature* **449**, 862-866.

Lamb, A., and Chen, L. F. (2013). Role of the *Helicobacter pylori*-induced inflammatory response in the development of gastric cancer. *J Cell Biochem* **114**, 491-497.

Lillington, J., Geibel, S., and Waksman, G. (2014). Biogenesis and adhesion of type 1 and P pili. *Biochim Biophys Acta* **1840**, 2783-2793.

Low, H. H., Gubellini, F., Rivera-Calzada, A., Braun, N., Connery, S., Dujeancourt, A., Lu, F., Redzej, A., Fronzes, R., Orlova, E. V., and Waksman, G. (2014). Structure of a type IV secretion system. *Nature* **508**, 550-553.

Luo, B. H., Carman, C. V., and Springer, T. A. (2007). Structural basis of integrin regulation and signaling. *Annu Rev Immunol* **25**, 619-647.

Mahdavi, J., Sonden, B., Hurtig, M., Olfat, F. O., Forsberg, L., Roche, N., Angstrom, J., Larsson, T., Teneberg, S., Karlsson, K. A., Altraja, S., Wadstrom, T., Kersulyte, D., Berg, D. E., Dubois, A., Petersson, C., Magnusson, K. E., Norberg, T., Lindh, F., Lundskog, B. B., Arnqvist, A., Hammarstrom, L., and Boren, T. (2002). *Helicobacter pylori* SabA adhesin in persistent infection and chronic inflammation. *Science* **297**, 573-578.

Marshall, B. J., and Warren, J. R. (1984). Unidentified curved bacilli in the stomach of patients with gastritis and peptic ulceration. *Lancet* **1**, 1311-1315.

Mauch, F., Bode, G., Ditschuneit, H., and Malfertheiner, P. (1993). Demonstration of a phospholipid-rich zone in the human gastric epithelium damaged by *Helicobacter pylori*. *Gastroenterology* **105**, 1698-1704.

McClain, M. S., Duncan, S. S., Gaddy, J. A., and Cover, T. L. (2013). Control of gene expression in *Helicobacter pylori* using the Tet repressor. *J Microbiol Methods* **95**, 336-341.

McGee, D. J., and Mobley, H. L. (2000). Pathogenesis of *Helicobacter pylori* infection. *Curr Opin Gastroenterol* **16**, 24-31.

Mizoguchi, H., Fujioka, T., Kishi, K., Nishizono, A., Kodama, R., and Nasu, M. (1998). Diversity in protein synthesis and viability of *Helicobacter pylori* coccoid forms in response to various stimuli. *Infect Immun* **66**, 5555-5560.

Morgan, D. R., Freedman, R., Depew, C. E., and Kraft, W. G. (1987). Growth of *Campylobacter pylori* in liquid media. *J Clin Microbiol* **25**, 2123-2125.

Murata-Kamiya, N., Kikuchi, K., Hayashi, T., Higashi, H., and Hatakeyama, M. (2010). *Helicobacter pylori* exploits host membrane phosphatidylserine for delivery, localization, and pathophysiological action of the CagA oncoprotein. *Cell Host Microbe* **7**, 399-411.

Naito, M., Yamazaki, T., Tsutsumi, R., Higashi, H., Onoe, K., Yamazaki, S., Azuma, T., and Hatakeyama, M. (2006). Influence of EPIYA-repeat polymorphism on the phosphorylation-dependent biological activity of *Helicobacter pylori* CagA. *Gastroenterology* **130**, 1181-1190.

Naumann, M., and Crabtree, J. E. (2004). *Helicobacter pylori*-induced epithelial cell signalling in gastric carcinogenesis. *Trends Microbiol* **12**, 29-36.

Noto, J. M., and Peek, R. M., Jr. (2012). The *Helicobacter pylori cag* Pathogenicity Island. *Methods Mol Biol* **921**, 41-50.

Nozawa, Y., Nishihara, K., Akizawa, Y., Orimoto, N., Nakano, M., Uji, T., Ajioka, H., Kanda, A., Matsuura, N., and Kiniwa, M. (2004). Protein kinase C activation by *Helicobacter pylori* in human gastric epithelial cells limits interleukin-8 production through suppression of extracellular signal-regulated kinase. *J Pharmacol Sci* **94**, 233-239.

O'Toole, P. W., Lane, M. C., and Porwollik, S. (2000). *Helicobacter pylori* motility. *Microbes Infect* **2**, 1207-1214.

Odenbreit, S., Puls, J., Sedlmaier, B., Gerland, E., Fischer, W., and Haas, R. (2000). Translocation of *Helicobacter pylori* CagA into gastric epithelial cells by type IV secretion. *Science* **287**, 1497-1500.

Odenbreit, S., Swoboda, K., Barwig, I., Ruhl, S., Boren, T., Koletzko, S., and Haas, R. (2009). Outer membrane protein expression profile in *Helicobacter pylori* clinical isolates. *Infect Immun* **77**, 3782-3790.

Olbermann, P., Josenhans, C., Moodley, Y., Uhr, M., Stamer, C., Vauterin, M., Suerbaum, S., Achtman, M., and Linz, B. (2010). A global overview of the genetic and functional diversity in the *Helicobacter pylori cag* pathogenicity island. *PLoS Genet* **6**, e1001069.

Oleastro, M., Cordeiro, R., Ferrand, J., Nunes, B., Lehours, P., Carvalho-Oliveira, I., Mendes, A. I., Penque, D., Monteiro, L., Megraud, F., and Menard, A. (2008). Evaluation of the clinical significance of homB, a novel candidate marker of *Helicobacter pylori* strains associated with peptic ulcer disease. *J Infect Dis* **198**, 1379-1387.

Oleastro, M., and Menard, A. (2013). The Role of *Helicobacter pylori* Outer Membrane Proteins in Adherence and Pathogenesis. *Biology (Basel)* **2**, 1110-1134.

Ottlecz, A., Romero, J. J., Hazell, S. L., Graham, D. Y., and Lichtenberger, L. M. (1993). Phospholipase activity of *Helicobacter pylori* and its inhibition by bismuth salts. Biochemical and biophysical studies. *Dig Dis Sci* **38**, 2071-2080.

Papini, E., Zoratti, M., and Cover, T. L. (2001). In search of the *Helicobacter pylori* VacA mechanism of action. *Toxicon* **39**, 1757-1767.

Parkin, D. M., Bray, F., Ferlay, J., and Pisani, P. (2005). Global cancer statistics, 2002. *CA Cancer J Clin* **55**, 74-108.

Parsonnet, J., Friedman, G. D., Orentreich, N., and Vogelman, H. (1997). Risk for gastric cancer in people with CagA positive or CagA negative *Helicobacter pylori* infection. *Gut* **40**, 297-301.

Parsonnet, J., Friedman, G. D., Vandersteen, D. P., Chang, Y., Vogelman, J. H., Orentreich, N., and Sibley, R. K. (1991). *Helicobacter pylori* infection and the risk of gastric carcinoma. *N Engl J Med* **325**, 1127-1131.

Parsonnet, J., Hansen, S., Rodriguez, L., Gelb, A. B., Warnke, R. A., Jellum, E., Orentreich, N., Vogelman, J. H., and Friedman, G. D. (1994). *Helicobacter pylori* infection and gastric lymphoma. *N Engl J Med* **330**, 1267-1271.

Partridge, A. W., Liu, S., Kim, S., Bowie, J. U., and Ginsberg, M. H. (2005). Transmembrane domain helix packing stabilizes integrin alphaIIbbeta3 in the low affinity state. *J Biol Chem* **280**, 7294-7300.

Pattis, I., Weiss, E., Laugks, R., Haas, R., and Fischer, W. (2007). The Helicobacter pylori CagF protein is a type IV secretion chaperone-like molecule that binds close to the C-terminal secretion signal of the CagA effector protein. *Microbiology* **153**, 2896-2909.

Peck, B., Ortkamp, M., Diehl, K. D., Hundt, E., and Knapp, B. (1999). Conservation, localization and expression of HopZ, a protein involved in adhesion of *Helicobacter pylori*. *Nucleic Acids Res* **27**, 3325-3333.

Penta, R., De Falco, M., Iaquinto, G., and De Luca, A. (2005). *Helicobacter pylori* and gastric epithelial cells: from gastritis to cancer. *J Exp Clin Cancer Res* **24**, 337-345.

Pinto-Santini, D., and Salama, N. R. (2005). The biology of *Helicobacter pylori* infection, a major risk factor for gastric adenocarcinoma. *Cancer Epidemiol Biomarkers Prev* **14**, 1853-1858.

Portal-Celhay, C., and Perez-Perez, G. I. (2006). Immune responses to *Helicobacter pylori* colonization: mechanisms and clinical outcomes. *Clin Sci (Lond)* **110**, 305-314.

Pounder, R. E., and Ng, D. (1995). The prevalence of *Helicobacter pylori* infection in different countries. *Aliment Pharmacol Ther* **9 Suppl 2**, 33-39.

Rohde, M., Puls, J., Buhrdorf, R., Fischer, W., and Haas, R. (2003). A novel sheathed surface organelle of the *Helicobacter pylori* cag type IV secretion system. *Mol Microbiol* **49**, 219-234.

Salama, N. R., Hartung, M. L., and Muller, A. (2013). Life in the human stomach: persistence strategies of the bacterial pathogen *Helicobacter pylori*. *Nat Rev Microbiol* **11**, 385-399.

Salama, N. R., Otto, G., Tompkins, L., and Falkow, S. (2001). Vacuolating cytotoxin of *Helicobacter pylori* plays a role during colonization in a mouse model of infection. *Infect Immun* **69**, 730-736.

Schmitt, W., and Haas, R. (1994). Genetic analysis of the *Helicobacter pylori* vacuolating cytotoxin: structural similarities with the IgA protease type of exported protein. *Mol Microbiol* **12**, 307-319.

Schroder, G., Krause, S., Zechner, E. L., Traxler, B., Yeo, H. J., Lurz, R., Waksman, G., and Lanka, E. (2002). TraG-like proteins of DNA transfer systems and of the *Helicobacter pylor*i type IV secretion system: inner membrane gate for exported substrates? *J Bacteriol* **184**, 2767-2779.

Segal, E. D., and Tompkins, L. S. (1993). Transformation of *Helicobacter pylori* by electroporation. *Biotechniques* **14**, 225-226.

Selbach, M., Moese, S., Meyer, T. F., and Backert, S. (2002). Functional analysis of the *Helicobacter pylori cag* pathogenicity island reveals both VirD4-CagA-dependent and VirD4-CagA-independent mechanisms. *Infect Immun* **70**, 665-671.

Senkovich, O. A., Yin, J., Ekshyyan, V., Conant, C., Traylor, J., Adegboyega, P., McGee, D. J., Rhoads, R. E., Slepenkov, S., and Testerman, T. L. (2011). *Helicobacter pylori* AlpA and AlpB bind host laminin and influence gastric inflammation in gerbils. *Infect Immun* **79**, 3106-3116.

Shaffer, C. L., Gaddy, J. A., Loh, J. T., Johnson, E. M., Hill, S., Hennig, E. E., McClain, M. S., McDonald, W. H., and Cover, T. L. (2011). *Helicobacter pylori* exploits a unique repertoire of type IV

secretion system components for pilus assembly at the bacteria-host cell interface. *PLoS Pathog* **7**, e1002237.

Sharma, C. M., Hoffmann, S., Darfeuille, F., Reignier, J., Findeiss, S., Sittka, A., Chabas, S., Reiche, K., Hackermuller, J., Reinhardt, R., Stadler, P. F., and Vogel, J. (2010). The primary transcriptome of the major human pathogen *Helicobacter pylori*. *Nature* **464**, 250-255.

Sharma, S. A., Tummuru, M. K., Blaser, M. J., and Kerr, L. D. (1998). Activation of IL-8 gene expression by *Helicobacter pylori* is regulated by transcription factor nuclear factor-kappa B in gastric epithelial cells. *J Immunol* **160**, 2401-2407.

Sharma, S. A., Tummuru, M. K., Miller, G. G., and Blaser, M. J. (1995). Interleukin-8 response of gastric epithelial cell lines to *Helicobacter pylori* stimulation in vitro. *Infect Immun* **63**, 1681-1687.

Shibata, W., Hirata, Y., Maeda, S., Ogura, K., Ohmae, T., Yanai, A., Mitsuno, Y., Yamaji, Y., Okamoto, M., Yoshida, H., Kawabe, T., and Omata, M. (2006). CagA protein secreted by the intact type IV secretion system leads to gastric epithelial inflammation in the Mongolian gerbil model. *J Pathol* **210**, 306-314.

Shimaoka, M., Takagi, J., and Springer, T. A. (2002). Conformational regulation of integrin structure and function. *Annu Rev Biophys Biomol Struct* **31**, 485-516.

Shimizu, T., Akamatsu, T., Sugiyama, A., Ota, H., and Katsuyama, T. (1996). *Helicobacter pylori* and the surface mucous gel layer of the human stomach. *Helicobacter* **1**, 207-218.

Smeets, L. C., and Kusters, J. G. (2002). Natural transformation in *Helicobacter pylori*: DNA transport in an unexpected way. *Trends Microbiol* **10**, 159-162; discussion 162.

Smillie, C., Garcillan-Barcia, M. P., Francia, M. V., Rocha, E. P., and de la Cruz, F. (2010). Mobility of plasmids. *Microbiol Mol Biol Rev* **74**, 434-452.

Smith, T. G., Lim, J. M., Weinberg, M. V., Wells, L., and Hoover, T. R. (2007). Direct analysis of the extracellular proteome from two strains of Helicobacter pylori. *Proteomics* **7**, 2240-2245.

Sugimoto, M., Ohno, T., Graham, D. Y., and Yamaoka, Y. (2011). *Helicobacter pylori* outer membrane proteins on gastric mucosal interleukin 6 and 11 expression in Mongolian gerbils. *J Gastroenterol Hepatol* **26**, 1677-1684.

Sundrud, M. S., Torres, V. J., Unutmaz, D., and Cover, T. L. (2004). Inhibition of primary human T cell proliferation by *Helicobacter pylori* vacuolating toxin (VacA) is independent of VacA effects on IL-2 secretion. *Proc Natl Acad Sci U S A* **101**, 7727-7732.

Ta, L. H., Hansen, L. M., Sause, W. E., Shiva, O., Millstein, A., Ottemann, K. M., Castillo, A. R., and Solnick, J. V. (2012). Conserved transcriptional unit organization of the *cag* pathogenicity island among *Helicobacter pylori* strains. *Front Cell Infect Microbiol* **2**, 46.

Takada, Y., Ye, X., and Simon, S. (2007). The integrins. *Genome Biol* **8**, 215.

Tanaka, J., Suzuki, T., Mimuro, H., and Sasakawa, C. (2003). Structural definition on the surface of *Helicobacter pylori* type IV secretion apparatus. *Cell Microbiol* **5**, 395-404.

Tegtmeyer, N., Hartig, R., Delahay, R. M., Rohde, M., Brandt, S., Conradi, J., Takahashi, S., Smolka, A. J., Sewald, N., and Backert, S. (2010). A small fibronectin-mimicking protein from bacteria induces cell spreading and focal adhesion formation. *J Biol Chem* **285**, 23515-23526.

Tegtmeyer, N., Wessler, S., and Backert, S. (2011). Role of the cag-pathogenicity island encoded type IV secretion system in *Helicobacter pylori* pathogenesis. *FEBS J* **278**, 1190-1202.

Telford, J. L., Ghiara, P., Dell'Orco, M., Comanducci, M., Burroni, D., Bugnoli, M., Tecce, M. F., Censini, S., Covacci, A., Xiang, Z., and et al. (1994). Gene structure of the *Helicobacter pylori* cytotoxin and evidence of its key role in gastric disease. *J Exp Med* **179**, 1653-1658.

Terradot, L., Bayliss, R., Oomen, C., Leonard, G. A., Baron, C., and Waksman, G. (2005). Structures of two core subunits of the bacterial type IV secretion system, VirB8 from *Brucella suis* and ComB10 from *Helicobacter pylori*. *Proc Natl Acad Sci U S A* **102**, 4596-4601.

Terradot, L., and Waksman, G. (2011). Architecture of the *Helicobacter pylori* Cag-type IV secretion system. *FEBS J* **278**, 1213-1222.

Vannini, A. (2013). Tile *Universitita Di Bologna*

Vannini, A., Roncarati, D., Spinsanti, M., Scarlato, V., and Danielli, A. (2014). In depth analysis of the *Helicobacter pylori cag* pathogenicity island transcriptional responses. *PLoS One* **9**, e98416.

Vergunst, A. C., van Lier, M. C., den Dulk-Ras, A., and Hooykaas, P. J. (2003). Recognition of the *Agrobacterium tumefaciens* VirE2 translocation signal by the VirB/D4 transport system does not require VirE1. *Plant Physiol* **133**, 978-988.

Viala, J., Chaput, C., Boneca, I. G., Cardona, A., Girardin, S. E., Moran, A. P., Athman, R., Memet, S., Huerre, M. R., Coyle, A. J., DiStefano, P. S., Sansonetti, P. J., Labigne, A., Bertin, J., Philpott, D. J., and Ferrero, R. L. (2004). Nod1 responds to peptidoglycan delivered by the *Helicobacter pylori cag* pathogenicity island. *Nat Immunol* **5**, 1166-1174.

Wallden, K., Rivera-Calzada, A., and Waksman, G. (2010). Type IV secretion systems: versatility and diversity in function. *Cell Microbiol* **12**, 1203-1212.

Walz, A., Odenbreit, S., Mahdavi, J., Boren, T., and Ruhl, S. (2005). Identification and characterization of binding properties of *Helicobacter pylori* by glycoconjugate arrays. *Glycobiology* **15**, 700-708.

Walz, A., Odenbreit, S., Stuhler, K., Wattenberg, A., Meyer, H. E., Mahdavi, J., Boren, T., and Ruhl, S. (2009). Identification of glycoprotein receptors within the human salivary proteome for the lectin-like BabA and SabA adhesins of *Helicobacter pylori* by fluorescence-based 2-D bacterial overlay. *Proteomics* **9**, 1582-1592.

Wang, H., Han, J., Chen, D., Duan, X., Gao, X., Wang, X., and Shao, S. (2012). Characterization of CagI in the cag pathogenicity island of *Helicobacter pylori*. *Curr Microbiol* **64**, 191-196.

Watanabe, T., Asano, N., Fichtner-Feigl, S., Gorelick, P. L., Tsuji, Y., Matsumoto, Y., Chiba, T., Fuss, I. J., Kitani, A., and Strober, W. (2010). NOD1 contributes to mouse host defense against *Helicobacter pylori* via induction of type I IFN and activation of the ISGF3 signaling pathway. *J Clin Invest* **120**, 1645-1662.

Wessel, D., and Flugge, U. I. (1984). A method for the quantitative recovery of protein in dilute solution in the presence of detergents and lipids. *Anal Biochem* **138**, 141-143.

Wiedemann, T., Hofbaur, S., Tegtmeyer, N., Huber, S., Sewald, N., Wessler, S., Backert, S., and Rieder, G. (2012). *Helicobacter pylori* CagL dependent induction of gastrin expression via a novel alphavbeta5-integrin-integrin linked kinase signalling complex. *Gut* **61**, 986-996.

Worku, M. L., Sidebotham, R. L., Walker, M. M., Keshavarz, T., and Karim, Q. N. (1999). The relationship between *Helicobacter pylori* motility, morphology and phase of growth: implications for gastric colonization and pathology. *Microbiology* **145 (Pt 10)**, 2803-2811.

Wozniak, R. A., and Waldor, M. K. (2010). Integrative and conjugative elements: mosaic mobile genetic elements enabling dynamic lateral gene flow. *Nat Rev Microbiol* **8**, 552-563.

Xiang, Z., Censini, S., Bayeli, P. F., Telford, J. L., Figura, N., Rappuoli, R., and Covacci, A. (1995). Analysis of expression of CagA and VacA virulence factors in 43 strains of *Helicobacter pylori* reveals that clinical isolates can be divided into two major types and that CagA is not necessary for expression of the vacuolating cytotoxin. *Infect Immun* **63**, 94-98.

Xiong, J. P., Stehle, T., Diefenbach, B., Zhang, R., Dunker, R., Scott, D. L., Joachimiak, A., Goodman, S. L., and Arnaout, M. A. (2001). Crystal structure of the extracellular segment of integrin alpha Vbeta3. *Science* **294**, 339-345.

Xiong, J. P., Stehle, T., Zhang, R., Joachimiak, A., Frech, M., Goodman, S. L., and Arnaout, M. A. (2002). Crystal structure of the extracellular segment of integrin alpha Vbeta3 in complex with an Arg-Gly-Asp ligand. *Science* **296**, 151-155.

Yamaoka, Y. (2010). Mechanisms of disease: *Helicobacter pylori* virulence factors. *Nat Rev Gastroenterol Hepatol* **7**, 629-641.

Yamaoka, Y., Kwon, D. H., and Graham, D. Y. (2000). A M(r) 34,000 proinflammatory outer membrane protein (oipA) of *Helicobacter pylori*. *Proc Natl Acad Sci U S A* **97**, 7533-7538.

Yuan, Q., Carle, A., Gao, C., Sivanesan, D., Aly, K. A., Hoppner, C., Krall, L., Domke, N., and Baron, C. (2005). Identification of the VirB4-VirB8-VirB5-VirB2 pilus assembly sequence of type IV secretion systems. *J Biol Chem* **280**, 26349-26359.

Yucel, O. (2014). Prevention of *Helicobacter pylori* infection in childhood. *World J Gastroenterol* **20**, 10348-10354.

Zechner, E. L., Lang, S., and Schildbach, J. F. (2012). Assembly and mechanisms of bacterial type IV secretion machines. *Philos Trans R Soc Lond B Biol Sci* **367**, 1073-1087.

Zehr, B. D., Savin, T. J., and Hall, R. E. (1989). A one-step, low background coomassie staining procedure for polyacrylamide gels. *Anal Biochem* **182**, 157-159.

Zhang, S., Yanaka, A., Tauchi, M., Suzuki, H., Shibahara, T., Matsui, H., Nakahara, A., and Tanaka, N. (2006). Hyperosmotic stress enhances interleukin-1beta expression in *Helicobacter pylori*-infected murine gastric epithelial cells in vitro. *J Gastroenterol Hepatol* **21**, 759-766.

Zheng, P. Y., Hua, J., Ng, H. C., and Ho, B. (1999). Unchanged characteristics of *Helicobacter pylori* during its morphological conversion. *Microbios* **98**, 51-64.

ABBREVIATIONS AND UNITS

Abbreviations

A	Adenin
amp^R	Ampicillin resistance
AP	Adenosintriphosphate
APS	Ammoniumpersulphate
ATP	Adenosine triphosphate
BB	Brucella Broth
BCIP	5-Brom-4-chlor-3-indolylphosphate
BSA	Bovines Serumalbumin
C	Cytosine
cag	Cytotoxin-associated gene
Cag-T4SS	Cag Type IV Secretion System
cam^R	Chloramphenicol resistance
C-termimus	Carboxyl terminal end of a protein
Δ	Delta (Deletion)
D	Aspartat
DEPC	diethylpyrocarbonate
dATP	Desoxyadenosintriphosphate
dCTP	Desoxycytidintriphosphat
dGTP	Desoxyguanosintriphosphate
DMF	DMF Dimethylformamide
DMSO	DMSO Dimethylsulfoxide
DNA	Deoxyribonucleic acid
DNAse	Deoxyribonuclease
dNTP	Deoxynucleotide Triphosphates (Mixture of dATP, dCTP, dGTP, dTTP)
DTT	Dithiothreitol

dTTP	Desoxythiymidintriphosphate
EDTA	Ethylenediaminetetraacetic acid
ERK	extracellular signal-regulated kinases
erm^R	Erythromycin resistance
et al.,	From Latin, abbreviation of et (“and”) and alii (“others”)
FACS	Fluorescence-activated cell sorting
FCS	fetal calf serum
G	Glycine
G	Guanin
GEBS	Glycerol EDTA bromphenol blue sarkosyl buffer
His	Histidine
Ig	Immunoglobulin
IL	Interleukin
IPTG	Isopropyl β-D-1-thiogalactopyranoside
kan^R	Kanamycin resistance
LB-Medium	Luria-Bertani-Medium
MAPK	Mitogen-activated protein kinase
M-MuLVRT	Moloney Murine Leukemia Virus
MOPS	Morpholinepropanesulfonic acid
MOI	Multiplicity of infection
NaCl	Sodium chloride
NBT	Nitrotetrazoliumbluechloride
N-terminus	Amino terminal end of protein
OD	Optical density
ORF	Open reading frame
PAGE	Polyacrylamide gel electrophoresis
PAI	Pathogenicity island
PBS	Phosphate Buffered Saline

PCR	Polymerase Chain Reaction
qPCR (RT PCR)	Quantitative polymerase chain reaction (Real-time polymerase chain reaction)
RNA	Ribonucleic acid
RNase	RNA endonuclease
RT-PCR	Reverse transcription polymerase chain reaction
PMSF	Phenylmethylsulfonyl fluoride
POX	Peroxidase
P-Tyr	Phosphotyrosine
PVDF	Polyvinylidinfluoride
RIPA	Radioimmunoprecipitation assay buffer
SDS	Sodium dodecyl sulfate
Src	Tyrosine kinase
$strep^R$	Streptomycin resistance
T	Thymin
TEMED	Tetramethylethylendiamin
Tris	Tris-(hydroxymethyl)-Aminomethan
Tris HCl	Tris-HCl Tris-(hydroxymethyl)-Aminomethan-Hydrochloride
(w/v)	weight/volume
w/w	weight/weight

Units

^oC	Grad Celsisus
µ	Micro- (10^{-6})
A	Amper
bp	Base pair
Da	Dalton
g	Gram

(x)*g*	Standard gravities
h	Hour
k	Kilo-, 10^3
l	Liter
M	Molar (mol/g)
m	Milli- (10^{-3})
n	Nano- (10^{-9})
rpm	Rounds per minute
sec	Seconds
U	Unit (Enzyme activity = moles of substrate converted per unit time)
V	Volts

ACKNOWLEDGEMENT

Foremost, I would like to express my gratitude to my supervisor, Prof. Rainer Haas, for giving me a great opportunity to join an excellent environment for learning and doing research. Thank you for reading and correcting my thesis.

I would like to say a great thank you and to express my sincere gratitude to my advisor PD. Dr. Wolfgang Fischer for the continuous support of my P.h.D study and research, for your patience, motivation, enthusiasm, and immense knowledge, in building my background. Your expertise and guidance helped me in every step of my research and writing of this thesis. Thank you for putting a lot of effort on correcting my thesis. I could not have imagined having a better advisor and mentor for my P.h.D study.

I would like to say thank you, Dr. Beate Kern, who is the first German friend of mine. Thank you for being always so nice to me, helping me and reminding me that everything will work.

Many thanks to my friend, Caro, for sharing a good time and venting of frustration during my time in the lab. I appreciate everything you have done to help me overcome the earlier difficulties of a foreigner and get to know German culture, which I would have never found in a book.

A lot of thanks, I would like to say thank you, Evelyn, who was always helping and willing to do any favor I asked. Thank you for your enthusiasm. I enjoyed the time when we were 'bench-mates' every morning, and talking when you had a break in between your experiments.

My thanks also go to my dear Friederike for motivating me and for giving me helpful advices. I always felt like talking to my mom when I talked to you.

I would like to thank to my 'Nachbarin', Lea, for your help whenever I needed. You are the cleverest girl I have ever met and always come up with ideas and solutions. I would like to say thank you to Verana as well, I always liked having a short talk to you about work and life.

I would like to thank Luisa for being always so helpful. I learned a lot from your professional attitude at work.

It is never enough words to say thank to other friends, Benjamin, Qing, Franzi, Kathrin, Ute. I enjoyed every moment when I talked to you all. I realized that I never felt lonely in the lab because of having many friendly friends.

This research would not have been possible without the financial assistance of the Vietnamese Government, and support from the Vietnam Academy of Science and Technology, Institute of Biology, Department of Microorganism and I would like to express my gratitude to those agencies.

Last but not the last, I would like to thank my husband. I would have never finished my study without your support, patience and understanding. You are always beside me and show me the positive side of every problem, encouraging me to keep going forward, which helps me to find the balance between life and work. My thanks also go to my son who joined us during the time of my P.h.D, for making unlimited happiness and pleasure. You are the most wonderful 'result' I have ever got in my life. A very special thank goes to my family in Vietnam. Your encouragement and your belief in me always make me stronger eventhough you are not by my side.